MOLECULAR ECOLOGY

Molecular Ecology (2015) doi: 10.1111/mec.13343

Phylogeographic inference using Bayesian model comparison across a fragmented chorus frog species complex

LISA N. BARROW,* ALYSSA T. BIGELOW,* CHRISTOPHER A. PHILLIPS† and EMILY MORIARTY LEMMON*

*Department of Biological Science, Florida State University, 319 Stadium Drive, P.O. Box 3064340, Tallahassee, FL 32306-4340, USA, †Illinois Natural History Survey, Prairie Research Institute, University of Illinois, 185 Natural Resources Bldg, 607 E. Peabody Drive, Champaign, IL 61820, USA

Abstract

Fragmented species complexes provide an interesting system for investigating biogeographic history and the present distribution of genetic variation. Recent advances in sequencing technology and statistical phylogeography enable the collection and rigorous analysis of large multilocus data sets, but designing studies that produce meaningful phylogeographic inferences remains challenging. We implemented a Bayesian model comparison approach to investigate previous biogeographic hypotheses while simultaneously inferring the presence of genetic structure in a chorus frog species complex. The Illinois chorus frog (*Pseudacris illinoensis*), originally described as a subspecies of the broadly distributed Strecker's chorus frog (*Pseudacris streckeri*), occurs in small, disjunct regions associated with scarce sand prairie habitats that have been impacted by human development. We used high-throughput sequencing to develop and collect a multitiered genetic data set comprised of three different marker types (23 anonymous nuclear sequence loci, four mitochondrial genes and 14 microsatellite loci) designed to address questions across different evolutionary timescales. Phylogenetic analyses uncovered a deep divergence between populations in the Edwards Plateau of central Texas and all other *P. streckeri*/*P. illinoensis* populations, but suggest the disjunct distribution of *P. illinoensis* occurred more recently. Our best-supported migration model is consistent with the hypothesis that central Texas represented a refugium from which populations expanded via multiple routes. This model also indicates that disjunct northern and southern regions of *P. illinoensis* should be considered genetically distinct management units. Our study provides an evolutionary context for future studies and conservation efforts in *P. illinoensis* and demonstrates the utility of model-based approaches for phylogeographic inference.

Keywords: Illinois chorus frog, Illumina, migrate-n, parallel tagged sequencing, phylogeography, *Pseudacris*

Received 20 October 2014; revision received 24 July 2015; accepted 8 August 2015

Introduction

Geography has a pronounced influence on the structuring of populations and the diversification of lineages (Avise 2000; Epperson 2003). In addition to habitat and climatic variation, the inherent properties of the species in question, such as dispersal ability or habitat requirements, dictate the physical connectivity of and gene flow between populations (Endler 1977; Burney & Brumfield 2009). Species complexes with disjunct ranges provide interesting systems for investigating the impact of historical environmental change and contemporary issues such as human development on the evolutionary

Correspondence: Lisa N. Barrow, Fax: 850 644 0989; E-mail: barrow@bio.fsu.edu

history and genetic structure of natural populations. This situation can also pose challenges for taxonomic designations and conservation decisions (e.g. Coates 2000; Cook *et al.* 2001; Smith 2005), and because the factors involved span different timescales, different types of genetic markers with varying mutation rates (reviewed in Sunnucks 2000) are needed to elucidate patterns and the underlying processes.

Phylogeographic research is undergoing rapid improvements with the application of recent sequencing technologies to collect large multilocus data sets from nonmodel organisms (reviewed in McCormack *et al.* 2013; Garrick *et al.* 2015). In addition, analytical tools and methods for statistical inference continue to improve allowing researchers to rigorously test *a priori* hypotheses (Knowles 2009; Nielsen & Beaumont 2009; Hickerson *et al.* 2010; Bouckaert *et al.* 2012; Carstens *et al.* 2013; Pelletier & Carstens 2014). Alternative approaches for phylogeographic inference have been developed that differ primarily on whether they involve reconstructing the phylogenetic history of individuals sampled within species or between closely related species, or use population genetic models in a coalescent framework to infer population-level information (Smouse 1998; Hey & Machado 2003; Bloomquist *et al.* 2010). Each approach can provide useful insights, but challenges remain in designing studies, including sufficient geographic and genetic sampling, and conducting analyses of empirical data sets that allow us to draw meaningful inferences. Existing analytical methods incorporate different underlying assumptions to simplify the complex history being estimated, for example by allowing or ignoring gene flow, population divergence or changes in population size through time. Although some assumptions may be violated by empirical data sets, simulations indicate certain methods are robust to model violations and parameters can still be estimated reliably (Beerli 2010; Strasburg & Rieseberg 2010). In this study, we use a coalescent-based model selection framework to simultaneously test hypotheses regarding the biogeographic history and level of genetic structure in a fragmented chorus frog species complex. We employed high-throughput sequencing to collect a large multilocus data set consisting of three different types of genetic markers and analysed data in both phylogenetic and population genetic contexts to address questions both above and below the species level. This combined approach allows us to better understand the evolutionary history and current status of a species of conservation concern.

Strecker's chorus frog (*Pseudacris streckeri*) is a member of the 'Fat Frog' clade of the North American chorus frogs (Moriarty & Cannatella 2004) and is widely distributed throughout eastern Texas, Oklahoma, southern Kansas and western Arkansas along the Arkansas River Valley. The Illinois chorus frog (*Pseudacris illinoensis*), originally described as a subspecies of *P. streckeri* based on subtle morphological differences (Smith 1951), occurs in three disjunct clusters (counties of record separated by >60 km; IUCN 2012) in south-central Illinois, south-eastern Missouri, and north-eastern Arkansas (Fig. 1). *Pseudacris illinoensis* is of conservation concern because of its limited range and habitat loss due to agricultural practices (Brown & Rose 1988; Trauth *et al.* 2006), but formal efforts to list this taxon under the Endangered Species Act have not yet been successful. In addition, the taxonomic status of *P. illinoensis* is still unsettled. Collins (1991) listed *P. illinoensis* as a distinct species presumably because of its allopatric distribution and morphological distinctiveness described by Smith (1951). More recent studies have found that (i) morphology varies geographically but does not distinguish between the two taxa (Trauth *et al.* 2007), and (ii) mitochondrial sequence data from limited samples demonstrate that *P. streckeri* is paraphyletic with respect to *P. illinoensis* (Moriarty & Cannatella 2004; Lemmon *et al.* 2007a). We follow Frost *et al.* (2012) and refer to populations using their current taxonomic designations, but our analyses and conclusions do not rely on *a priori* species designations. Here, we focus on understanding the biogeographic history and genetic structure across the species complex, using regions and populations as the units of focus, and reserve species delimitation for future study.

The disjunct distribution of this species complex is similar to a number of other terrestrial vertebrates that consist of wide-ranging western segments in the Great Plains and relict populations in eastern sand prairies or grasslands (Smith 1957). The primary hypothesis explaining these distributional patterns posits that during the Xerothermic period (approx. 4000 years ago), these dry-adapted species occupied a wider, continuous range, but as the climate became cooler and more humid, eastern populations survived only in pockets of suitable habitat (Smith 1957). In addition to considering climatic factors that influence fauna of an entire region, natural history information from specific organisms can be incorporated into phylogeographic studies. An alternative hypothesis was proposed by Axtell & Haskell (1977) to explain the origin and distribution of *P. illinoensis* in particular, which requires specific soil types for its burrowing lifestyle (Brown *et al.* 1972; Brown 1978). Axtell & Haskell (1977) proposed that *P. illinoensis* was derived from populations of *P. streckeri* and that the dispersal route was likely limited to the Arkansas River Valley rather than dispersal along a 'broad front'. We investigate these hypotheses and a range of phylogeographic scenarios using genetic data in a model

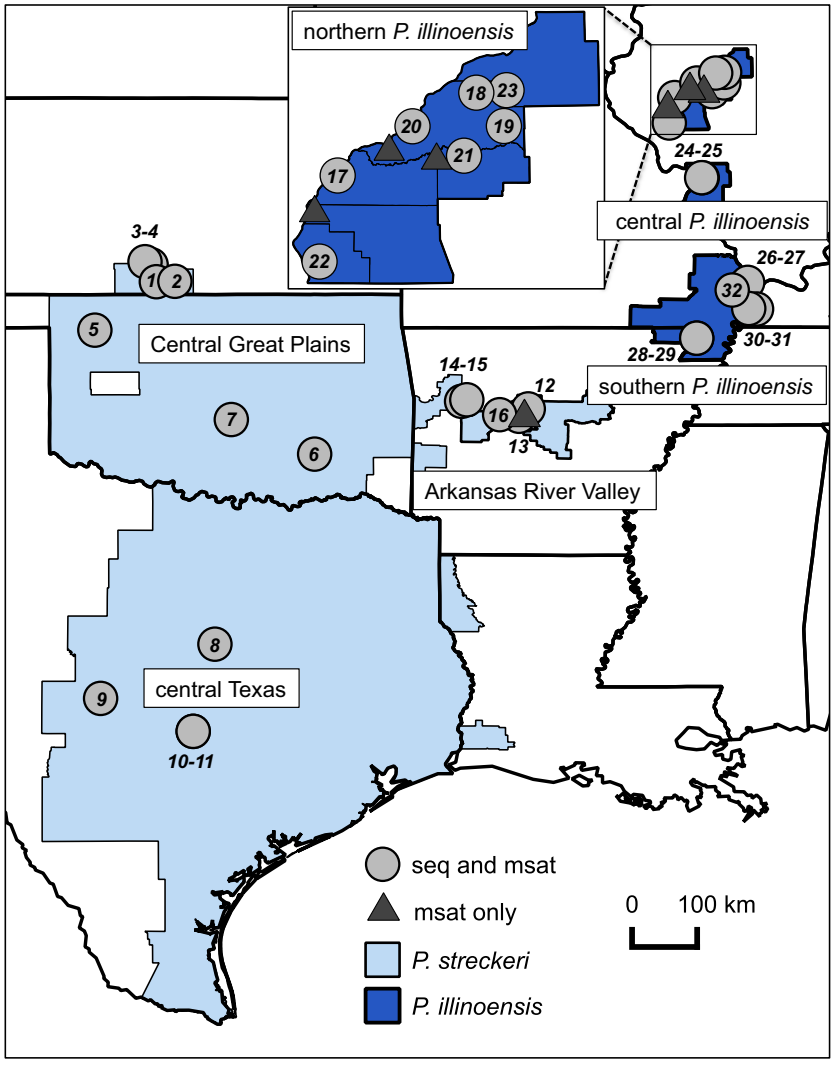

Fig. 1 Map of species ranges (IUCN 2012) and sample localities for *Pseudacris streckeri* and *Pseudacris illinoensis*. Numbers correspond to Seq ID in Table 1.

comparison framework to better understand the biogeographic history and current distribution of genetic variation of these taxa.

The goals of this study were to conduct the most comprehensive genetic assessment of this species complex to date in order to (i) determine the evolutionary relationships within and between *P. streckeri* and *P. illinoensis* populations and estimate divergence times within the group, (ii) discover the patterns of genetic structure and levels of genetic diversity across species and populations, and (iii) test previously proposed biogeographic hypotheses for this species complex using a Bayesian model comparison framework. Our findings will help inform conservation efforts in this species complex and provide a framework for future biogeographic studies of other taxa in this region. Furthermore, the model selection strategy we implement can be applied widely across phylogeographic studies.

Materials and methods

Geographic sampling and DNA extraction

We obtained tissue samples from across the range of *Pseudacris streckeri* and *Pseudacris illinoensis* through previous field collections or museum loans (Table S1, Supporting information; Fig. 1). A total of 294 individuals (103 *P. streckeri*, 191 *P. illinoensis*) were sampled from 32 sites (Table 1). Genomic DNA was isolated from liver tissue, toe clips or larval tail clips using either the EZNA Tissue DNA Kit (Omega Bio-Tek, Norcross, GA,

USA) following the manufacturer's protocols or a standard guanidine thiocyanate extraction protocol as follows. Tissues were digested in 300 μL cell lysis buffer (1.975 M NaCl, 125 mM Tris-Cl, 25 mM EDTA, 5% SDS) with 25 μL OB Protease (Omega Bio-Tek) overnight at 55°C. The DNA was purified with a protein precipitate solution (4 M guanidine thiocyanate, 100 mM Tris-Cl), 100% isopropanol precipitation and two 70% ethanol washes.

Table 1 List of sample sites included in this study for each taxon and region, number of individuals sequenced for 23 nDNA loci and four mtDNA genes (N Seq), and number of individuals genotyped at 14 microsatellite loci (N Msat). Seq ID corresponds to individuals that were sequenced (see Fig. 1); Site Name corresponds to the labels used for microsatellite data. Some sites combine individuals sampled from multiple nearby locations (see Methods and Table S1, Supporting information for location details)

Region	Seq ID	Site Name	N Seq	N Msat
Pseudacris streckeri (16 sites, 103 individuals)				
Central Texas (TEX)	10–11	TEX1	2	18
	9	TEX2	1	1
	8	TEX3	1	1
Central Great Plains (CGP)	5	OKL1	1	5
		OKL2A		8
	7	OKL2B	1	8
	6	OKL3	1	1
	3–4	KAN1	2	5
	1	KAN2	1	1
	2	KAN3	1	1
Arkansas River Valley (ARV)		ARK1		20
	13	ARK2	1	11
	12	ARK3	1	5
	16	ARK4	1	9
	15	ARK5A	1	6
	14	ARK5B	1	3
Pseudacris illinoensis (16 sites, 191 individuals)				
Southern cluster (ILLS)	28–29	ARK6	2	8
	30	MIS1A	1	1
	31	MIS1B	1	21
	32	MIS2	1	5
	26–27	ILLS	2	21
Central cluster (ILLC)	24–25	ILLC	2	5
Northern cluster (ILLN)	22	ILLN1	1	11
		ILLN2		4
	17	ILLN3	1	13
		ILLN4		21
	21	ILLN5	1	1
		ILLN6		10
	20	ILLN7	1	11
	19	ILLN8	1	17
	23	ILLN9	1	22
	18	ILLN10	1	20
Total Individuals			32	294

Sequence data collection

We used parallel tagged amplicon sequencing (Bybee *et al.* 2011; O'Neill *et al.* 2013) to cost-effectively sequence 23 anonymous nuclear (nDNA) loci and four mitochondrial (mtDNA) fragments from 34 individuals including 16 *P. streckeri*, 16 *P. illinoensis* and two *P. ornata* as out-groups. The nuclear loci in this study were designed for the chorus frog genus *Pseudacris* using a reduced representation library (RRL) approach described in Lemmon & Lemmon (2012). We included mtDNA from the following regions: cytochrome b (cytb; 707 bp), cytochrome oxidase I (COI; 710 bp), NADH dehydrogenase subunit 2 (ND2; 627 bp) and 16S ribosomal RNA (16S; 929 bp). Primer sequences and annealing temperatures are included in Table S2 (Supporting information). Amplification conditions and sequencing procedures are described in detail in Barrow *et al.* (2014a). Briefly, for each individual, the 23 nuclear loci and four mtDNA fragments were amplified in separate PCRs and purified with a magnetic bead wash protocol (Agencourt SprintPrep beads; Beckman Coulter, Inc.). For each individual, loci were pooled at equal concentrations and a library was prepared with a unique barcode adapter using a protocol modified from Meyer & Kircher (2010). All libraries for this study were pooled together with libraries from two other projects and sequenced in a single Illumina MiSeq run (150-bp paired end) at the FSU Biology Core Facility. Data processing was completed as in Barrow *et al.* (2014a). Briefly, we assembled reads for each individual using SEQMAN NGEN v. 4.1.2 (DNASTAR, Inc., Madison, WI, USA), sorted loci by aligning contigs to primer sequences, removed any loci that had lower than 10X coverage and phased alleles to haplotype by identifying single nucleotide polymorphisms (SNPs) in SEQMAN PRO v. 10.1.2 and using the paired read data to determine which bases were associated together in each allele. We constructed alignments for each locus using MUSCLE v. 3.8.31 (Edgar 2004) and visually inspected them in SEAVIEW v. 4.4.2 (Gouy *et al.* 2010).

Microsatellite data collection

We collected microsatellite data for 14 loci from 294 individuals (103 *P. streckeri*, 191 *P. illinoensis*). The microsatellite loci were recently developed for this species complex using the enrichment and sequencing protocols at Cornell University's Evolutionary Genetics Core Facility. We designed primers from the resulting 454 GS-FLX sequence data, screened them across a panel of individuals and designed multiplexes for PCR and genotyping. Details including multiplex compositions, reaction conditions and temperature profiles are

described in Barrow *et al.* (2014b). Fragment analysis was performed using an Applied Biosystems 3730 Genetic Analyzer at the FSU Biology Core Facility. Allele sizes were determined and binning was conducted using GENEIOUS v. 6.0.4 (created by Biomatters). We tested for the presence of scoring errors and null alleles using MICRO-CHECKER v. 2.2.3 (Van Oosterhout *et al.* 2004) and tested for genotypic linkage disequilibrium (LD) and departures from Hardy–Weinberg equilibrium (HWE) within sites using GENEPOP v. 4.2 (Raymond & Rousset 1995; Rousset 2008).

Mitochondrial phylogeny estimation

We used MRMODELTEST2 v. 2.3 (Nylander 2004) to determine appropriate models of nucleotide evolution for each locus using the Akaike information criterion (Table S3, Supporting information). Mitochondrial phylogeny estimation was completed using both maximum-likelihood and Bayesian approaches. We conducted a maximum-likelihood analysis of the concatenated mtDNA data set using the rapid hill-climbing algorithm in RAXML v. 7.7.8 (Stamatakis 2006). We partitioned the data set by gene and codon position given that different mitochondrial regions evolve at different rates and previous studies have demonstrated support for partitioning protein-coding loci by codon position (Nylander *et al.* 2004; Brandley *et al.* 2005). We used the GTR+G model of nucleotide substitution for each partition and conducted 1000 nonparametric bootstrap replicates. We also used Bayesian analysis implemented in BEAST v. 2.1.3 (Bouckaert *et al.* 2014) to estimate the mtDNA phylogeny from the partitioned data set. The clock models and trees were linked across partitions, and the site models specific to each gene fragment reported in Table S3 (Supporting information) were used. When initial runs failed to converge for all parameters, we also conducted an analysis with HKY substitution models for all gene fragments and found consistent topologies. Following the recommendations of Drummond & Bouckaert (2015), we conducted trial runs to test different clock models and tree priors. We found that a strict clock was most appropriate for our data set (the posterior distribution of the coefficient of variation had large probability mass near 0) and that an exponential coalescent tree prior was most suitable (the posterior distribution of the growth rate parameter did not include 0). We ran the full MCMC analysis for 100 million generations sampling every 10 000 generations. We examined the sampled parameter values in TRACER v. 1.5 (Rambaut & Drummond 2007) to assess convergence and found that after a burn-in period of 10%, stationarity was reached and the effective sample size (ESS) values exceeded 200. We used TREEANNOTATOR v. 2.1.2 (Drummond & Rambaut 2007) to visualize the maximum clade credibility (MCC) tree discarding the first 1000 trees as burn-in.

Species tree estimation

We used *BEAST v. 2.1.3 (Heled & Drummond 2010) to estimate a population tree for the species complex under a multispecies coalescent model using 23 nDNA loci. Implementing this framework requires assignment of individuals to operational taxonomic units (OTUs) of the tree. Our primary interest was to estimate the phylogenetic relationships among regions and between populations of *P. streckeri* and *P. illinoensis* (hereafter referred to as the region tree, containing 6 OTUs), but we also conducted analyses in which every sampled individual was an OTU (hereafter referred to as the nDNA tree, containing 32 OTUs) for comparison to the mtDNA phylogeny. For all analyses, we used both alleles for every individual to provide information about the coalescent history of each tip in the estimated tree. One assumption of the multispecies coalescent model is that there is no gene flow between taxa, which we are likely violating with individuals sampled from areas in close geographic proximity. Simulations have demonstrated that gene flow can influence species tree analyses resulting in overestimates of population sizes, underestimates of divergence times and low posterior probabilities (Leaché *et al.* 2014). For this analysis, we are only interested in tree topology and interpret our results with caution.

For the nDNA tree, we set every individual as an OTU and used locus-specific site models. In trial runs, we used the models of nucleotide substitution selected using MRMODELTEST2 (Table S3, Supporting information), and tested different clock models and tree priors. Initial runs failed to converge and suggested that some settings were too parameter-rich given this data set; therefore, we ran our full analyses choosing HKY models, strict clock models for all loci, a constant species tree population function and an exponential coalescent population tree prior. We conducted two independent runs with an MCMC length of two billion generations each sampling every 200 000 generations. We assessed convergence by examining the sampled distributions from both runs using TRACER v. 1.5 and comparing the MCC tree from each replicate to determine which nodes were strongly supported across runs. After discarding the first 50% of trees from each replicate as burn-in (after stationarity had been reached), we combined the runs using LOGCOMBINER v. 2.1.3 and constructed the MCC tree with TREEANNOTATOR v. 2.1.2.

For the region tree, we estimated the relationships among the six regions of interest in Table 1 – within

P. streckeri: central Texas, Central Great Plains and Arkansas River Valley; and within *P. illinoensis*: northern, central and southern clusters (Fig. 1). We chose these regions based on our biogeographic hypotheses, the disjunct nature of the range and the combined evidence from the mtDNA and nDNA trees (see Results) that these represented suitable groupings. Given our results from the nDNA tree, we verified that these region designations did not constrain genetically dissimilar individuals to a single population. We used HKY site models, a strict clock model, a constant species tree population size and a Yule model tree prior. We conducted one run with an MCMC length of one billion generations sampling every 100 000 generations and assessed convergence by examining ESS values and stationarity in TRACER v. 1.5. We constructed the MCC tree with TREEANNOTATOR v. 2.1.2 after discarding the first 2000 trees as burn-in.

Divergence time and demographic history

We used two approaches to estimate divergence times within this species complex. First, we used fossil calibrations to co-estimate a mtDNA gene phylogeny and divergence times in BEAST v. 2.1.3 with a larger family-level data set for Hylidae using sequences from GenBank (Table S4, Supporting information). These analyses were restricted to the 16S mtDNA gene given the availability of sequences for other hylid taxa, which were necessary for calibrating the tree. Taxon sampling was comparable to Smith *et al.* (2005) and Lemmon *et al.* (2007b). We used three external calibration points within Hylidae because there are no pre-Pleistocene *Pseudacris* fossils identified to species. The calibrations used are similar to those in Smith *et al.* (2005) and include (i) the root (minimum age 42 mya); (ii) the most recent common ancestor of the *Pseudacris–Acris* clade (at least 16 mya; based on an extinct *Acris barbouri* fossil described as the sister group to extant *Acris* species – Holman 2003); and (iii) the most recent common ancestor of North American *Hyla* (at least 34 mya; based on an extinct *Hyla swanstoni* fossil similar to *H. gratiosa* – Holman 2003). The other calibrations from Smith *et al.* (2005) were not used because we either did not recover the same nodes in our tree (e.g. *Hyla squirella* was not recovered as part of the *H. cinerea* clade) or because in our view the proper placement of these fossils was unclear based on the description from Holman (2003). We provide further justification for the fossil calibrations used in Data S1. We used lognormal priors for the calibration nodes, the HKY+I+G site model, a lognormal relaxed clock model and a calibrated Yule model tree prior. We ran the MCMC analysis for 100 million generations sampling every 10 000 generations and assessed convergence as above. We discarded the first 2000 trees as burn-in and constructed the MCC tree with TREEANNOTATOR.

Dating analyses based on a single gene tree can be problematic and overestimate divergence times (Edwards & Beerli 2000; Arbogast *et al.* 2002; McCormack *et al.* 2010); therefore, we also implemented a multilocus approach using the isolation with migration model in IMa2 (Hey & Nielsen 2007; Hey 2010). This approach estimates the timing of divergence from an ancestral population (τ), as well as the effective population size (θ) and migration rate (m) for each population. The method assumes population history can reasonably be described by the isolation with migration model, meaning there is no structure within populations and no gene flow from unsampled populations. We conducted separate analyses for the mtDNA and nDNA data sets, using the mtDNA phylogeny and the * BEAST population tree to determine the starting trees, respectively. To reduce the number of parameters estimated, we conducted two sets of two-population models for the divergence times of interest: (i) between the Texas clade and the rest of the species complex, hereafter TEX; and (ii) after removing the Texas clade, between *P. illinoensis* and the remaining *P. streckeri*, hereafter ILL. We experimented with prior settings and heating schemes following the recommendations of the IMa2 documentation before choosing the following upper prior bounds: mtDNA TEX ($\theta = 80$, $m = 0.5$, $\tau = 40$); mtDNA ILL ($\theta = 50$, $m = 1$, $\tau = 8$); nDNA TEX ($\theta = 4$, $m = 5$, $\tau = 2$); nDNA ILL ($\theta = 0.5$, $m = 100$, $\tau = 0.5$); and geometric heating settings: mtDNA (20 chains, a = 0.96, b = 0.9); nDNA (100 chains, a = 0.99, b = 0.9). We conducted two separate runs for each analysis to ensure convergence in addition to examining effective sample sizes and trend plots of the parameters. We stopped the burn-in phase of each run and began collecting samples once there were no visible trends in the plots, sampling 300 000 genealogies for the mtDNA analyses and at least 60 000 for the nDNA analyses.

We explored past population dynamics using extended Bayesian skyline plots (EBSP) of multilocus sequence data sets in BEAST v. 1.8.2 (Drummond *et al.* 2005; Heled & Drummond 2008). This approach can be used to detect whether population size remained constant or changed in the past, and reconstructs the signal of population bottlenecks or population growth provided there is sufficient data (Heled & Drummond 2008). We conducted analyses with mtDNA only and combined mtDNA and nDNA, subsampling the data sets to evaluate demographic changes for each lineage with sufficient samples. Additional details are provided in Data S1.

Characterizing microsatellite variation

We assessed the level of variation for *P. streckeri* and *P. illinoensis* across 14 microsatellite loci using genetic diversity estimates (number of alleles, heterozygosities and fixation indices) in GENALEX v. 6.5 (Peakall & Smouse 2012). We also estimated allelic richness, which accounts for differences in sample size, using the R package DIVERSITY v. 1.9.73 (Keenan *et al.* 2013). Because small sample sizes are problematic for some diversity estimates, we analysed two separate data sets. The first included all individuals and considered each sample location, or unique set of geographic coordinates, as a population (294 individuals, 50 locations), and the second combined individuals sampled within 10 km (unless they were separated by a potential barrier such as the Arkansas River) and excluded sites with fewer than five individuals (280 individuals, 23 sites; Table 1). For this study, because we are addressing questions on a broad geographic scale and the results were qualitatively similar between data sets, we report the results from the combined data set to avoid small sample sizes where possible. Although this distance is greater than the expected dispersal in a single generation for these taxa (maximum dispersal from natal ponds has been measured at 0.9 km in *P. illinoensis*; Tucker & Philipp 1995), we examined pairwise differentiation (R_{st} and F_{st}) and used Bayesian clustering analyses (Pritchard *et al.* 2000) to verify that combined individuals were not genetically distinct (details in Data S1).

We performed an analysis of molecular variance (AMOVA) to examine the hierarchical partitioning of genetic variation across populations, regions and species using ARLEQUIN v. 3.5 (Excoffier & Lischer 2010). We conducted two separate AMOVAs: the first to determine the amount of variance among species, among populations within species and among individuals within populations, and the second to determine the amount of variance among regions, among populations within regions and among individuals within populations. To investigate patterns of isolation by distance (IBD) in our data set, we conducted Mantel tests in ARLEQUIN v. 3.5 (Excoffier & Lischer 2010). We tested for a significant correlation between pairwise geographic distances (coordinates transformed into distances using the GEOGRAPHIC DISTANCE MATRIX GENERATOR v. 1.2.3; Ersts Internet) and genetic distances (using R_{st}, an analog to F_{st} for microsatellites based on allele size differences; Slatkin 1995) between populations. We initially analysed the species complex across its range and then analysed *P. streckeri* and *P. illinoensis* separately to determine whether a pattern of IBD was present within each taxon.

To visually depict the spatial patterns of microsatellite genetic variation across this species complex, we conducted a principal coordinates analysis (PCoA) using GENALEX v. 6.5 (Peakall & Smouse 2012). We calculated pairwise, individual-by-individual codominant genetic distances and used the standardized covariance matrix option. Because we were interested in the variation attributed to both species and geographic regions, but sample sizes across regions were uneven, we subsampled the northern cluster of *P. illinoensis* for this analysis. We analysed 228 individuals comprised of 103 *P. streckeri* and 125 *P. illinoensis* and report the first three PCoA axes with 50% bivariate normal density ellipses.

Bayesian model comparison

We designed migration models for comparison using MIGRATE-N v. 3.6.4 (Beerli & Felsenstein 2001; Beerli 2006; Beerli & Palczewski 2010) to make inferences regarding previous biogeographic hypotheses in this species complex and investigate genetic structure within *P. illinoensis*. MIGRATE-N estimates effective population size ($\theta = 4N_e\mu$) and migration rates ($M = m/\mu$) for multiple populations in a coalescent framework. The method assumes an n-island model in which genetic material is exchanged only through migration and not population divergence. Marginal likelihoods can be used to compare models that differ in the number of migration parameters to test the directionality of gene flow and connectivity of populations, and models that combine populations can be compared to those that divide populations in order to determine whether individuals come from the same randomly mating population. We used the data from 14 microsatellite loci to compare 24 different models that addressed three main hypotheses (Fig. 2). First, we hypothesized that Texas represented a refugium during glacial periods, which has been inferred previously for other taxa (Waltari *et al.* 2007 and references therein). Because a refugial population would have contributed alleles to the founded populations, and MIGRATE-N estimates a long-term average of gene flow, this method can be used to test predictions about refugial structure and migration direction from putative refugia (Carstens *et al.* 2013). We constructed models with unidirectional migration routes from Texas (e.g. Fig. 2a) as well as competing models with refugia in other regions (e.g. Fig. 2b,c) to determine whether the inferred directionality of gene flow was consistent with the Texas refugium hypothesis. If a model with migration rates from Texas to other regions has the highest probability given the data, we interpret this as support for the Texas refugium hypothesis. Second, we tested the hypothesis that *P. illinoensis* is derived from

1 Texas was a refugium from which populations expanded northward into other regions.
2 *P. illinoensis* is derived from *P. streckeri* that expanded through the Arkansas River Valley.
3 There is detectable genetic structure within *P. illinoensis* consistent with the disjunct range.

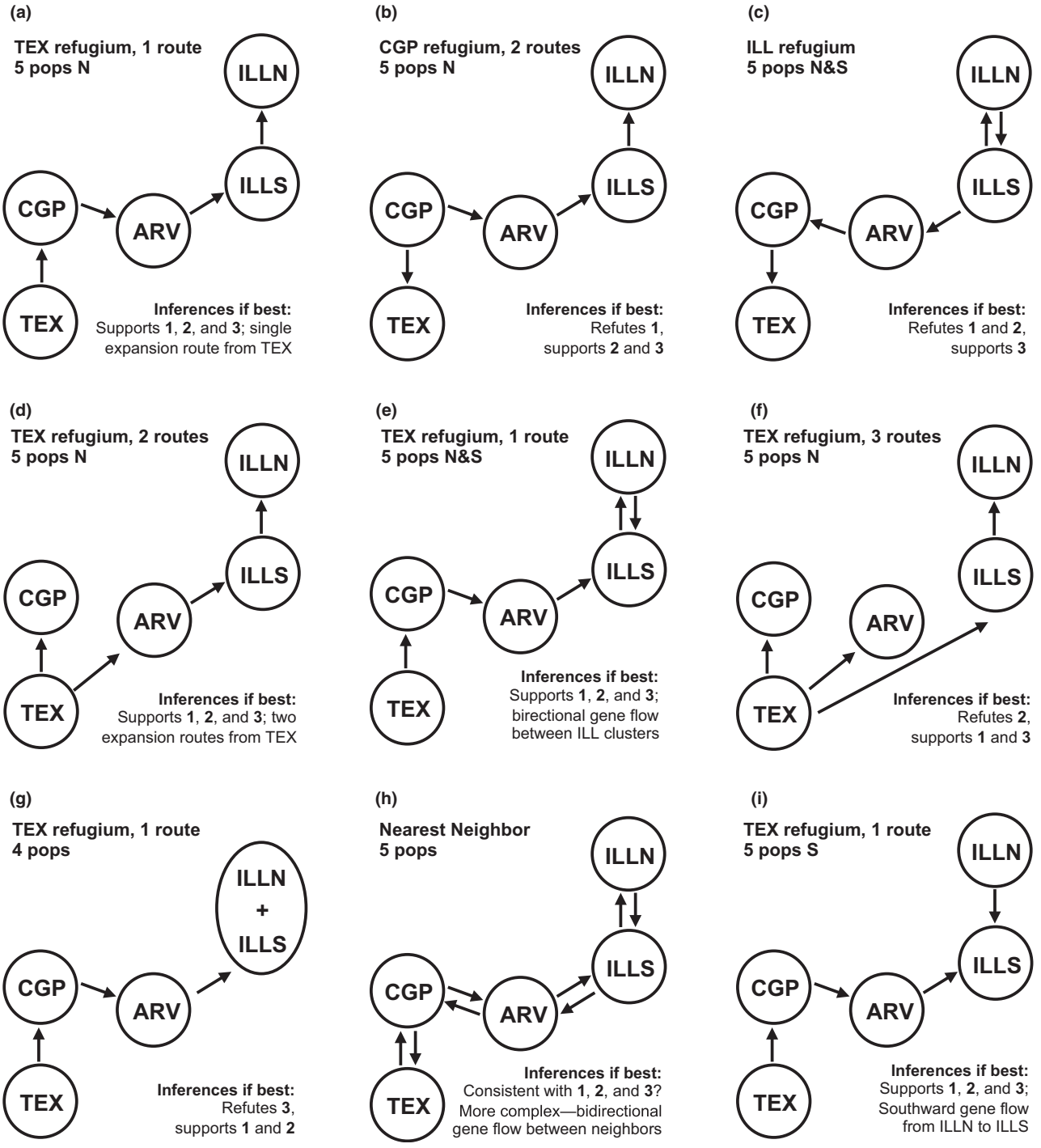

Fig. 2 Example models compared in MIGRATE-N to make inferences regarding the hypotheses described (1–3). Each circle represents an effective population size parameter, and each arrow represents a migration parameter. Region labels as in Table 1. Note that only a subset of the models tested is illustrated; all 24 tested models are shown in Data S1.

P. streckeri populations that expanded through the Arkansas River Valley (ARV; Axtell & Haskell 1977) by constructing models that include unidirectional gene flow from the ARV to *P. illinoensis* (e.g. Fig. 2d,e) and competing models that exclude this parameter (e.g. Fig. 2f). Third, we investigated the structure and direction of gene flow within *P. illinoensis* by comparing models with four populations (southern and northern *P. illinoensis* populations combined; e.g. Fig. 2g) to models with five populations (three *P. streckeri*, southern *P. illinoensis* and northern *P. illinoensis*; e.g. Fig. 2h,i). We did not include the central *P. illinoensis* population because of low sample size. Although Smith (1957) hypothesized that the range of this species complex was fragmented fairly recently (during the Xerothermic period, approx. 4000 ya), we predict restricted gene flow associated with the disjunct range will result in genetic structure within *P. illinoensis*, such that five-population models will be better supported.

All models were run on the FSU High Performance Computing Cluster and were then compared against all other models using marginal likelihoods approximated by thermodynamic integration with Bézier approximation (as in Beerli & Palczewski 2010). We chose a representative population from a single site for each region, with sample size ≥16 individuals. We used Bayesian inference, a Brownian motion microsatellite model, allowed mutation rates to vary among loci and experimented with prior settings with a full model (all parameters estimated) before choosing uniform priors for θ (Min. = 0, Max. = 200, Delta = 20) and M (Min. = 0, Max. = 100, Delta = 10). We conducted 20 replicates for each model with a static heating scheme using four chains, discarded 40 000 trees as burn-in and recorded 40 000 steps with an increment of 100 (resulting in 80 million samples). To assess convergence, we examined ESS values (much >1000) and the posterior distributions of the parameters to determine whether they were single peaks with smooth curves. Bayes factors (BF) were calculated as a ratio of the marginal likelihoods to calculate model probabilities.

Results

Sequence data obtained

The Illumina MiSeq run produced 2 058 514 reads that were sorted by individual barcode for the 34 individuals in this study with an average of 60 545 ± 14 067 (SD) reads per individual. For the nDNA loci, full sequence alignments were recovered for 99.87% (781 of 782) of the targeted amplicons. Of these alignments, we obtained phased haplotypes for 98.72% (771 of 781). For the mtDNA loci, full sequence alignments were recovered for 96.3% (131 of 136) of the targeted amplicons. Within the in-group, individuals were heterozygous for an average of 28.33% of their loci. On average, *Pseudacris streckeri* individuals were heterozygous for a higher proportion of loci compared to *Pseudacris illinoensis* (37.23% versus 18.75%). Sequence data generated and files from the analyses are available on Dryad (doi:10.5061/dryad.h2082).

We analysed a total of 13 893 bp that included 357 (2.57%) variable sites and 249 (1.79%) parsimony-informative sites within the in-group (Table S3, Supporting information). The four mtDNA loci totalled 2769 bp and included 202 (7.30%) variable sites and 145 (5.24%) informative sites, while the 23 nDNA loci totalled 11 124 bp and included 155 (1.39%) variable sites and 104 (0.93%) informative sites. On average, each mtDNA locus contained 51 variable sites (range: 27–71) and 36 parsimony-informative sites (range: 4–67). On average, each nDNA locus contained 7 variable sites (range: 2–21) and 5 parsimony-informative sites (range: 0–15).

Phylogenetic relationships

Although *P. streckeri* and *P. illinoensis* were not reciprocally monophyletic (Fig. 3a–b), we found two strongly supported groups (RAXML bootstrap values = 100 and BEAST posterior probabilities = 1) within this species complex for both the mtDNA and nDNA data sets. One of these groups consisted of central Texas *P. streckeri* individuals, while the other included the remaining *P. streckeri* and *P. illinoensis* populations. The average sequence divergence (calculated in MEGA5 using the maximum composite likelihood model; Tamura *et al*. 2011) between the Texas clade and the rest of the species complex was 5.99% for mtDNA and 0.54% for nDNA. Within *P. illinoensis*, the average sequence divergence among the disjunct clusters was 0.09% for mtDNA and 0.11% for nDNA. The mtDNA tree included monophyletic Central Great Plains (CGP) and Arkansas River Valley (ARV) *P. streckeri* groups, but the ARV group was nested within *P. illinoensis*. Overall, the nDNA tree had very few well-supported branches, likely due to the limited number of variable sites in these loci. One strongly supported difference between the mtDNA and nDNA trees was the placement of the Bosque County, TX, individual with the central Texas clade in the nDNA tree, while its position in the mtDNA tree suggested mitochondrial introgression. The *BEAST population tree indicated that *P. streckeri* is paraphyletic with respect to *P. illinoensis* and again provided strong support for a highly divergent TEX clade (Fig. 3c). The population tree also suggested that *P. illinoensis* is a monophyletic group nested within *P. streckeri*, but support for monophyly was moderate (posterior probability = 0.84).

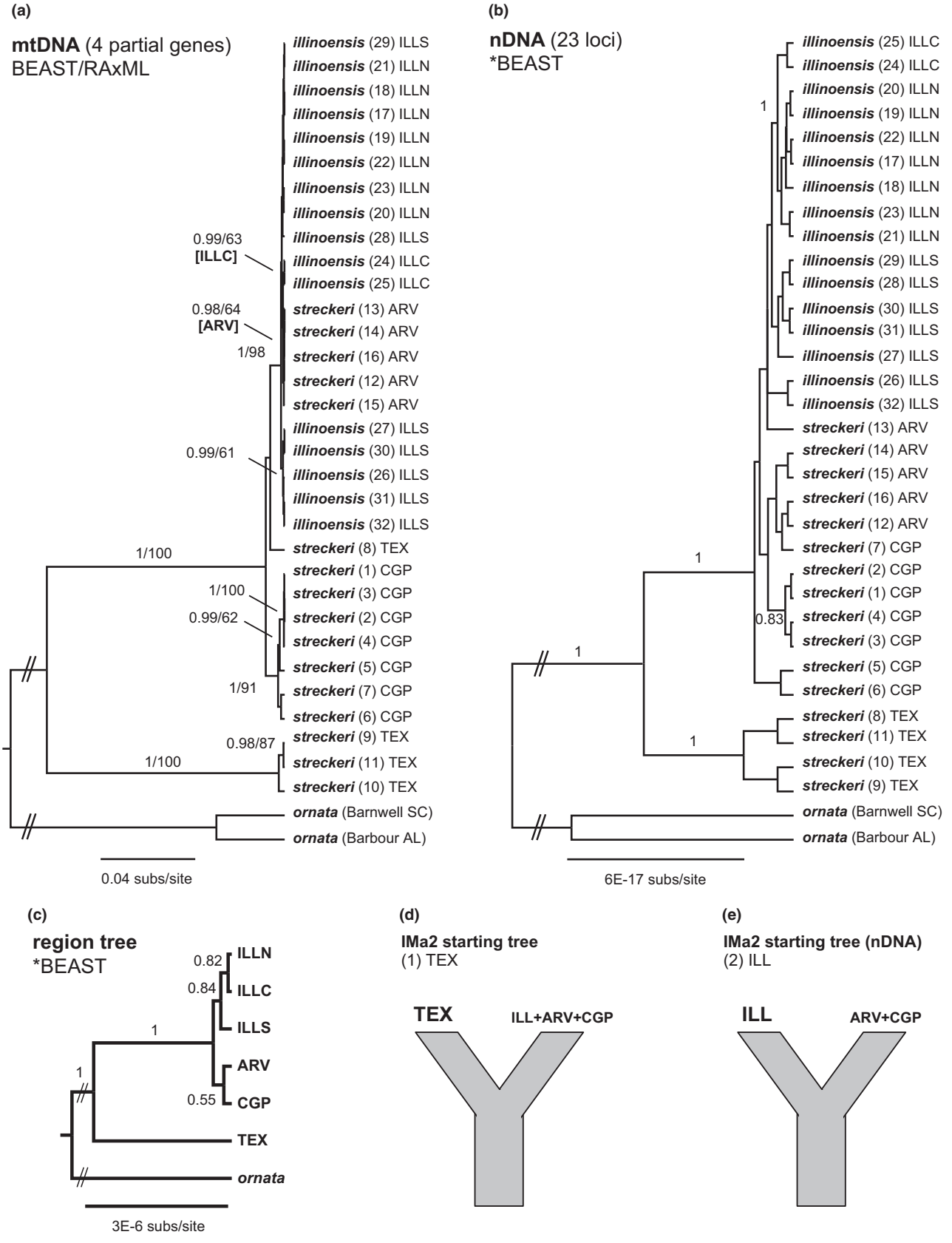

Fig. 3 Results from phylogenetic analyses (a–c) and starting trees for IMa2 (d–e). (a) Topology from BEAST mtDNA analysis with posterior probabilities shown to the left of the slash and RAxML bootstrap support values shown to the right. (b, c) Posterior probabilities >50 are shown. Branch lengths are in substitutions per site. Numbers in tip labels correspond to Seq ID in Table 1 and Fig. 1. Region labels as in Table 1. Note that (e) depicts the starting tree for the nDNA analysis only; the mtDNA starting tree differs slightly (ARV combined with ILL).

Divergence time and demographic history

The nodes within this species complex for which we were interested in estimating divergence times had strong support in the 16S mtDNA BEAST analysis (posterior probability = 1; Fig. S1, Supporting information). The divergence time between the central Texas clade and the rest of the species complex was estimated at 4.126 mya (95% highest posterior density, hereafter HPD: 1.83–7.008). The divergence time between the non-Texas *P. streckeri* and *P. illinoensis* (including the Arkansas River Valley *P. streckeri* individuals) was estimated at 1.482 mya (95% HPD: 0.576–2.938). The parameter estimates from IMa2 were similar across replicates for the mtDNA and nDNA TEX analyses. The nDNA ILL analysis did not converge perhaps because of the low number of variable sites in these loci. The posterior densities of the migration rate parameters and some of the divergence time parameters did not reach low limits near the upper prior boundaries; thus, results should be treated with caution (Table 2). The marginal posterior probability of the divergence time between TEX and the rest of the species complex was 18.82 (95% HPD: 10.3–38.82) for mtDNA and 0.593 (95% HPD: 0.303–1.987) for nDNA. If we apply mutation rates estimated for other amphibians (details in Data S1), conversion into years suggests that based on mtDNA, the Texas clade diverged from the rest of species complex approximately 2.644 (95% HPD: 1.447–5.453) mya and *P. illinoensis* diverged from the non-Texas *P. streckeri* approximately 0.35 (95% HPD: 0.1826–1.123) mya. These date estimates were generally younger than the BEAST estimates using 16S mtDNA, but the intervals overlap. Based on nDNA, the divergence time estimate between the Texas clade and the rest of the species complex was approximately 1.004 (95% HPD: 0.513–3.366) mya. Without mutation rate information for the anonymous nuclear loci in this study or genomewide estimates for anurans, we based these calculations on other nuclear genes that may have very different rates (see Data S1); thus, these results should be interpreted carefully. The EBSP results indicated that we could not reject constant population size in the past for any of the lineages examined (Fig. S2, Supporting information).

Population genetic structure

We observed a total of 195 alleles across 14 microsatellite loci (9–23 alleles per locus) and our final data set contained <0.559% missing data. We found no evidence of scoring errors, but there was evidence of null alleles for five loci (Pst12856, Pst3261, Pst14601, Pst5995 and Pst1854) in three or fewer sites for each locus. Three locus by site combinations significantly deviated from HWE after a Bonferroni correction (Pst3261 and Pst14601 for TEX1, and Pst5995 for ILLN8). One locus pair showed significant linkage disequilibrium for a single site (Pst11102 and Pst1854 for MIS1). Because these patterns were not consistent across sites, we did not exclude any loci from the following analyses.

For *P. streckeri*, the average number of alleles per population ranged from 2.429 to 10, allelic richness ranged from 2.25 to 5.25, observed heterozygosity ranged from 0.443 to 0.781, expected heterozygosity ranged from 0.508 to 0.843 and the fixation index ranged from −0.124 to 0.133 (Table S5, Supporting information). For *P. illinoensis*, the average number of alleles per population ranged from 2.571 to 5.643, allelic richness ranged from 2.23 to 3.66, observed heterozygosity ranged from 0.381 to 0.694, expected heterozygosity ranged from 0.410 to 0.689 and the fixation index ranged from −0.206 to 0.037. The higher average diversity estimates for *P. streckeri* (Table S5, Supporting information) were largely driven by the TEX1 population, which also had 42 private alleles (all other populations had 0–4 private alleles). Within *P. illinoensis*, the population from Clay County, Arkansas (ARK6), had the lowest average number of alleles and lowest heterozygosity estimates. There was a trend of decreasing allelic richness as geographic distance from the TEX1 population increased, consistent with a putative Texas refugium (Fig. S3, Supporting information). Average pairwise differentiation (R_{st}) across the species complex was 0.254 ± 0.140 (see Table S6, Supporting information for pairwise R_{st} and F_{st} values). The AMOVAs indicated significant genetic structure among species ($F_{CT} = 0.179$, $P < 0.0001$) and among regions ($F_{CT} = 0.254$, $P < 0.0001$; Table 3). The Mantel test across the entire range of the species complex indicated a significant correlation between geographic distance and genetic distance consistent with a pattern of isolation by distance (correlation coefficient = 0.603, $P < 0.0001$; Fig. S4, Supporting information). Within each species, Mantel tests also indicated a significant pattern of isolation by distance (*P. streckeri*: correlation coefficient = 0.490, $P = 0.007$; *P. illinoensis*: correlation coefficient = 0.643, $P < 0.0001$). The first three PCoA axes accounted for 25.5% of the genetic

Table 2 Parameter estimates from IMa2 including divergence time (τ), effective population size (θ) and migration rate (*m*); and divergence time estimates in years from IMa2 and BEAST

	mtDNA TEX	mtDNA ILL	nDNA TEX	nDNA ILL
IMa2 parameter estimates				
θ_0	10.44 (6.6–15.88)	2.825 (1.175–5.775)	0.37 (0.230–0.546)	0.0178 (0.00725–0.0458)
θ_1	5.72 (1.16–30.52*)	5.675 (2.525–12.12)	1.086 (0.642–1.926)	0.0523 (0.0203–0.134)
$m_{0>1}$	0.00025 (0–0.0523*)	0.0005 (0–0.4035*)	0.4475 (0.0225–1.657*)	99.95 (24.85–99.95*)
$m_{1>0}$	0.00025 (0–0.0828*)	0.0005 (0–0.3225*)	1.363 (0.303–2.658*)	32.05 (0–91.85*)
τ	18.82 (10.3–38.82)	2.492 (1.30–7.996*)	0.593 (0.303–1.987)	0.0738 (0.0528–0.5*)
Divergence time estimates in millions of years				
IMa2	2.644 (1.447–5.453)	0.3500 (0.1826–1.123)	1.004 (0.513–3.366)	Failed to converge
BEAST	4.126 (1.83–7.008)	1.482 (0.576–2.938)	n/a	

95% highest posterior density intervals are shown in parentheses. TEX models: 1 = TEX, 0 = rest of the species complex (Fig. 3d). ILL models: 0 = ILL, 1 = non-TEX *Pseudacris streckeri* (Fig. 3e).
*The posterior density did not reach low limits near the upper limit of the prior.

Table 3 AMOVA results across species (samples divided across two species, *Pseudacris streckeri* and *Pseudacris illinoensis*) and regions (samples divided across six regions, as in Table 1)

Source of variation	d.f.	Sum of Squares	Variance components		Percentage of variation	Fixation indices		*P*-value
Among species	1	6769.191	24.24618	Va	17.85	0.17850	F_{CT}	<0.0001
Among populations within species	21	12625.908	21.38932	Vb	15.75	0.19156	F_{SC}	<0.0001
Within populations	537	48436.831	90.19894	Vc	66.40	0.33596	F_{ST}	<0.0001
Total	559	67831.930	135.83444					
Among regions	5	14757.938	33.31044	Va	25.39	0.25394	F_{CT}	<0.0001
Among populations within regions	17	4637.161	7.66368	Vb	5.84	0.07831	F_{SC}	<0.0001
Within populations	537	48436.831	90.19894	Vc	68.76	0.31237	F_{ST}	<0.0001
Total	559	67831.930	131.17306					

variation in the species complex (Fig. 4). The first axis of variation separated *P. streckeri* and *P. illinoensis* with substantial overlap of neighbouring regions. The second axis separated the southern *P. illinoensis* cluster from the northern *P. illinoensis* cluster, and the third axis separated the central Texas region from all other regions.

Bayesian model comparison

The best-supported model tested in MIGRATE-N was a five-population model with a Texas refugium, two migration routes from Texas and northward migration from the southern *P. illinoensis* cluster to the northern cluster (Table 4; Fig. 5). This model had very strong support with a model probability>0.999, and the second-ranked model with the remaining model probability represented the same scenario but with one additional parameter (southward migration from the northern *P. illinoensis* cluster to the southern cluster). The remaining models have effectively no probability given the data, indicating that of the models tested, there was overwhelming support for the best model. This selected model (i) supported the gene flow predictions of the Texas refugium hypothesis, (ii) suggested that populations expanded northward from Texas along multiple routes, (iii) provided support for Axtell & Haskell's (1977) hypothesis that *P. illinoensis* was founded from populations that expanded through the ARV and (iv) suggested that the northern and southern clusters of *P. illinoensis* are genetically distinct. The relatively high migration rate parameter estimate between the northern and southern *P. illinoensis* clusters (mode = 5.50, 95% posterior = 1.60–12.2) compared to all other migration parameter estimates (modes ≤1.03, 95% posterior including 0) was consistent with a relatively recent fragmentation of the *P. illinoensis* range. The effective number of migrants per generation ($4N_em$, calculated as the product of the θ and M modes) was ~0.369 between the northern and southern *P. illinoensis* clusters.

Discussion

The suite of genetic markers we targeted and the range of analyses implemented enabled us to investigate the biogeography of this fragmented species complex across

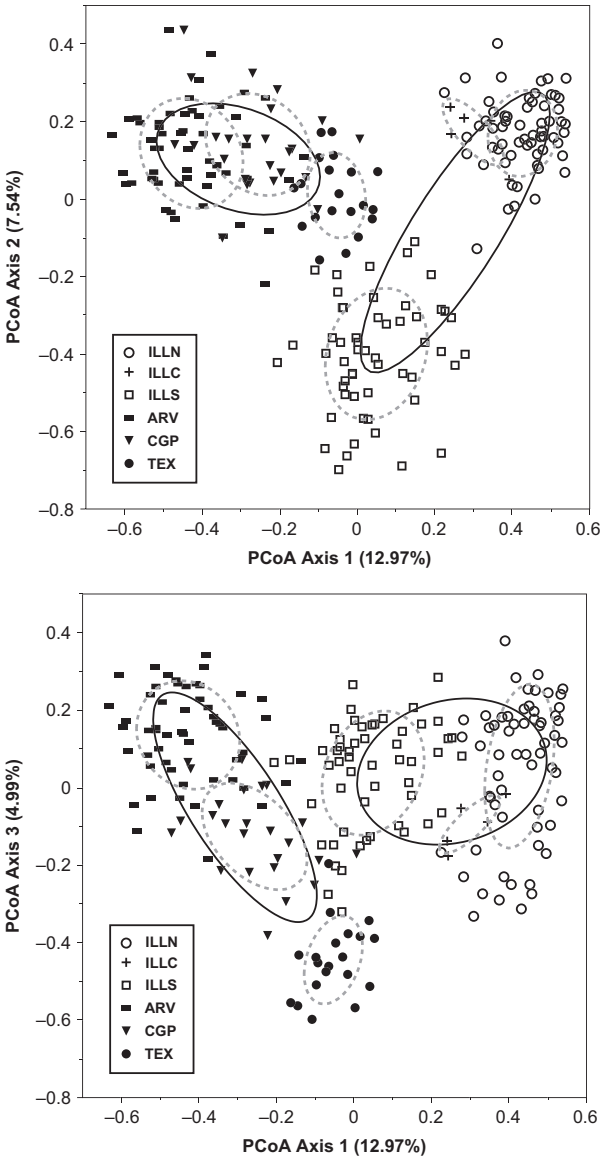

Fig. 4 Results from principal coordinates analysis (PCoA) depicting genetic variation across this species complex. Ellipses are 50% bivariate normal density ellipses, within which 50% of the points are expected to be contained assuming a bivariate normal distribution (solid = species, dotted = region).

different timescales (from ~4 mya to the present). Phylogenetic analysis of mitochondrial and nuclear sequence data allowed estimation of the evolutionary relationships both between and within *Pseudacris streckeri* and *Pseudacris illinoensis*, and faster-evolving microsatellites depicted contemporary genetic structure at a finer resolution. The model-testing framework we implemented provided us with a more complete picture of the processes that have influenced the fragmented range of these taxa. Through comparison of carefully designed population models, we simultaneously provided evidence for the location of a glacial refugium, the direction of migration between populations and the presence of substructure within a species of conservation concern.

Evolutionary history of the Pseudacris streckeri–Pseudacris illinoensis species complex

Our findings from mtDNA, nuclear sequence and microsatellite loci suggest that environmental changes associated with climate have influenced this species complex on historical and recent timescales. First, the central Texas samples contain higher microsatellite diversity and sequence divergence from the remaining *P. streckeri* and *P. illinoensis* populations. Taken together with the trend of decreasing allelic richness as distance from Texas increases and the best-supported TEX 2-route model in Migrate-n, we find support for the biogeographic scenario in which Texas represented a glacial refugium and the species range expanded. Although our divergence time estimates are uncertain, results from mtDNA (BEAST and IMa2) indicate that the TEX clade diverged from the rest of the species complex during the Early Pleistocene (0.781–2.588 mya; Cohen *et al.* 2013) or much earlier. Interestingly, our samples from central Texas also lie within the Edwards Plateau, the eastern edge of which is typically called Texas Hill Country. The Edwards Plateau is an important ecological region with unique vegetation (Van Auken *et al.* 1979; Fowler & Dunlap 1986) and a number of endemic cave invertebrates, fishes and salamanders (Culver & Sket 2000; Culver *et al.* 2000). Biogeographic analyses of the mammal, reptile, amphibian and bird fauna in the region have suggested that the Edwards Plateau may act as a transition zone or barrier to dispersal for terrestrial vertebrates (Blair 1950; Gehlbach 1991; Goetze 1995). Future genetic studies of *P. streckeri* that include sampling from eastern and northern Texas may better determine the degree to which the Edwards Plateau samples are isolated or unique. The decisively supported TEX 2-route model in MIGRATE-N indicates that populations expanded from Texas along more than one route, which is plausible assuming a gradual change in climate and environment across the region (Nordt *et al.* 1994; Cooke *et al.* 2003).

Second, our results are consistent with the idea that *P. illinoensis* was derived from *P. streckeri* on a more recent timescale. We base this conclusion first on the low amount of sequence divergence between the non-Texas *P. streckeri* and *P. illinoensis* resulting in short branches in both the mtDNA and nDNA trees. We also corroborate the findings of Moriarty & Cannatella (2004) and Lemmon *et al.* (2007a) that *P. streckeri* is paraphyletic with respect to *P. illinoensis*. This pattern is

Table 4 Results from model comparisons in Migrate-n, listed from best model to worst. Model descriptions as in Fig. 2. The number of parameters for each model, Bézier approximation scores of log marginal likelihoods (l mL), log Bayes factors (LBF) and model probabilities are shown. LBF values <−2 indicate strong preference for the top model (Kass & Raftery 1995)

Model description	Parameters	Bézier l mL	LBF	Probability
TEX refugium, 2 routes, 5 pops N	9 (5 θ, 4 M)	−10696.64	0	0.99977
TEX refugium, 2 routes, 5 pops N&S	10 (5 θ, 5 M)	−10705.03	−16.78	0.00023
ILL refugium, 4 pops	7 (4 θ, 3 M)	−10971.66	−550.04	<0.00001
ILL refugium, 5 pops S	9 (5 θ, 4 M)	−11514.39	−1635.50	<0.00001
TEX refugium, 1 route, 4 pops	7 (4 θ, 3 M)	−11883.12	−2372.96	<0.00001
ILL refugium, 5 pops N	9 (5 θ, 4 M)	−11919.50	−2445.72	<0.00001
TEX refugium, 3 routes, 4 pops	7 (4 θ, 3 M)	−12144.62	−2895.96	<0.00001
TEX refugium, 2 routes, 4 pops	7 (4 θ, 3 M)	−12171.00	−2948.72	<0.00001
TEX refugium, 3 routes, 5 pops N	9 (5 θ, 4 M)	−12714.98	−4036.68	<0.00001
ILL refugium, 5 pops N&S	10 (5 θ, 5 M)	−14337.50	−7281.72	<0.00001
CGP refugium, 2 routes, 4 pops	7 (4 θ, 3 M)	−17598.64	−13804.00	<0.00001
TEX refugium, 1 route, 5 pops N&S	10 (5 θ, 5 M)	−19503.73	−17614.18	<0.00001
TEX refugium, 3 routes, 5 pops N&S	10 (5 θ, 5 M)	−20868.28	−20343.28	<0.00001
TEX refugium, 1 route, 5 pops N	9 (5 θ, 4 M)	−26436.46	−31479.64	<0.00001
CGP refugium, 2 routes, 5 pops N	9 (5 θ, 4 M)	−31235.57	−41077.86	<0.00001
Nearest neighbour, 4 pops	10 (4 θ, 6 M)	−32577.76	−43762.24	<0.00001
CGP refugium, 2 routes, 5 pops N&S	10 (5 θ, 5 M)	−37350.43	−53307.58	<0.00001
Nearest neighbour, 5 pops	13 (5 θ, 8 M)	−64917.70	−108442.12	<0.00001
Full Model, 4 pops	16 (4 θ, 12 M)	−104370.33	−187347.38	<0.00001
TEX refugium, 1 route, 5 pops S	9 (5 θ, 4 M)	−146022.89	−270652.50	<0.00001
CGP refugium, 2 routes, 5 pops S	9 (5 θ, 4 M)	−182532.56	−343671.84	<0.00001
Full Model, 5 pops	25 (5 θ, 20 M)	−203383.47	−385373.66	<0.00001
TEX refugium, 2 routes, 5 pops S	9 (5 θ, 4 M)	−216233.59	−411073.90	<0.00001
TEX refugium, 3 routes, 5 pops S	9 (5 θ, 4 M)	−230621.54	−439849.80	<0.00001

TEX = central Texas, CGP = Central Great Plains, ILL = Illinois; N&S = bidirectional gene flow between northern and southern *Pseudacris illinoensis* clusters, N = northward gene flow only, S = southward gene flow only.

consistent with the scenario put forth by Smith (1957), in which a wide-ranging ancestor experienced range fragmentation resulting in the disjunct *P. streckeri* and *P. illinoensis* range. Our results could not substantiate whether the timing of this divergence is consistent with the Xerothermic period (approx. 4000 ya). The results from the BEAST and IMa2 analyses suggest that the mtDNA lineages diverged sometime between 0.1826 and 2.938 mya, but the nDNA ILL analyses never converged presumably because of the limited variation in the loci. Our best-supported model does provide evidence for a more detailed geographic scenario in which populations dispersed through the Arkansas River Valley, as proposed by Axtell & Haskell (1977). Although few sequence differences have accumulated, the faster-evolving microsatellite loci demonstrate genetic variation across the fragmented range of this species complex, including sufficient signal to differentiate the northern and southern clusters within *P. illinoensis* in a coalescent framework. The signal of isolation by distance both within species and across the whole range is not surprising given the probable limited dispersal ability of a small terrestrial anuran, in addition to the apparent habitat specificity of *P. illinoensis* (Brown *et al.* 1972; Brown 1978).

Conservation implications for the Illinois chorus frog

Concerns for the persistence of *P. illinoensis* populations include a paucity of suitable habitat, small population sizes and the ephemeral nature of breeding ponds that are susceptible to variable weather conditions (Brown & Rose 1988; Trauth *et al.* 2006). Our findings provide an evolutionary context for future studies and conservation efforts for this taxon. It seems clear that the isolation of *P. illinoensis* from *P. streckeri* occurred recently. Although there is only moderate support for monophyly from multilocus sequence data, the faster-evolving microsatellites indicate genetic differences have already accumulated. Our results can be used to evaluate criteria for defining conservation units (Moritz 1994; Mills & Allendorf 1996; Waples & Gaggiotti 2006; see Dufresnes *et al.* 2013 for an empirical example). Moritz (1994) suggested that management units should be defined as populations with significant divergence at nuclear or mitochondrial loci, and we find that

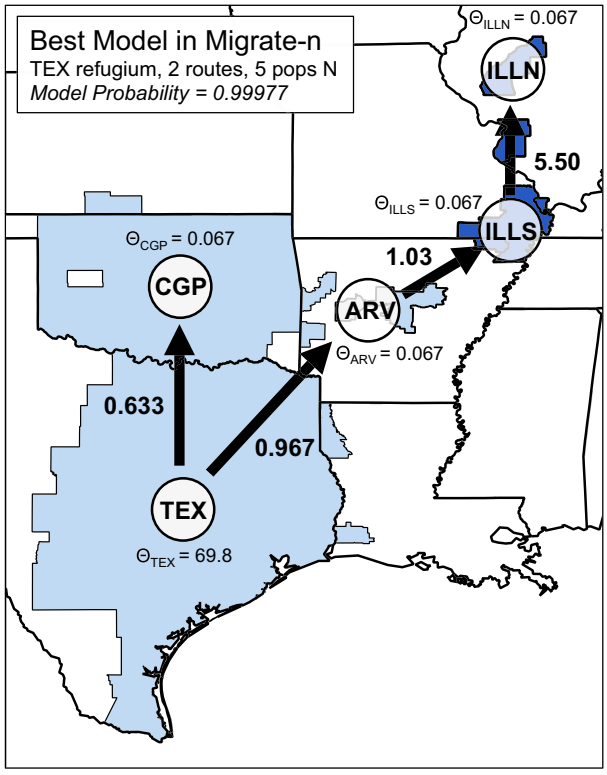

Fig. 5 Best model tested in MIGRATE-N depicted on species range map. The mode of each parameter estimate for effective population size (θ) and migration rate (M, bold text with arrows) is shown.

P. illinoensis and the disjunct clusters within this taxon are differentiated at nuclear microsatellites. Furthermore, under the evolutionary population concept of Waples & Gaggiotti (2006), we find that the northern and southern clusters within *P. illinoensis* meet even the most stringent criteria for defining units important for conservation. In addition to rejecting models of panmixia within *P. illinoensis*, the effective number of migrants estimated (~0.369 between northern and southern *P. illinoensis*) was well below the stringent value of $N_em = 1$, which is the suggested lower limit for maintaining connectivity in population management (Mills & Allendorf 1996). These disjunct clusters are clearly genetically distinct and can be considered separate management units. We did not include the central *P. illinoensis* cluster in these analyses because of low sample size, although other results (Fig. 4) indicate these individuals are genetically similar to the northern cluster.

The allopatric distribution of *P. illinoensis*, lack of suitable intermediate habitat and the evidence that the nearest populations (Clay County, Arkansas) to *P. streckeri* are declining (Trauth *et al.* 2006) underscore the importance of preserving these populations. Here, we outline topics that deserve further study, both to address taxonomy and inform management efforts. First, additional genetic sampling of *P. streckeri* in Texas and surrounding areas is warranted to determine whether other lineages or management units should be recognized, and whether geographic range boundaries need to be redefined. The application of species delimitation methods (e.g. Yang & Rannala 2014) with more complete geographic sampling across this region may help resolve the taxonomic issues in this species complex. Behavioural studies that measure male acoustic signals and test female preferences between multiple populations of *P. streckeri* and *P. illinoensis* may be of interest to determine the degree of reproductive isolation between these taxa. It would also be useful to investigate the ecological requirements of both *P. streckeri* and *P. illinoensis* in relation to available habitat, given the unique burrowing lifestyle and association with sand prairies that has been highlighted in *P. illinoensis* (Brown *et al.* 1972; Axtell & Haskell 1977; Brown 1978). Perhaps most importantly, fine-scale studies of population connectivity within *P. illinoensis* incorporating landscape information will further inform conservation efforts and population management.

Model testing in phylogeography

As the amount of data in phylogeographic studies continues to grow rapidly, efforts will need to focus on the development and refinement of approaches for making inferences from large data sets (e.g. Carstens *et al.* 2013; Smith *et al.* 2014). In this study, we took the approach of evaluating models that either support or contradict previously proposed biogeographic hypotheses. Although this is not the same as traditional hypothesis testing in the sense that there is not a null hypothesis to reject or fail to reject, we demonstrate that model-based approaches are useful for choosing among *a priori* hypotheses to make meaningful inferences. We recognize that there are shortcomings to this strategy, most important of which is that we may not have considered a model that could be better supported by the data (Hickerson 2014). We chose to evaluate a set of models designed to test specific hypotheses because it is more tractable than trying to compare all possible models and provides more useful insights than comparing several models that do not have a meaningful biological interpretation. Emerging methods for generating and evaluating all or many phylogeographic models for a given data set (B. C. O'Meara, A. E. Morales-Garciá, N. D. Jackson, B. C. Carstens, in review) have the potential to provide additional insights and may be particularly useful if limited prior knowledge of the system in question is available to inform model design.

A significant challenge to phylogeographic research is the computational effort involved in estimating complex

demographic parameters (Stephens 1999, 2008; Beerli 2009). Consequently, model-based approaches require a number of simplifying assumptions, and it is important to consider how violation of assumptions in empirical systems might influence our interpretation of results. Three main assumptions are relevant to our study. First, we assumed there was no structure within groups when we pooled individuals to evaluate two-population models in IMa2. Simulations indicate that violation of this assumption may result in an upward bias of divergence time estimates (Strasburg & Rieseberg 2010). Although the sequence data we used for these analyses contained limited structure, we have also interpreted these results with caution. Second, we assumed gene flow with unsampled or 'ghost' populations was negligible for our IMa2 and MIGRATE-N analyses. Describing the effects of gene flow with ghost populations remains a challenge (Slatkin 2005), although simulations in MIGRATE-N suggest that migration rate parameters are fairly robust if migration with unsampled populations is low (Beerli 2004). Third, we assumed that alleles were shared only through migration and not population divergence in our MIGRATE-N analyses. Even with fairly recent divergences between populations, MIGRATE-N produces accurate parameter estimates if effective population sizes are sufficiently small or migration rates are high (Beerli 2010). In our case, although the divergence between the northern and southern *P. illinoensis* populations is presumably recent, the effective population sizes are indeed small.

One final challenge to designing phylogeographic studies is deciding how to group individuals into populations. We were interested in specific biogeographic regions and used these to demarcate our populations, but we also used MIGRATE-N to test whether structure within *P. illinoensis* could be detected compared to a model of panmixia. Recent studies have used a similar strategy to evaluate the level of panmixia in other systems including broadly distributed birds (Roshier *et al.* 2012; Kraus *et al.* 2013), lichens (Fernández-Mendoza & Printzen 2013) and marine organisms (Vogler *et al.* 2012; Horne & van Herwerden 2013; Lee *et al.* 2013). This approach is a useful complement to common methods for investigating genetic structure (e.g. PCoA, AMOVA, F-statistics, clustering analyses), some of which may be biased by isolation by distance (Frantz *et al.* 2009; Meirmans 2012). Our model design also revealed a more complete picture of the system by testing the directionality of migration. Future study of other taxa with similar disjunct distributions across the Great Plains and Prairie Peninsula (Smith 1957) in this framework would provide an interesting comparison. Although challenges remain in properly designing phylogeographic studies, particularly with the influx of data and the computational demands those data pose, we have the unprecedented ability to greatly refine our understanding of biogeographic history and contemporary genetic structure.

Acknowledgements

Funding for this project was provided by the East Texas Herpetological Society to LNB, NSF DEB1120516 to EML and start-up funds from Florida State University (FSU) to EML. The work was supported by the NSF Graduate Research Fellowship Program under Grant No. DGE0952090 to LNB. We thank Peter Beerli, Scott J. Steppan and Moses J. Michelsohn for helpful discussions and assistance with analyses; Steven Miller at the FSU Biology Core Facility for assistance with sequencing and fragment analysis; Mallory Bedwell and Sandra A. Emme for laboratory support; Kory Roberts, Curtis Schmidt and Travis Taggart for field collections; Janalee Caldwell and Janet Braun at the Sam Noble Oklahoma Museum of Natural History, University of Oklahoma, Joseph T. Collins and Curtis Schmidt at the Sternberg Museum of Natural History, Fort Hays State University, and David Cannatella and Travis LaDuc at the Texas Natural History Collection, University of Texas, Austin for tissue loans; seven anonymous reviewers for comments that greatly improved our manuscript; and the FSU Research Computing Center facility and staff for computational resources and support.

References

Arbogast BS, Edwards SV, Wakeley J, Beerli P, Slowinski JB (2002) Estimating divergence times from molecular data on phylogenetic and population genetic timescales. *Annual Review of Ecology, Evolution, and Systematics*, **33**, 707–740.

Avise JC (2000) *Phylogeography: The History and Formation of Species*. Harvard University Press, Cambridge, Massachusetts.

Axtell RW, Haskell N (1977) An interhiatal population of *Pseudacris streckeri* from Illinois, with an assessment of its postglacial dispersion history. *Chicago Academy of Sciences, Natural History Miscellanea*, **202**, 1–8.

Barrow LN, Ralicki HF, Emme SA, Lemmon EM (2014a) Species tree estimation of North American chorus frogs (Hylidae: *Pseudacris*) with parallel tagged amplicon sequencing. *Molecular Phylogenetics and Evolution*, **75**, 78–90.

Barrow LN, Phillips CA, Lemmon EM (2014b) Development and characterization of 24 microsatellite loci for the Illinois chorus frog (*Pseudacris illinoensis*) and Strecker's chorus frog (*P. streckeri*). *Conservation Genetics Resources*, **6**, 633–636.

Beerli P (2004) Effect of unsampled populations on the estimation of population sizes and migration rates between sampled populations. *Molecular Ecology*, **13**, 827–836.

Beerli P (2006) Comparison of Bayesian and maximum-likelihood inference of population genetic parameters. *Bioinformatics*, **22**, 341–345.

Beerli P (2009) How to use MIGRATE or why are Markov chain Monte Carlo programs difficult to use? In: *Population Genetics for Animal Conservation* (eds Bertorelle G, Bruford

MW, Hauffe HC, Rizzoli A, Vernesi C), pp. 42–79. Cambridge University Press, Cambridge, UK.

Beerli P (2010) Violation of assumptions: or are your migration estimates wrong when the populations split in the recent past [Web log]. Available from <http://popgen.sc.fsu.edu/Migrate/Blog/Entries/2010/8/15_Violation_of_assumptions,_or_are_your_migration_estimates_wrong_when_the_populations_split_in_the_recent_past.html>. Accessed on 14 July 2015.

Beerli P, Felsenstein J (2001) Maximum likelihood estimation of a migration matrix and effective population sizes in n subpopulations by using a coalescent approach. *Proceedings of the National Academy of Sciences USA*, **98**, 4563–4568.

Beerli P, Palczewski M (2010) Unified framework to evaluate panmixia and migration direction among multiple sampling locations. *Genetics*, **185**, 313–326.

Blair WF (1950) Biotic provinces of Texas. *Texas Journal of Science*, **2**, 93–116.

Bloomquist EW, Lemey P, Suchard MA (2010) Three roads diverged? Routes to phylogeographic inference. *Trends in Ecology and Evolution*, **25**, 626–632.

Bouckaert R, Lemey P, Dunn M *et al.* (2012) Mapping the origins and expansion of the Indo-European language family. *Science*, **337**, 957–960.

Bouckaert R, Heled J, Kuhnert D *et al.* (2014) BEAST2: a software platform for Bayesian evolutionary analysis. *PLoS Computational Biology*, **10**, e1003537.

Brandley MC, Schmitz A, Reeder TW (2005) Partitioned Bayesian analyses, partition choice, and the phylogenetic relationships of scincid lizards. *Systematic Biology*, **54**, 373–390.

Brown LE (1978) Subterranean feeding by the chorus frog *Pseudacris streckeri* (Anura: Hylidae). *Herpetologica*, **34**, 212–216.

Brown LE, Rose GB (1988) Distribution, habitat, and calling season of the Illinois chorus frog (*Pseudacris streckeri illinoensis*) along the lower Illinois River. *Illinois Natural History Survey Biological Notes*, **132**, 1–13.

Brown LE, Jackson HO, Brown JR (1972) Burrowing behavior of the chorus frog, *Pseudacris streckeri*. *Herpetologica*, **28**, 325–328.

Burney CW, Brumfield RT (2009) Ecology predicts levels of genetic differentiation in Neotropical birds. *The American Naturalist*, **174**, 358–368.

Bybee SM, Bracken-Grissom H, Haynes BD *et al.* (2011) Targeted amplicon sequencing (TAS): a scalable next-gen approach to multilocus, multitaxa phylogenetics. *Genome Biology and Evolution*, **3**, 1312–1323.

Carstens BC, Brennan RS, Chua V *et al.* (2013) Model selection as a tool for phylogeographic inference: an example from the willow *Salix melanopsis*. *Molecular Ecology*, **22**, 4014–4028.

Coates DJ (2000) Defining conservation units in a rich and fragmented flora: implications for the management of genetic resources and evolutionary processes in south-west Australian plants. *Australian Journal of Botany*, **48**, 329–339.

Cohen KM, Finney SC, Gibbard PL, Fan JX (2013) The ICS International chronostratigraphic chart. *Episodes*, **36**, 199–204.

Collins JT (1991) Viewpoint: a new taxonomic arrangement for some North American amphibians and reptiles. *Herpetological Review*, **22**, 42–43.

Cook JA, Bidlack AL, Conroy CJ *et al.* (2001) A phylogeographic perspective on endemism in the Alexander Archipelago of southeast Alaska. *Biological Conservation*, **97**, 215–227.

Cooke MJ, Stern LA, Banner JL, Mack LE, Stafford TWJ, Toomey RS III (2003) Precise timing and rate of massive late Quaternary soil denudation. *Geology*, **31**, 853–856.

Culver DC, Sket B (2000) Hotspots of subterranean biodiversity in caves and wells. *Journal of Cave and Karst Studies*, **62**, 11–17.

Culver DC, Master LL, Christman MC, Hobbs HH III (2000) Obligate cave fauna of the 48 contiguous United States. *Conservation Biology*, **14**, 386–401.

Drummond AJ, Bouckaert RR (2015) *Bayesian Evolutionary Analysis With BEAST*. Cambridge University Press, Cambridge, UK.

Drummond AJ, Rambaut A (2007) BEAST: Bayesian evolutionary analysis by sampling trees. *BMC Evolutionary Biology*, **7**, 214.

Drummond AJ, Rambaut A, Shapiro B, Pyrus OG (2005) Bayesian coalescent inference of past population dynamics from molecular sequences. *Molecular Biology and Evolution*, **22**, 1185–1192.

Dufresnes C, Wassef J, Ghali K *et al.* (2013) Conservation phylogeography: does historical diversity contribute to regional vulnerability in European tree frogs (*Hyla arborea*)? *Molecular Ecology*, **22**, 5669–5684.

Edgar RC (2004) MUSCLE: multiple sequence alignment with high accuracy and high throughput. *Nucleic Acids Research*, **32**, 1792–1797.

Edwards SV, Beerli P (2000) Perspective: gene divergence, population divergence, and the variance in coalescence time in phylogeographic studies. *Evolution*, **54**, 1839–1854.

Endler JA (1977) *Geographic Variation, Speciation, and Clines*. Princeton University Press, Princeton, New Jersey.

Epperson BK (2003) *Geographical Genetics (MPB-38)*. Princeton University Press, Princeton, New Jersey.

Ersts PJ (Internet) Geographic Distance Matrix Generator (version 1.2.3). American Museum of Natural History, Center for Biodiversity and Conservation. Available from http://biodiversityinformatics.amnh.org/open_source/gdmg. Accessed on 13 April 2014.

Excoffier L, Lischer HEL (2010) Arlequin suite v. 3.5: a new series of programs to perform population genetics analyses under Linux and Windows. *Molecular Ecology Resources*, **10**, 564–567.

Fernández-Mendoza F, Printzen C (2013) Pleistocene expansion of the bipolar lichen *Cetraria aculeata* into the Southern hemisphere. *Molecular Ecology*, **22**, 1961–1983.

Fowler NL, Dunlap DW (1986) Grassland vegetation of the eastern Edwards Plateau. *American Midland Naturalist*, **115**, 146–155.

Frantz AC, Cellina S, Krier A, Schley L, Burke T (2009) Using spatial Bayesian methods to determine the genetic structure of a continuously distributed population: clusters or isolation by distance? *Journal of Applied Ecology*, **46**, 493–505.

Frost DR, McDiarmid RW, MendelsonIII JR, Green DM (2012) Anura—Frogs. In: *Scientific and Standard English Names of Amphibians and Reptiles of North America North of Mexico, With Comments Regarding Confidence in our Understanding*, Vol. **39**, 7th edn (ed. Crother BI), pp. 11–22. Herpetological Circular. Society for the Study of Amphibians and Reptiles, Shoreview, Minnesota.

Garrick RC, Bonatelli IAS, Hyseni C *et al.* (2015) The evolution of phylogeographic data sets. *Molecular Ecology*, **24**, 1164–1171.

Gehlbach FR (1991) The east-west transition zone of terrestrial vertebrates in Central Texas—A biogeographical analysis. *Texas Journal of Science*, **43**, 415–427.

Goetze JR (1995) Distribution, natural history, and biogeographic relationships of mammals on the Edwards Plateau of Texas. Dissertation, Texas Tech University.

Gouy M, Guindon S, Gascuel O (2010) SeaView version 4: a multiplatform graphical user interface for sequence alignment and phylogenetic tree building. *Molecular Biology and Evolution*, **27**, 221–224.

Heled J, Drummond AJ (2008) Bayesian inference of population size history from multiple loci. *BMC Evolutionary Biology*, **8**, 289.

Heled J, Drummond AJ (2010) Bayesian inference of species trees from multilocus data. *Molecular Biology and Evolution*, **27**, 570–580.

Hey J (2010) Isolation with migration models for more than two populations. *Molecular Biology and Evolution*, **27**, 905–920.

Hey J, Machado CA (2003) The study of structured populations—new hope for a difficult and divided science. *Nature Reviews Genetics*, **4**, 535–543.

Hey J, Nielsen R (2007) Integration within the Felsenstein equation for improved Markov chain Monte Carlo methods in population genetics. *Proceedings of the National Academy of Sciences USA*, **104**, 2785–2790.

Hickerson MJ (2014) All models are wrong. *Molecular Ecology*, **23**, 2887–2889.

Hickerson MJ, Carstens BC, Cavender-Bares J *et al.* (2010) Phylogeography's past, present, and future: 10 years after Avise, 2000. *Molecular Phylogenetics and Evolution*, **54**, 291–301.

Holman JA (2003) *Fossil Frogs and Toads of North America*. Indiana University Press, Bloomington, Indiana.

Horne JB, van Herwerden L (2013) Long-term panmixia in a cosmopolitan Indo-Pacific coral reef fish and a nebulous genetic boundary with its broadly sympatric sister species. *Journal of Evolutionary Biology*, **26**, 783–799.

IUCN (2012) IUCN Red List of threatened species. Version 2012.1. Available from http://www.iucnredlist.org. accessed on 13 February 2013.

Kass RE, Raftery AE (1995) Bayes factors. *Journal of the American Statistical Association*, **90**, 773–795.

Keenan K, McGinnity P, Cross TF, Crozier WW, Prodöhl PA (2013) Diversity: an R package for the estimation and exploration of population genetics parameters and their associated errors. *Methods in Ecology and Evolution*, **4**, 782–788.

Knowles LL (2009) Statistical phylogeography. *Annual Review of Ecology, Evolution, and Systematics*, **40**, 593–612.

Kraus RH, Hooft P, Megens HJ *et al.* (2013) Global lack of flyway structure in a cosmopolitan bird revealed by a genome wide survey of single nucleotide polymorphisms. *Molecular Ecology*, **22**, 41–55.

Leaché AD, Harris RB, Rannala B, Yang Z (2014) The influence of gene flow on species tree estimation: a simulation study. *Systematic Biology*, **63**, 17–30.

Lee PL, Dawson MN, Neill SP *et al.* (2013) Identification of genetically and oceanographically distinct blooms of jellyfish. *Journal of The Royal Society Interface*, **10**, 20120920.

Lemmon AR, Lemmon EM (2012) High-throughput identification of informative nuclear loci for shallow-scale phylogenetics and phylogeography. *Systematic Biology*, **61**, 745–761.

Lemmon EM, Lemmon AR, Collins JT, Lee-Yaw JA, Cannatella DC (2007a) Phylogeny-based delimitation of species boundaries and contact zones in the trilling chorus frogs (*Pseudacris*). *Molecular Phylogenetics and Evolution*, **44**, 1068–1082.

Lemmon EM, Lemmon AR, Cannatella DC (2007b) Geological and climatic forces driving speciation in the continentally distributed trilling chorus frogs (*Pseudacris*). *Evolution*, **61**, 2086–2103.

McCormack JE, Heled J, Delaney KS, Peterson AT, Knowles LL (2010) Calibrating divergence times on species trees versus gene trees: Implications for speciation history of *Aphelocoma* jays. *Evolution*, **65**, 184–202.

McCormack JE, Hird SM, Zellmer AJ, Carstens BC, Brumfield RT (2013) Applications of next-generation sequencing to phylogeography and phylogenetics. *Molecular Phylogenetics and Evolution*, **66**, 526–538.

Meirmans PG (2012) The trouble with isolation by distance. *Molecular Ecology*, **21**, 2839–2846.

Meyer M, Kircher M (2010) Illumina sequencing library preparation for highly multiplexed target capture and sequencing. *Cold Spring Harbor Protocols*, **2010**, doi:10.1101/pdb.prot5448.

Mills LS, Allendorf FW (1996) The one-migrant-per generation rule in conservation and management. *Conservation Biology*, **10**, 1509–1518.

Moriarty EC, Cannatella DC (2004) Phylogenetic relationships of the North American chorus frogs (*Pseudacris*: Hylidae). *Molecular Phylogenetics and Evolution*, **30**, 409–420.

Moritz C (1994) Defining 'Evolutionarily Significant Units' for conservation. *Trends in Ecology and Evolution*, **9**, 373–375.

Nielsen R, Beaumont MA (2009) Statistical inferences in phylogeography. *Molecular Ecology*, **18**, 1034–1047.

Nordt LC, Boutton TW, Hallmark CT, Waters MR (1994) Late Quaternary vegetation and climate changes in central Texas based on the isotopic composition of organic carbon. *Quaternary Research*, **41**, 109–120.

Nylander JAA (2004) *MrModeltest v2*. Program Distributed by the Author. Evolutionary Biology Centre, Uppsala University, Uppsala, Sweden.

Nylander JAA, Ronquist F, Huelsenbeck JP, Nieves-Aldrey JL (2004) Bayesian phylogenetic analysis of combined data. *Systematic Biology*, **53**, 47–67.

O'Neill EM, Schwartz R, Bullock CT *et al.* (2013) Parallel tagged amplicon sequencing reveals major lineages and phylogenetic structure in the North American tiger salamander (*Ambystoma tigrinum*) species complex. *Molecular Ecology*, **22**, 111–129.

Peakall R, Smouse PE (2012) GenAlEx 6.5: genetic analysis in Excel. Population genetic software for teaching and research–an update. *Bioinformatics*, **28**, 2537–2539.

Pelletier TA, Carstens BC (2014) Model choice for phylogeographic inference using a large set of models. *Molecular Ecology*, **23**, 3028–3043.

Pritchard JK, Stephens M, Donnelly P (2000) Inference of population structure using multilocus genotype data. *Genetics*, **155**, 945–959.

Rambaut A, Drummond AJ (2007) Tracer v1.4. Available from http://beast.bio.ed.ac.uk/Tracer.

Raymond M, Rousset F (1995) GENEPOP (version 1.2): population genetics software for exact tests and ecumenicism. *Journal of Heredity*, **86**, 248–249.

Roshier DA, Heinsohn R, Adcock GJ, Beerli P, Joseph L (2012) Biogeographic models of gene flow in two waterfowl of the Australo-Papuan tropics. *Ecology and Evolution*, **2**, 2803–2814.

Rousset F (2008) Genepop'007: a complete re-implementation of the genepop software for Windows and Linux. *Molecular Ecology Resources*, **8**, 103–106.

Slatkin M (1995) A measure of population subdivision based on microsatellite allele frequencies. *Genetics*, **139**, 457–462.

Slatkin M (2005) Seeing ghosts: the effect of unsampled populations on migration rates estimated for sampled populations. *Molecular Ecology*, **14**, 67–73.

Smith PW (1951) A new frog and a new turtle from the western Illinois sand prairies. *Bulletin of the Chicago Academy of Sciences*, **9**, 189–199.

Smith PW (1957) An analysis of post-Wisconsin biogeography of the Prairie Peninsula region based on distributional phenomena among terrestrial vertebrate populations. *Ecology*, **38**, 205–218.

Smith WP (2005) Evolutionary diversity and ecology of endemic small mammals of southeastern Alaska with implications for land management planning. *Landscape and Urban Planning*, **72**, 135–155.

Smith SA, Stephens PR, Wiens JJ (2005) Replicate patterns of species richness, historical biogeography, and phylogeny in Holarctic treefrogs. *Evolution*, **59**, 2433–2450.

Smith BT, Harvey MG, Faircloth BC, Glenn TC, Brumfield RT (2014) Target capture and massively parallel sequencing of ultraconserved elements (UCEs) for comparative studies at shallow evolutionary time scales. *Systematic Biology*, **63**, 83–95.

Smouse PE (1998) To tree or not to tree. *Molecular Ecology*, **7**, 399–412.

Stamatakis A (2006) RAxML-VI-HPC: maximum likelihood-based phylogenetic analyses with thousands of Taxa and mixed models. *Bioinformatics*, **22**, 2688–2690.

Stephens M (1999) Problems with computational methods in population genetics. Bulletin of the 52nd Session of the International Statistical Institute, Helsinki, pp. 273–276.

Stephens M (2008) Inference under the coalescent. *Handbook of Statistical Genetics*, 3rd edn, pp. 878–908. John Wiley & Sons, Ltd., Hoboken, New Jersey.

Strasburg JL, Rieseberg LH (2010) How robust are "Isolation with Migration" analyses to violations of the IM model? A simulation study. *Molecular Biology and Evolution*, **27**, 297–310.

Sunnucks P (2000) Efficient genetic markers for population biology. *Trends in Ecology and Evolution*, **15**, 199–203.

Tamura K, Peterson D, Peterson N, Stecher G, Nei M, Kumar S (2011) MEGA5: Molecular Evolutionary Genetic Analysis using maximum likelihood, evolutionary distance, and maximum parsimony methods. *Molecular Biology and Evolution*, **28**, 2731–2739.

Trauth JB, Trauth SE, Johnson RL (2006) Best management practices and drought combine to silence the Illinois chorus frog in Arkansas. *Wildlife Society Bulletin*, **34**, 514–517.

Trauth JB, Johnson RL, Trauth SE (2007) Conservation implications of a morphometric comparison between the Illinois Chorus Frog (*Pseudacris streckeri illinoensis*) and Strecker's Chorus Frog (*P. s. streckeri*) (Anura: Hylidae) from Arkansas, Illinois, Missouri, Oklahoma, and Texas. *Zootaxa*, **1589**, 23–32.

Tucker JK, Philipp DP (1995) Population status of the Illinois chorus frog (*Pseudacris streckeri illinoensis*) in Madison County, Illinois: Results of 1994 surveys. Illinois Natural History Survey Aquatic Ecology Technical Report. 78 pp.

Van Auken OW, Ford AL, Stein A (1979) A comparison of some woody upland and riparian plant communities of the southern Edwards Plateau. *The Southwestern Naturalist*, **24**, 165–180.

Van Oosterhout C, Hutchinson WF, Wills DP, Shipley P (2004) MICRO-CHECKER: software for identifying and correcting genotyping errors in microsatellite data. *Molecular Ecology Notes*, **4**, 535–538.

Vogler C, Benzie J, Barber PH *et al.* (2012) Phylogeography of the crown-of-thorns starfish in the Indian Ocean. *PLoS ONE*, **7**, e43499.

Waltari E, Hijmans RJ, Peterson AT, Nyári ÁS, Perkins SL, Guralnick RP (2007) Locating Pleistocene refugia: comparing phylogeographic and ecological niche model predictions. *PLoS ONE*, **2**, e563.

Waples RS, Gaggiotti O (2006) What is a population? An empirical evaluation of some genetic methods for identifying the number of gene pools and their degree of connectivity. *Molecular Ecology*, **15**, 1419–1439.

Yang Z, Rannala B (2014) Unguided species delimitation using DNA sequence data from multiple loci. *Molecular Biology and Evolution*, **31**, 3125–3135.

L.N.B. obtained funding, planned the project, led the laboratory work, designed and conducted analyses, and led the writing. A.T.B. conducted laboratory work and analyses. C.A.P. conceived the original project idea and provided funding and tissues. E.M.L. assisted with project planning and provided funding, tissues and laboratory space. All authors edited the manuscript.

Data accessibility

Sequence and microsatellite data generated in this study, alignments, tree files, and input/output files from IMa2, Migrate-n, and additional analyses are available on Dryad (doi:10.5061/dryad.h2082).

Supporting information

Additional supporting information may be found in the online version of this article.

Fig. S1 BEAST tree for divergence time estimation.

Fig. S2 Results of demographic analyses.

Fig. S3 Allelic richness across the species complex.

Fig. S4 Geographic distance by genetic distance.

Fig. S5 Mean likelihoods from Bayesian clustering analyses.

Fig. S6 Assignment plots from Bayesian clustering analyses.

Fig. S7 All 24 models compared in Migrate-n.

Data S1 Methods.

Table S1 List of samples in this study including field numbers and locality information.

Table S2 Primer sequences and annealing temperatures for sequenced loci.

Table S3 Sequence locus information including variable sites and nucleotide models.

Table S4 List of sequences from GenBank used for divergence time estimation.

Table S5 Genetic diversity estimates for 14 microsatellite loci.

Table S6 Pairwise differentiation and geographic distances for 23 combined sites.

Table S7 Pairwise differentiation for full microsatellite dataset.

Supplementary Materials

Supporting Information [brief captions]

Table S1. List of samples in this study including field numbers and locality information.
Table S2. Primer sequences and annealing temperatures for sequenced loci.
Table S3. Sequence locus information including variable sites and nucleotide models.
Table S4. List of sequences from GenBank used for divergence time estimation.
Table S5. Genetic diversity estimates for 14 microsatellite loci.
Table S6. Pairwise differentiation and geographic distances for 23 combined sites.
Table S7. Pairwise differentiation for full microsatellite dataset.
Fig. S1. BEAST tree for divergence time estimation.
Fig. S2. Results of demographic analyses.
Fig. S3. Allelic richness across the species complex.
Fig. S4. Geographic distance by genetic distance.
Fig. S5. Mean likelihoods from Bayesian clustering analyses.
Fig. S6. Assignment plots from Bayesian clustering analyses.
Fig. S7. All 24 models compared in Migrate-n.

[Supplementary Tables included in Excel spreadsheet]

Table S1. List of samples in this study including taxon labels, location labels (one for each set of geographic coordinates), site labels (samples within 10 km combined), field numbers, museum catalog numbers, and locality information. Museum abbreviations are as follows: Sternberg Museum of Natural History, Fort Hays State University (MHP), Texas Natural History Collection Genetic Diversity Collection (TNHC-GDC), Texas Natural History Collection, University of Texas, Austin (TNHC), Illinois Natural History Survey (INHS), and Sam Noble Oklahoma Museum of Natural History (OMNH). An "n/a" under Collection No. indicates that vouchers and additional specimen information are available from the authors. All samples were genotyped in this study, and samples that were also sequenced are indicated in the last column.

Table S2. Primer sequences and annealing temperatures (ºC) for the 23 nDNA loci and 4 mtDNA fragments in this study. All primers were developed in Lemmon and Lemmon (2012) unless otherwise noted.

Table S3. Sequence locus information including length analyzed (after excluding primer regions), ingroup variable sites, ingroup parsimony-informative sites, and model of nucleotide evolution.

Table S4. List of mitochondrial 16S sequences from GenBank used for divergence time estimation.

Table S5. Genetic diversity estimates for 14 microsatellite loci. N = number of individuals, Na = average number of alleles per locus, Ar = allelic richness, Np = number

of private alleles, Ho = observed heterozygosity, uHe = unbiased expected heterozygosity [(2N/(2N - 1)) * (1 - sum of squared allele frequencies)], F = fixation index = 1 - (Ho/He).

Table S6. Pairwise differentiation values and pairwise geographic distances between 23 sites (280 individuals) used for AMOVAs and Mantel tests. Below diagonal: Differentiation values (Top = Rst, Bottom = Fst). Bold italicized values are significant at a level of p=0.001, using 10,000 permutations in Arlequin v. 3.5. Above diagonal: Pairwise geographic distances in km, calculated by transforming GPS coordinate data using the Geographic Distance Matrix Generator v. 1.2.3.

Table S7. Pairwise differentiation for entire microsatellite dataset (294 individuals, 50 sites) with combined sites highlighted. Greyed boxes are locations that were excluded from combined analyses because they had sample size n<5 and were not within 10km of any other sample locality. Fst values were calculated and significance testing was done using 10,000 permutations in Arlequin v. 3.5; locations with n=1 are indicated in the left column and should not be interpreted (see Bayesian clustering analyses for evidence that combined sites are not genetically differentiated in these cases). Bold, italicized values are significant at a level of p=0.05. Two pairs of combined sites (ILLN3B-ILLN3D and ILLN9A-ILLN9B) are significant at a level of p=0.05, but not after correction for multiple tests.

Fig. S1. BEAST divergence time estimation using 16S mtDNA from additional hylid taxa to calibrate the tree. Fossil calibrations include (1) the root (minimum age 42 mya), (2) the most recent common ancestor of the *Pseudacris-Acris* clade (at least 16 mya), and (3) the most recent common ancestor of North American *Hyla* (at least 34 mya). The median height and 95% highest posterior density (HPD) of divergence times of interest within *P. streckeri* and *P. illinoensis* are shown. Node bars represent 95% HPD for each divergence time.

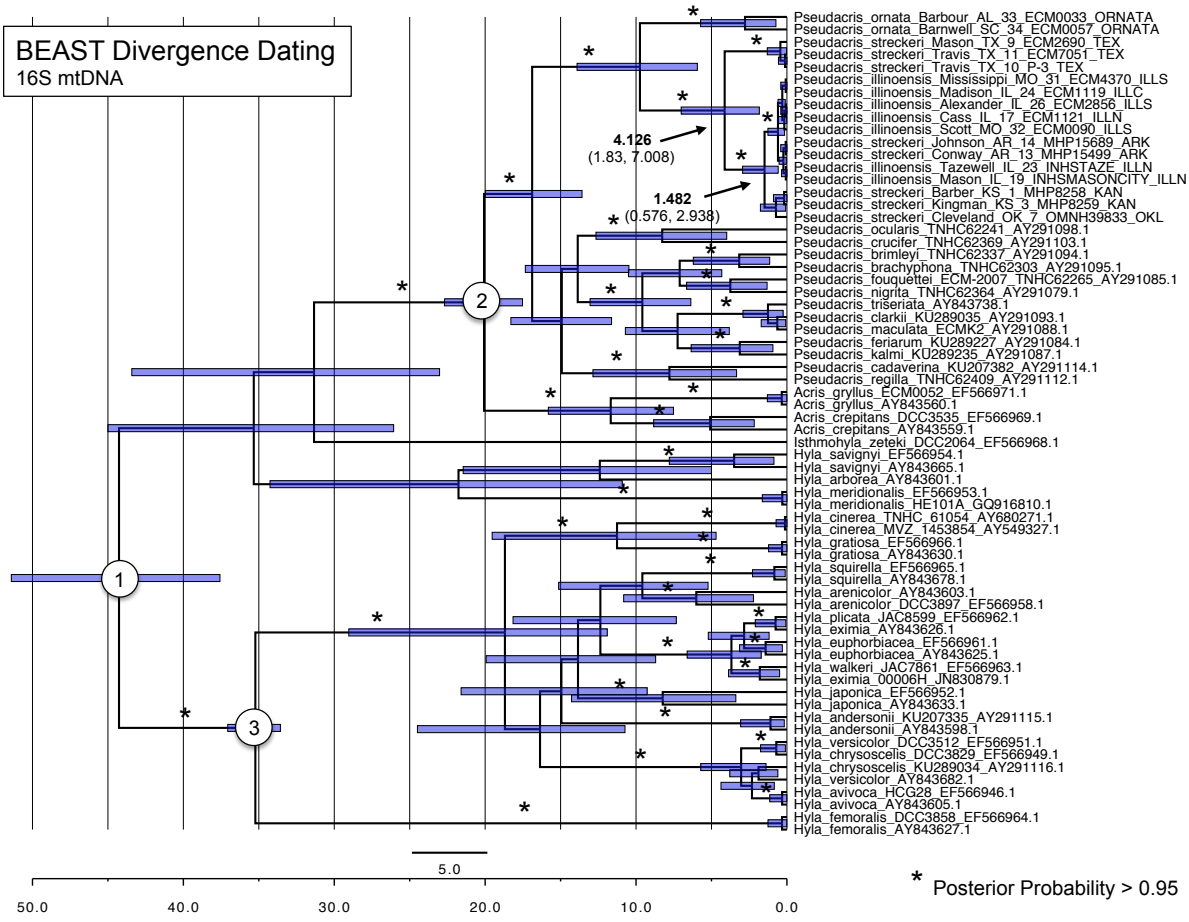

Fig. S2. Results of demographic analyses. (a, c, e, g): number of population size changes estimated from EBSP analyses. All 95% HPD intervals include 0 changes, indicating that we cannot reject constant size. (b, d, f, h): Population size (Ne, log-transformed) through time from present into the past; grey shading indicates 95% HPD interval. The x-axes are not directly comparable; (b) not scaled so time is in substitutions/site; (d, f, h) scaled by 16S rate of 0.00249 subs/site/million years. Inset plots in (f, h) depicted to show full time scale, rectangles indicate the area of larger plots.

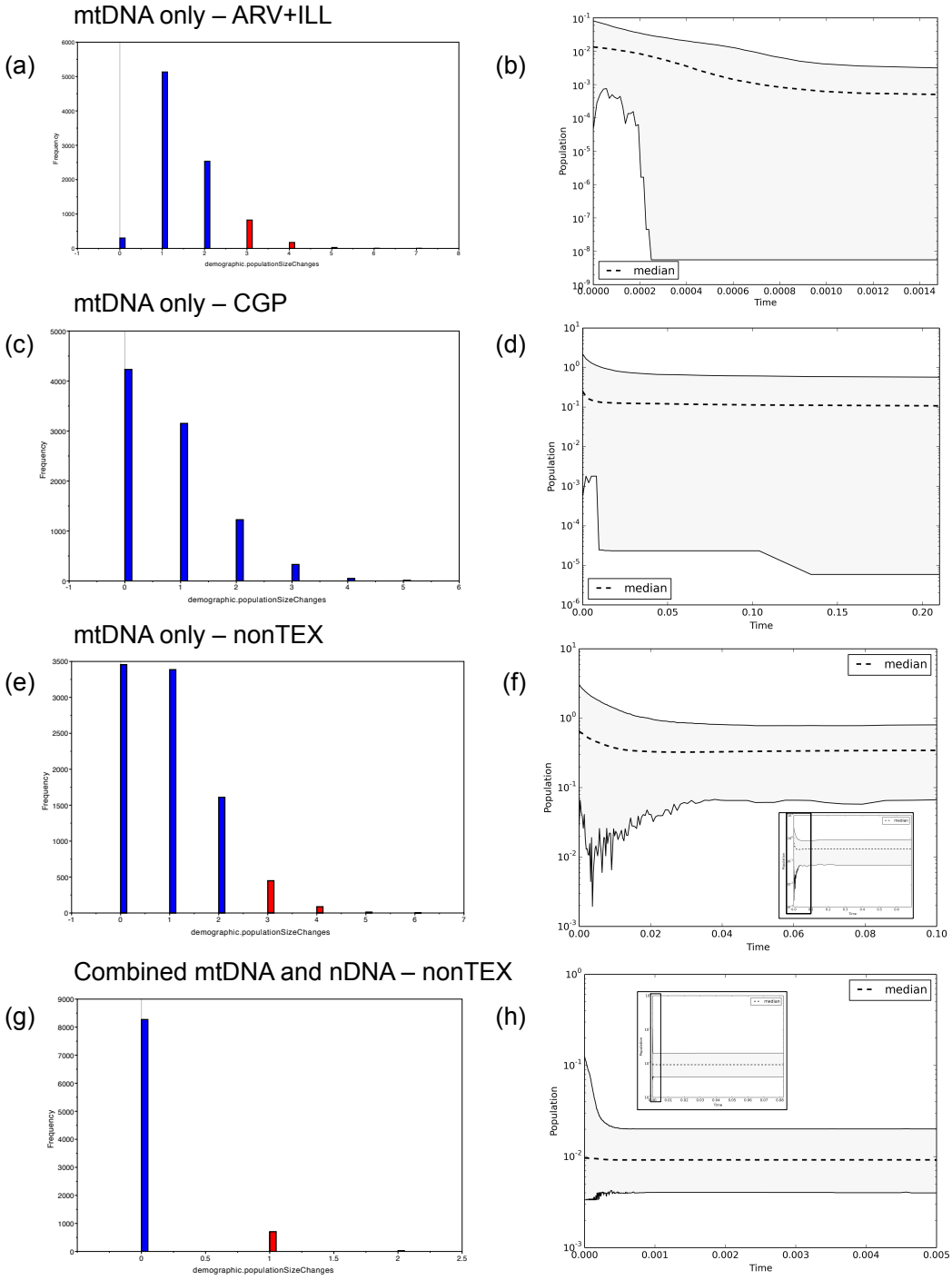

Fig. S3. Allelic richness across the *P. streckeri*/*P. illinoensis* species complex. (a) Map depicting allelic richness for each site. (b) Distance from the putative Texas refugium compared to allelic richness shows a trend of decreasing genetic diversity as distance from the refugium increases (Pearson's product-moment correlation).

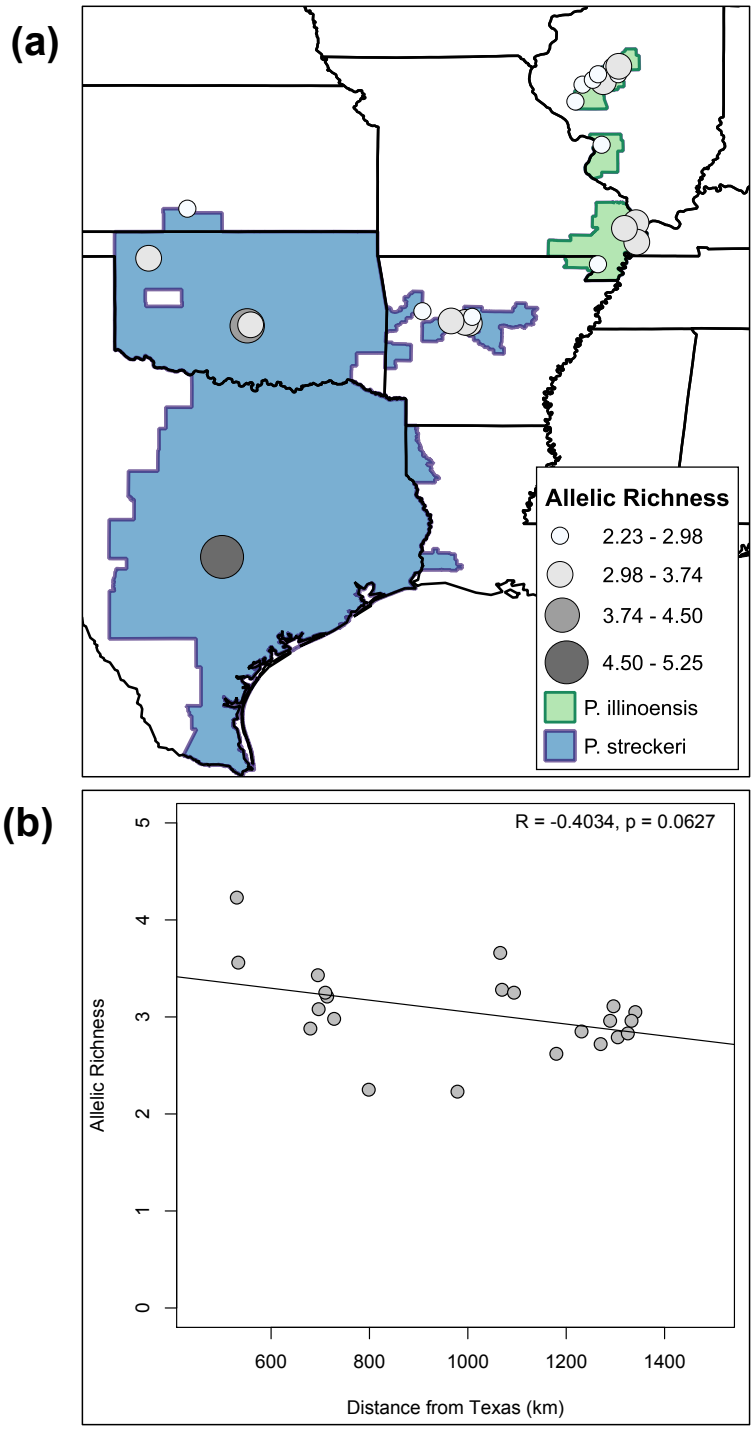

94 Fig. S4. Geographic distance by genetic distance (R_{st}) within and between *P. streckeri*
95 and *P. illinoensis* population-by-population pairs. Solid line depicts line of best fit (R^2 =
96 0.4144) through all points estimated using JMP Pro 10 (SAS Institute Inc., Cary, NC).

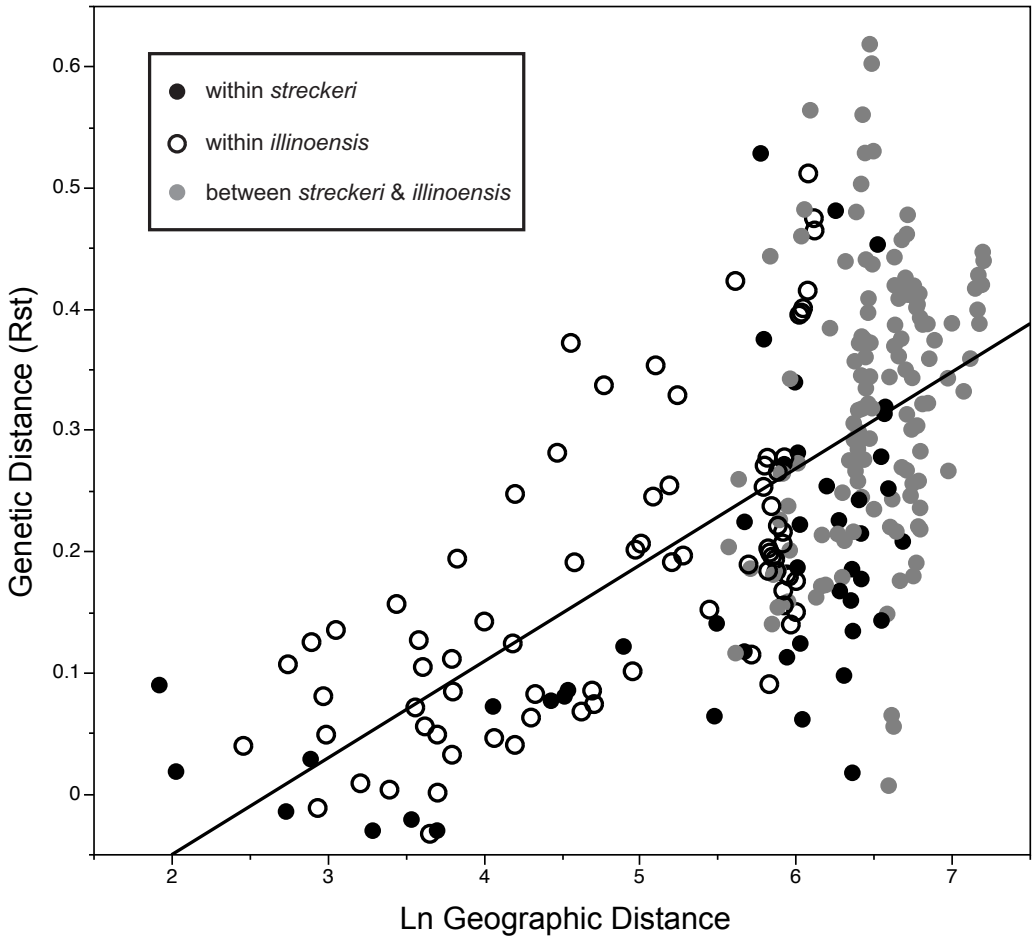

97

Fig. S5. Mean likelihoods from STRUCTURE analyses conducted with 14 microsatellite loci. Each value of K was run with 10 replicates, 1 million MCMC generations burn-in, and 1 million additional generations.

Full Dataset

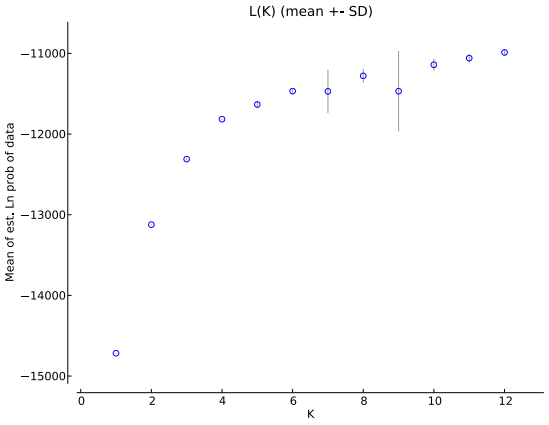

P. streckeri

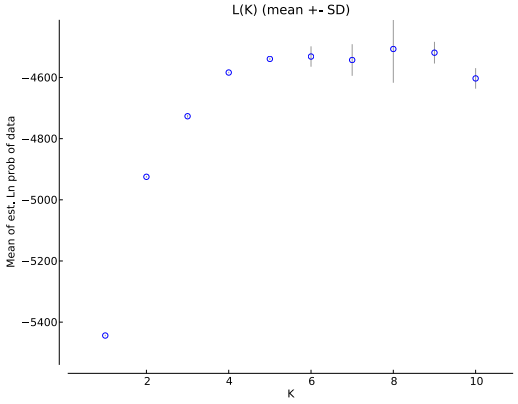

P. Illinoensis – ILLS

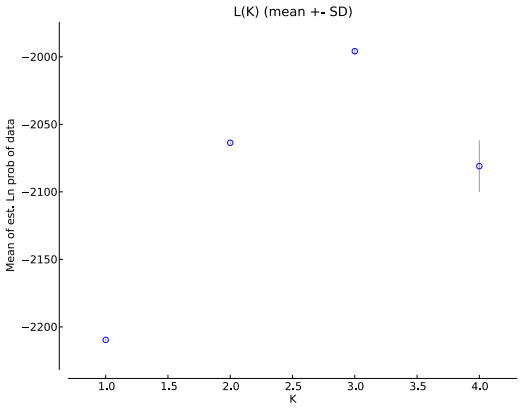

P. Illinoensis – ILLN

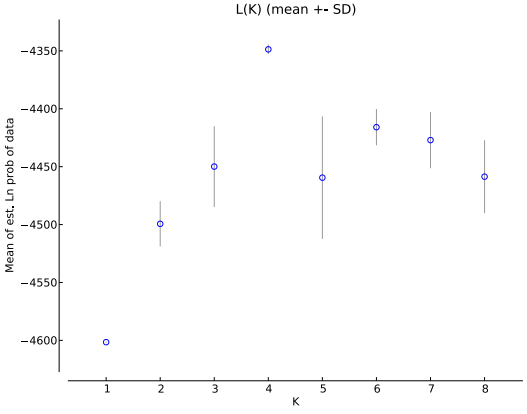

P. streckeri + ILLS

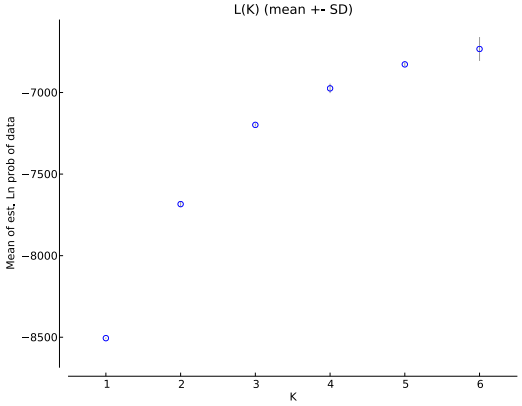

Fig. S6a. Cluster assignments from STRUCTURE analysis of full microsatellite dataset (14 loci, 294 individuals), summarized across 10 replicates using Structure Harvester, CLUMPP, and distruct. Each horizontal bar depicts an individual and its probability of assignment to one or more genetic clusters, represented by different colors. Across the full dataset, about six clusters that closely associate with geography can be recognized.

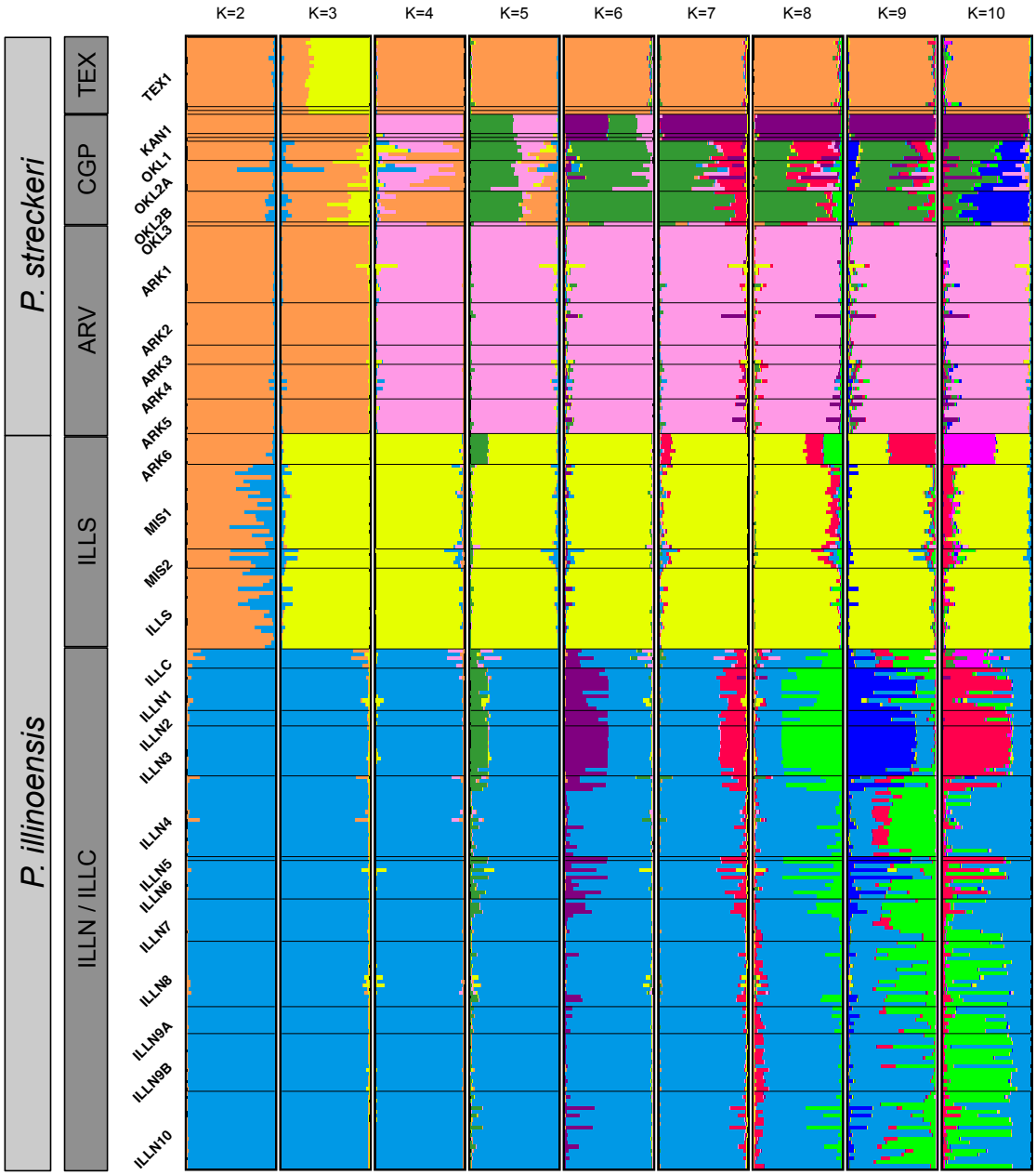

Fig. S6b. Cluster assignments from STRUCTURE analysis of subsets of the data to identify additional substructure. Left panel: top=*P. streckeri,* middle=Southern *P. illinoensis*, bottom=Northern *P. illinoensis*. Right panel: top=*P. streckeri* + Southern *P. illinoensis*, bottom=Northern *P. illinoensis*. At most, eight clusters that closely associate with geography can be recognized: K=4 for *P. streckeri*, K=3 for Southern *P. illinoensis*, and K=1 for Northern *P. illinoensis*.

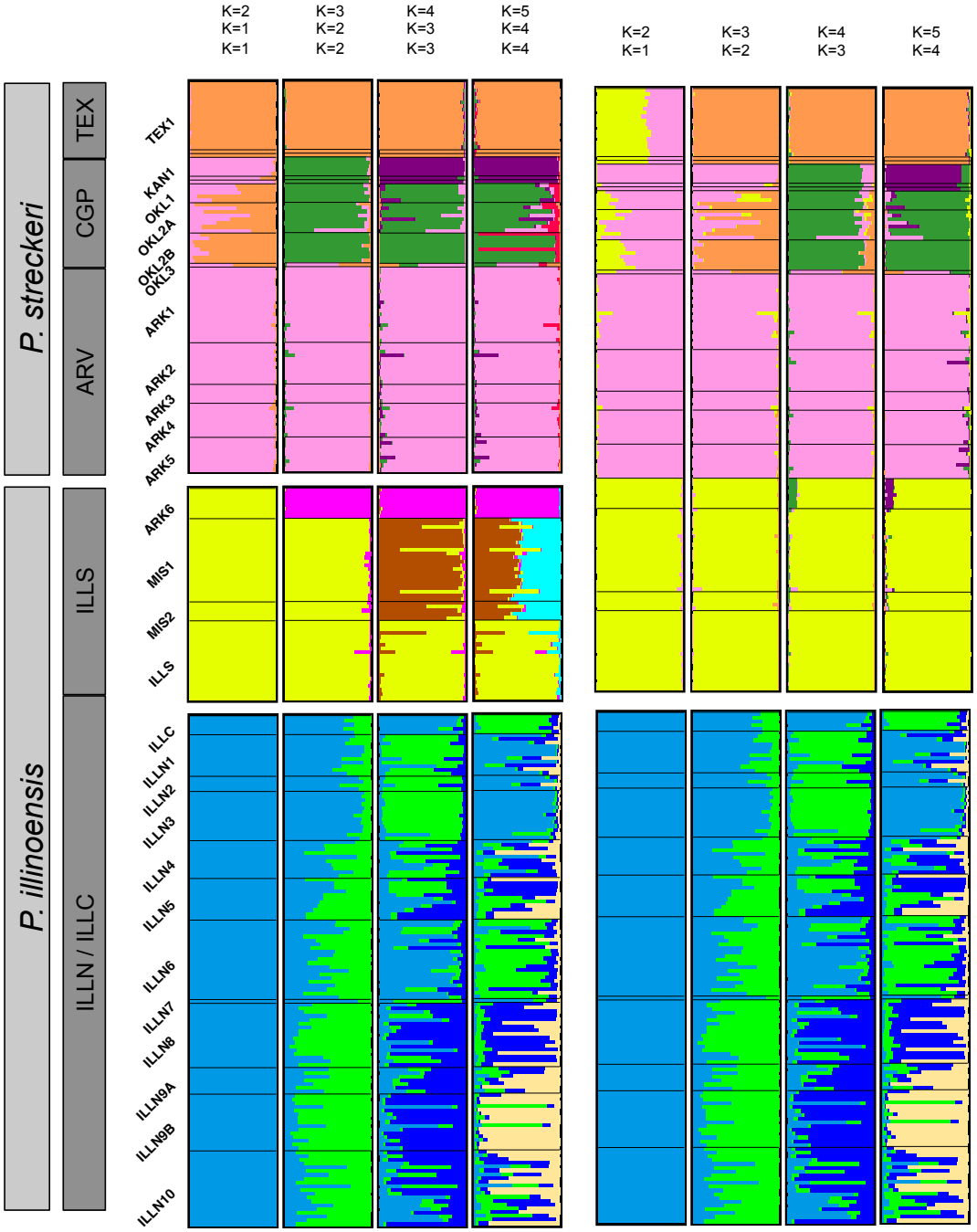

Fig. S7. All 24 models compared in Migrate-n. The best model is shown with a square.

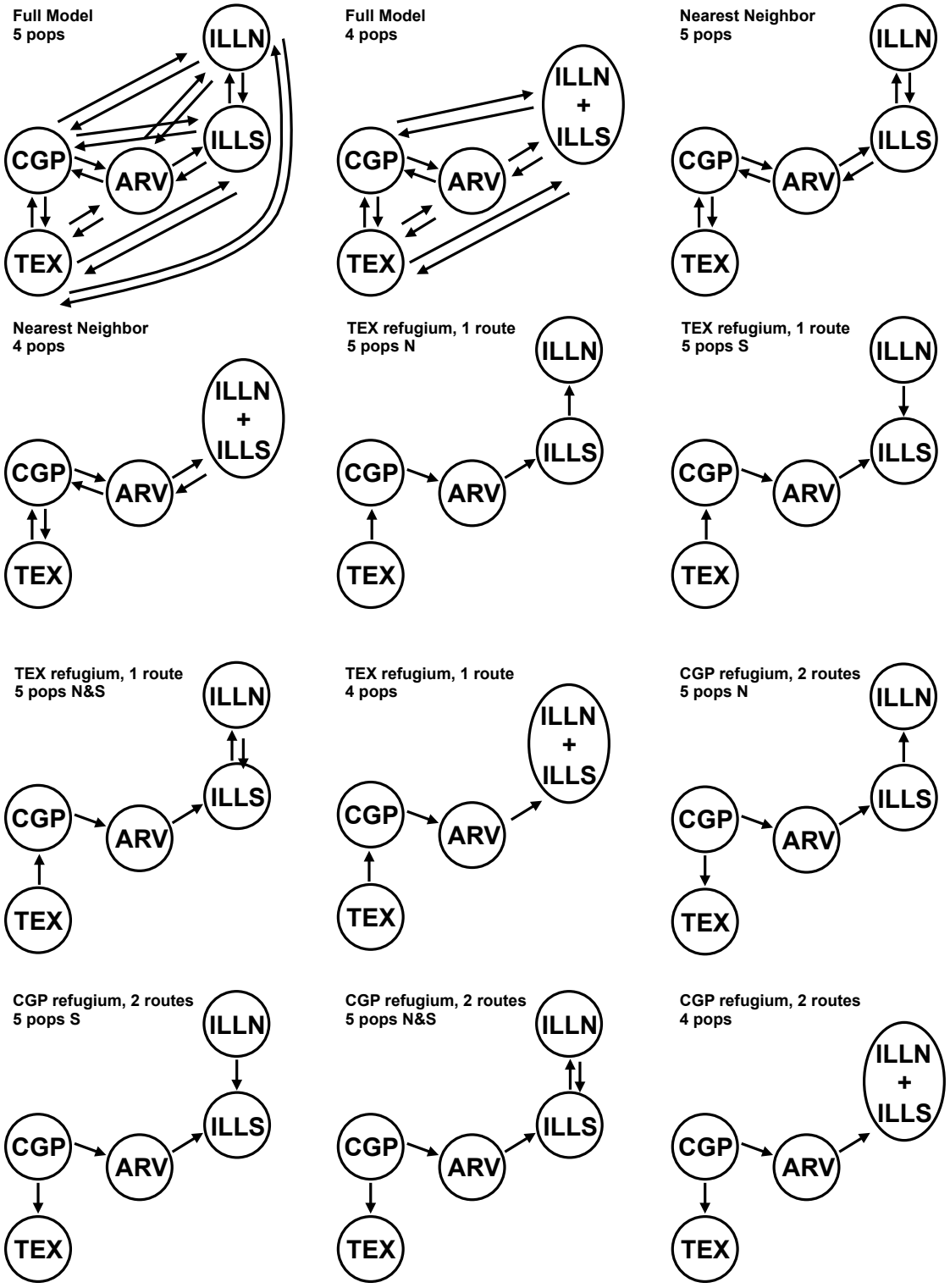

Fig. S7 (cont). All 24 models compared in Migrate-n. The best model is shown with a square.

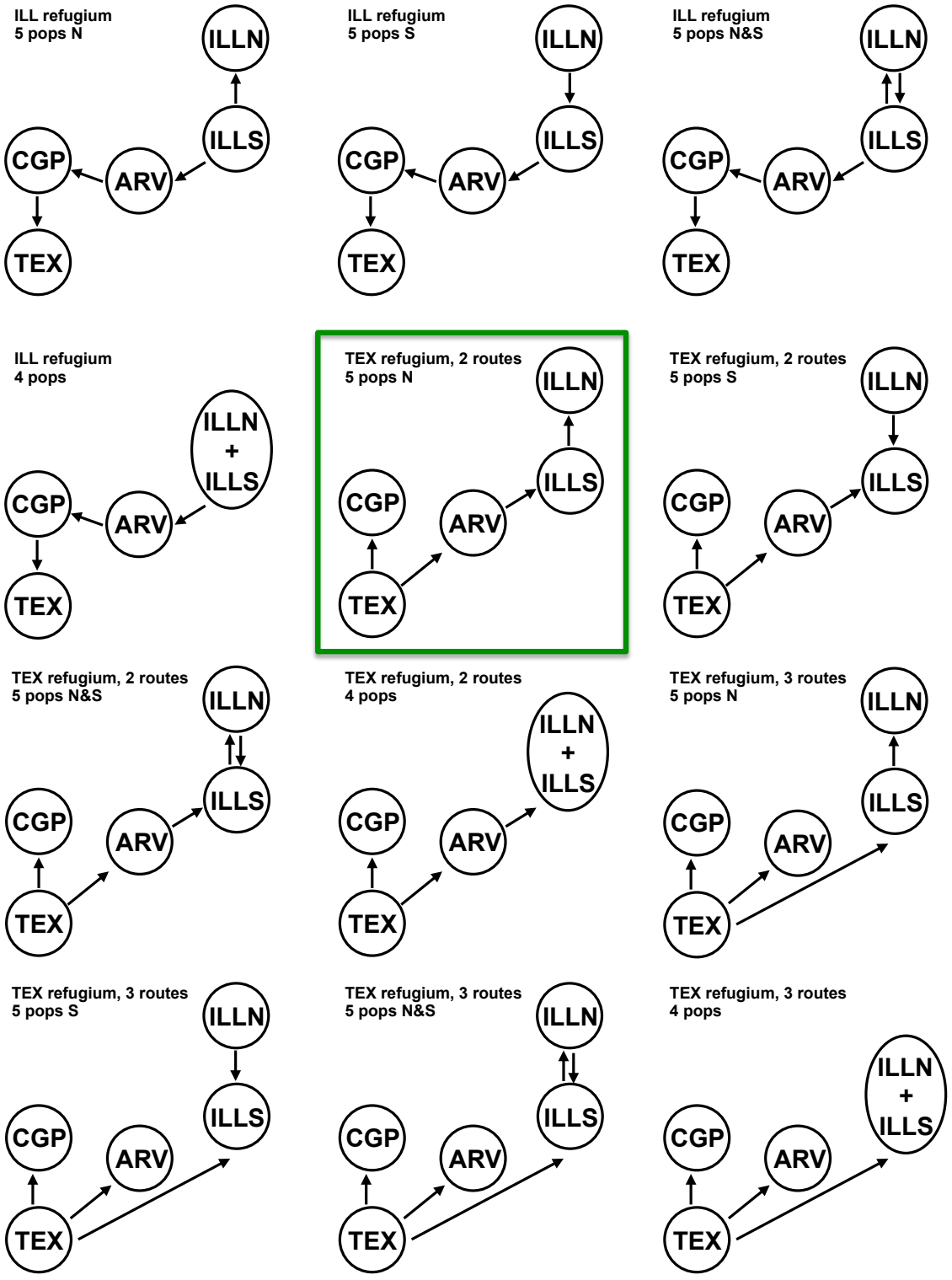

Supplementary Methods

Fossil calibrations for divergence time estimation

We used external calibrations within the treefrog family Hylidae and sequences from other Hylid taxa obtained from GenBank to date a mtDNA phylogeny that included *P. streckeri* and *P. illinoensis*. These calibrations have been used previously for divergence time estimation within *Pseudacris* (Lemmon et al. 2007) and *Hyla* (Smith et al. 2005; Wiens et al. 2006). Here we describe as much detail of these fossil calibrations as possible following the recommendations of Parham et al. (2012) – "Best Practices for Justifying Fossil Calibrations." It should be noted that identification of fossil hylids to species is extremely difficult since most material consists of small, broken individual elements (Holman 2003). We use minimum ages and incorporate error into our estimates by allowing a range of dates to be specified by lognormal priors (root: M = 3.9, S = 0.085 resulting in a 95% central prior interval of 41.8–58.4 my; *Pseudacris-Acris*: M = 2.9, S = 0.065 resulting in a 95% central prior interval of 16.0–20.6 my; and *Hyla*: M = 3.57, S = 0.025 resulting in a 95% central prior interval of 33.8–37.3 my). We also interpret our result cautiously given the level of uncertainty in the fossil calibrations and wide 95% HPD intervals that we observed.

Root of the Middle American *Hyla* clade, constrained to be at least 42 million years ago. There were no clear fossils to calibrate the root of our tree, so we followed Smith et al. (2005) and Lemmon et al. (2007) and constrained the root to at least 42 mya. The approximate overall age of hylids in the fossil record is 55–65 mya (Duellman and Trueb 1986), but it is uncertain whether fossils can be assigned to a clade within extant hylids. The minimum age used is based on previous analyses of Hylidae that include many additional outgroup taxa and additional calibration points (Wiens et al. 2006).

Most Recent Common Ancestor (MRCA) of the *Acris-Pseudacris* clade, at least 16 million years ago. This minimum age is based on the extinct *Acris barbouri* fossil thought to be the sister taxon to extant *Acris* species. (1) *Museum numbers of specimens that demonstrate all the relevant characters.* Florida Museum of Natural History: UF 10208, holotype a right ilium of *Acris barbouri* Holman (1967). Other material: a right ilium (Florida Geological Survey: FGS V6088) was designated as a paratype (Holman 1967). (2) *An apomorphy-based diagnosis of the specimen or up-to-date phylogenetic analysis that includes the specimen*. Several morphological characters were used to assign to specimen to genus (details in Holman 2003). The specimen is distinguished from extant *Acris* by having a low dorsal crest, rounded dorsal tubercle, and nearly straight ilial shaft. (3) *Reconciliation of morphological and molecular data sets*. We are unaware of any phylogenetic analyses that include the specimen, and to our knowledge molecular analysis of this fossil material has not been attempted. Molecular phylogenies of extant *Acris* species place them as the sister group of *Pseudacris* (Smith et al. 2005; Wiens et al. 2006). (4) *The locality and stratigraphic level from which the calibrating fossil was collected.* Thomas Farm Local Fauna, Gilchrist County, Florida: Torreya Formation. (5) *Reference to a published radioisotopic age and/or numeric time scale and details of numeric age selection.* Miocene (Hemingfordian North American Land Mammal Age, NALMA hereafter). Previous studies have used the dates 15–19 mya for this calibration, but revised dates of the Hemingfordian NALMA based on paleontological mammal information set the range at 15.97–20.43 mya (Alroy 2000).

MRCA of the North American *Hyla*, at least 34 million years ago. This minimum age is based on the extinct *Hyla swanstoni* fossil, which is similar to the extant *Hyla gratiosa*. It should be noted that the assignment of this fossil to *Hyla* has been called into question by some authors (Faivovich et al. 2005; Wiens et al. 2006). (1) *Museum numbers of specimens that demonstrate all the relevant characters.* Saskatchewan Museum of Natural History: SMNH 1435, holotype a left ilium described by Holman (1968). Other material: a left ilium (SMNH 1436) was designated as a paratype and three partial tibiofibulae (SMNH 1437) designated referred material (Holman 1968). (2) *An apomorphy-based diagnosis of the specimen or up-to-date phylogenetic analysis that includes the specimen*. The specimen is most similar to *Hyla miofloridana* with differences described in detail by Holman (2003). (3) *Reconciliation of morphological and molecular data sets*. We are unaware of any phylogenetic analyses that include the specimen, and to our knowledge molecular analysis of this fossil material has not been attempted. (4) *The locality and stratigraphic level from which the calibrating fossil was collected.* Calf Creek Local Fauna, near East End, Saskatchewan, Canada: Cypress Hills Formation. (5) *Reference to a published radioisotopic age and/or numeric time scale and details of numeric age selection.* Eocene (Chadronian NALMA). Previous studies have used the dates 33–35 mya for this calibration, but revised dates of the Chadronian NALMA based on paleontological mammal information set the range at 33.9–37.2 mya (Alroy 2000).

IMa2 divergence time conversions

In order to convert the divergence time parameters estimated from IMa2 into time in years, we obtained mutation rates previously estimated for anuran amphibians from the literature. We converted per site estimates into estimates for each locus by scaling by locus length (number of base pairs analyzed). For the 16S mitochondrial gene, we used the mutation rate of 0.00249 substitutions per site per million years estimated by Evans et al. (2004) for the frog family Pipidae for the 12S/16S region. This rate has previously been applied to estimates of divergence time in *Pseudacris* (Lemmon et al. 2007) and other frog taxa (e.g. Evans et al. 2008). For the ND2 gene, Crawford (2003) estimated a rate of between 1.48×10^{-8} and 2.45×10^{-8} substitutions per site per year for the frog genus *Eleutherodactylus*. Because we could find no mutation rates for anurans for either COI or cytb, we decided to apply an average rate of 1.9×10^{-8} as in García-R et al. (2012) to the three other mitochondrial genes (COI, cytb, ND2) and took the geometric mean of all four loci after scaling by locus length (geometric mean = 4.73×10^{-6}).

For the nuclear loci, we are unaware of any published overall estimates of mutation rate for the amphibian nuclear genome. Crawford (2003) estimated the divergence rate for the nuclear c-*myc* gene to be between 9.24×10^{-10} and 1.53×10^{-9} substitutions per site per year. Although far from ideal, we again applied an average mutation rate of 1.23×10^{-9} to the nuclear loci, converted to per locus mutation rates based on the number of base pairs analyzed, and calculated the geometric mean for the nuclear loci (5.90×10^{-7}). The divergence times in years were then calculated as $t = \tau / \mu$ where τ is the divergence time parameter from IMa2 and μ is the geometric mean of the mutation rates per year for either mitochondrial or nuclear loci.

Demographic analyses

We explored past population dynamics using extended Bayesian skyline plots (EBSP) of multi-locus sequence datasets in BEAST v. 1.8.2 (Drummond et al. 2005; Heled & Drummond 2008). This approach can be used to detect whether population size remained constant or changed in the past, and reconstructs the signal of population bottlenecks or population growth provided there is sufficient data (Heled & Drummond 2008). We conducted analyses using mtDNA only and combined mtDNA and nDNA, subsampling the datasets to evaluate demographic changes for each lineage with sufficient samples and informative sites.

For the mtDNA only dataset, we analyzed the ARV+ILL samples (N=21), CGP samples (N=7), and combined all non-TEX samples (N=28). The ARV+ILL analysis was conducted with only 3 mtDNA genes (COI, cytb, ND2) because there were no variable sites within 16S for this lineage. For each of the other analyses, the clock rate for 16S was set at 0.00249 substitutions/site/million years based on previous studies (Evans et al. 2004; Lemmon et al. 2007). We used HKY site models as in the other mtDNA and nDNA phylogenetic analyses in this study, and we adjusted other parameter settings for the EBSP analyses following Heled (2010). We ran each analysis for 100 million generations, sampling every 10,000 for a total of 10,000 samples, and examined the output in Tracer v. 1.5 to assess convergence. We used the python scripts described in Heled (2010) to graph population size over time with 95% HPD intervals.

For the nDNA and mtDNA combined analysis, we only analyzed non-TEX samples (N=28) given the lack of resolution in the nDNA tree. Preliminary analyses were conducted with all nuclear loci that had at least one variable site, but we had difficulty reaching convergence with additional (less informative) loci, and found inconsistent results across analyses. We included 12 loci in the full analysis (4 mtDNA, 8 nDNA) removing the nuclear loci that had fewer than 3 variable sites within this lineage, and again scaling time by the 16S clock rate as above. We ran the analysis for 200 million generations sampling every 20,000 generations. Post-run processing was completed as for the mtDNA analyses.

Bayesian clustering analysis

We used clustering analyses implemented in STRUCTURE v. 2.3.4 (Pritchard et al. 2000) to investigate patterns of genetic structure across the range of the *P. streckeri*/*P. illinoensis* species complex. STRUCTURE probabilistically assigns individuals to a genetic cluster based on their multi-locus genotype, assuming Hardy-Weinberg equilibrium and linkage equilibrium within populations. These analyses were performed to explore the level of structure under different sampling schemes and verify that locations we combined to characterize microsatellite variation were not genetically distinct. Using Structure to define genetic clusters is somewhat arbitrary, so we tested different values of K, the number of genetic clusters, and examined cluster membership of individuals at these varying levels to determine the maximum number of clusters that might be observed in our dataset.

We first analyzed our full dataset of 294 individuals across 14 microsatellite loci under models assuming 1–12 genetic clusters. Preliminary analyses with up to K=15 genetic clusters indicated that likelihood scores did not continue to increase substantially, so we ran full analyses with 10 replicates per value of K from 1–12. No prior information about the sampling location of individuals was used. For each replicate, 1

million MCMC generations were run for burn-in followed by an additional 1 million generations. We used an admixture model that allows some individuals to have mixed cluster ancestry and allowed correlated allele frequencies among populations. When similar values of the log probability of the data were obtained across replicate runs of the same K, convergence of the run was assumed. After analyzing the full dataset, we subsampled the populations to explore whether additional substructure could be detected. These smaller datasets included: (1) all *P. streckeri* individuals, (2) Southern cluster of *P. illinoensis*, (3) Northern cluster of *P. illinoensis*, and (4) all *P. streckeri* and the Southern cluster of *P. illinoensis*. The last grouping was chosen because of the patterns detected in the full dataset for K=2 (see Fig. S6a).

We used Structure Harvester v. 0.6.94 (Earl et al. 2012) to summarize the replicates for each value of K, calculate the mean likelihoods for each K, and generate infiles for further summarizing in CLUMPP v. 1.1.2 (Jakobsson and Rosenberg 2007). The estimated coefficient matrices of all runs for each value of K were permuted in CLUMPP so that the replicates had as close a match as possible, before visualizing the clusters in *distruct* (Rosenberg 2004). Results are depicted in Fig. S6.

References for Supplementary Materials

Alroy J (2000) New methods for quantifying macroevolutionary patterns and processes. *Paleobiology*, **26**, 707–733.

Crawford AJ (2003) Relative rates of nucleotide substitution in frogs. *Journal of Molecular Evolution*, **57**, 636–641.

Drummond AJ, Rambaut A, Shapiro B, Pyrus OG (2005) Bayesian coalescent inference of past population dynamics from molecular sequences. *Molecular Biology and Evolution*, **22**, 1185–1192.

Duellman WE, Trueb L (1986) Biology of amphibians. McGraw-Hill, New York.

Earl DA, vonHoldt BM (2012) STRUCTURE HARVESTER: a website and program for visualizing STRUCTURE output and implementing the Evanno method. *Conservation Genetics Resources*, **4**, 359–361.

Evans BJ, Kelley DB, Tinsley RC, Melnick DJ, Cannatella DC (2004) A mitochondrial DNA phylogeny of African clawed frogs: phylogeography and implications for polyploidy evolution. *Molecular Phylogenetics and Evolution*, **33**, 197–213.

Evans BJ, McGuire JA, Brown RM, Andayani N, Supriatna J (2008) A coalescent framework for comparing alternative models of population structure with genetic data: evolution of Celebes toads. *Biology Letters*, **4**, 430–433.

Faivovich J, García PC, Ananias F, Lanari L, Basso NG, Wheeler WC (2004) A molecular perspective on the phylogeny of the *Hyla pulchella* species group (Anura, Hylidae). *Molecular Phylogenetics and Evolution*, **32**, 938–950.

Faivovich J, Haddad CFB, Garcia PCA, Frost DR, Campbell JA, Wheeler WC (2005) Systematic review of the frog family Hylidae, with special reference to the Hylinae: phylogenetic analysis and taxonomic revision. *Bulletin of the American Museum of Natural History*, **294**, 1–240.

García-R JC, Crawford AJ, Mendoza ÁM, Ospina O, Cardenas H, Castro F (2012) Comparative phylogeography of direct-developing frogs (Anura: Craugastoridae: *Pristimantis*) in the Southern Andes of Colombia. *PLOS One*, **7**, e46077.

Gvozdik V, Moravec J, Klütsch C, Kotlík P (2010) Phylogeography of the Middle Eastern tree frogs (*Hyla*, Hylidae, Amphibia) as inferred from nuclear and mitochondrial DNA variation, with a description of a new species. *Molecular Phylogenetics and Evolution*, **55**, 1146–1166.

Heled J (2010) Extended Bayesian skyline plot tutorial. Accessed from: http://beast.bio.ed.ac.uk/tutorials.

Heled J, Drummond AJ (2008) Bayesian inference of population size history from multiple loci. *BMC Evolutionary Biology*, **8**, 289.

Holman JA (1967) Additional Miocene anurans from Florida. Florida Academy of Sciences, Quarterly Journal, **30**, 121–140.

Holman JA (1968) Lower Oligocene amphibians from Saskatchewan. Florida Academy of Sciences, Quarterly Journal, **31**, 273–289.

Holman JA (2003) Fossil Frogs and Toads of North America. Indiana University Press, Bloomington, Indiana.

Ivanova NV, Dewaard JR, Hebert PDN (2006) An inexpensive, automation-friendly protocol for recovering high-quality DNA. *Molecular Ecology Notes*, **6**, 998–1002.

328 Jakobsson M, Rosenberg NA (2007) CLUMPP: a cluster matching and permutation
329 program for dealing with label switching and multimodality in analysis of
330 population structure. *Bioinformatics*, **23**, 1801–1806.
331 Klymus KE, Gerhardt HC (2012) AFLP markers resolve intra-specific relationships and
332 infer genetic structure among lineages of the canyon treefrog, *Hyla arenicolor*.
333 *Molecular Phylogenetics and Evolution*, **65**, 654–667.
334 Kumazawa Y, Ota H, Nishida M, Ozawa T (1996) Gene rearrangements in snake
335 mitochondrial genomes: Highly concerted evolution of control-region-like
336 sequences duplicated and inserted into a tRNA gene cluster. *Molecular Biology*
337 *and Evolution*, **13**, 1242–1254.
338 Lemmon AR, Lemmon EM (2012) High-throughput identification of informative nuclear
339 loci for shallow-scale phylogenetics and phylogeography. *Systematic Biology*, **61**,
340 745–761.
341 Lemmon EM, Lemmon AR, Cannatella DC (2007) Geological and climatic forces
342 driving speciation in the continentally distributed trilling chorus frogs
343 (*Pseudacris*). *Evolution*, **61**, 2086–2103.
344 Moriarty EC, Cannatella DC (2004) Phylogenetic relationships of the North American
345 chorus frogs (*Pseudacris*: Hylidae). *Molecular Phylogenetics and Evolution*, **30**,
346 409–420.
347 Moritz C, Schneider CJ, Wake DB (1992) Evolutionary relationships within the *Ensatina*
348 *eschscholtzii* complex confirm the ring species interpretation. *Systematic Biology*,
349 **41**, 273–291.
350 Parham JF, Donoghue PCJ, Bell CJ, Calway TD, Head JJ, Holroyd PA, Inoue JG, Irmis
351 RB, Joyce WG< Ksepka DT, Patane JSL, Smith ND, Tarver JE, van Tuinen M,
352 Yan Z, Angielczyk KD, Greenwood JM, Hipsley CA, Jacobs L, Makovicky PJ,
353 Muller J, Smith KT, Theodor JM, Warnock RCM, Benton MJ (2012) Best
354 practices for justifying fossil calibrations. *Systematic Biology*, **61**, 346–359.
355 Pauly GB, Hillis DM, Cannatella DC (2004) The history of a nearctic colonization:
356 molecular phylogenetics and biogeography of the Nearctic toads (Bufo).
357 *Evolution*, **58**, 2517–2535.
358 Pritchard JK, Stephens M, Donnelly P (2000) Inference of population structure using
359 multilocus genotype data. *Genetics*, **155**, 945–959.
360 Rosenberg NA (2004) Distruct: a program for the graphical display of population
361 structure. *Molecular Ecology Notes*, **4**, 137–138.
362 Sadlier RA, Smith SA, Bauer AM, Whitaker AH (2004) A new genus and species of live
363 bearing scincid lizard (Reptilia: Scincidae) from New Caledonia. *Journal of*
364 *Herpetology*, **38**, 320–330.
365 Smith SA, Stephens PR, Wiens JJ (2005) Replicate patterns of species richness, historical
366 biogeography, and phylogeny in Holarctic treefrogs. *Evolution*, **59**, 2433–2450.
367 Wiens JJ, Graham CH, Moen DS, Smith SA, Reeder TW (2006) Evolutionary and
368 ecological causes of the latitudinal diversity gradient in hylid frogs: treefrog trees
369 unearth the roots of high tropical diversity. *The American Naturalist*, **168**, 579–
370 596.

Table S1. List of samples in this study including taxon labels, location labels (one for each set of geographic coordinates), site labels (samples within 10 km combined), field numbers, museum catalog numbers, and locality information. Museum abbreviations are as follows: Sternberg Museum of Natural History, Fort Hays State University (MHP), Texas Natural History Collection Genetic Diversity Collection (TNHC-GDC), Texas Natural History Collection, University of Texas, Austin (TNHC), Illinois Natural History Survey (INHS), and Sam Noble Oklahoma Museum of Natural History (OMNH). An "n/a" under Collection No. indicates that vouchers and additional specimen information are available from the authors. All samples were genotyped in this study except for the outgroup, and samples that were also sequenced are indicated in the last column with numbers corresponding to Fig. 1 (map) and Fig. 3 (phylogenies).

Taxon	Location Label	Site Label	Field No.	Collection No.	County	State	Latitude	Longitude	Sequence ID
P. illinoensis	ILLN1A	ILLN1	ECM1117	TNHC-GDC 19668	Scott	Illinois	39.61908	-90.52788	22
P. illinoensis	ILLN1A	ILLN1	ECM1118	TNHC-GDC 19669	Scott	Illinois	39.61908	-90.52788	
P. illinoensis	ILLN1B	ILLN1	INHS8240.1	INHS8240	Scott	Illinois	39.6296	-90.5359	
P. illinoensis	ILLN1B	ILLN1	INHS8240.2	INHS8240	Scott	Illinois	39.6296	-90.5359	
P. illinoensis	ILLN1C	ILLN1	INHS8241.1	INHS8241	Scott	Illinois	39.6711	-90.57	
P. illinoensis	ILLN1C	ILLN1	INHS8241.10	INHS8241	Scott	Illinois	39.6711	-90.57	
P. illinoensis	ILLN1C	ILLN1	INHS8241.2	INHS8241	Scott	Illinois	39.6711	-90.57	
P. illinoensis	ILLN1C	ILLN1	INHS8241.4	INHS8241	Scott	Illinois	39.6711	-90.57	
P. illinoensis	ILLN1C	ILLN1	INHS8241.5	INHS8241	Scott	Illinois	39.6711	-90.57	
P. illinoensis	ILLN1C	ILLN1	INHS8241.6	INHS8241	Scott	Illinois	39.6711	-90.57	
P. illinoensis	ILLN1C	ILLN1	INHS8241.7	INHS8241	Scott	Illinois	39.6711	-90.57	
P. illinoensis	ILLN2	ILLN2	INHS8239.1	INHS8239	Morgan	Illinois	39.83895	-90.55004	
P. illinoensis	ILLN2	ILLN2	INHS8239.2	INHS8239	Morgan	Illinois	39.83895	-90.55004	
P. illinoensis	ILLN2	ILLN2	INHS8239.3	INHS8239	Morgan	Illinois	39.83895	-90.55004	
P. illinoensis	ILLN2	ILLN2	INHS8239.4	INHS8239	Morgan	Illinois	39.83895	-90.55004	
P. illinoensis	ILLN3A	ILLN3	INHS3708.1	INHS3708	Cass	Illinois	39.92416	-90.39033	
P. illinoensis	ILLN3A	ILLN3	INHS8238.1	INHS8238	Cass	Illinois	39.92416	-90.39033	
P. illinoensis	ILLN3A	ILLN3	INHS8238.2	INHS8238	Cass	Illinois	39.92416	-90.39033	
P. illinoensis	ILLN3B	ILLN3	INHS3705.1	INHS3705	Cass	Illinois	39.95634	-90.40802	
P. illinoensis	ILLN3B	ILLN3	INHS3705.2	INHS3705	Cass	Illinois	39.95634	-90.40802	
P. illinoensis	ILLN3B	ILLN3	INHS3705.3	INHS3705	Cass	Illinois	39.95634	-90.40802	
P. illinoensis	ILLN3B	ILLN3	INHS3705.4	INHS3705	Cass	Illinois	39.95634	-90.40802	
P. illinoensis	ILLN3C	ILLN3	ECM1121	TNHC-GDC 19672	Cass	Illinois	40.00827	-90.44594	17
P. illinoensis	ILLN3C	ILLN3	ECM1122	TNHC-GDC 19673	Cass	Illinois	40.00827	-90.44594	
P. illinoensis	ILLN3D	ILLN3	INHS2003.3	TNHC-GDC 20343	Cass	Illinois	40.0175	-90.4242	
P. illinoensis	ILLN3D	ILLN3	INHS2003.4	TNHC-GDC 20344	Cass	Illinois	40.0175	-90.4242	
P. illinoensis	ILLN3D	ILLN3	INHS2003.5	TNHC-GDC 20345	Cass	Illinois	40.0175	-90.4242	
P. illinoensis	ILLN3D	ILLN3	INHS2003.6	TNHC-GDC 20328	Cass	Illinois	40.0175	-90.4242	
P. illinoensis	ILLN4	ILLN4	INHS1719.1	INHS1719	Cass	Illinois	40.0768	-89.9987	
P. illinoensis	ILLN4	ILLN4	INHS1719.10	INHS1719	Cass	Illinois	40.0768	-89.9987	
P. illinoensis	ILLN4	ILLN4	INHS1719.11	INHS1719	Cass	Illinois	40.0768	-89.9987	
P. illinoensis	ILLN4	ILLN4	INHS1719.12	INHS1719	Cass	Illinois	40.0768	-89.9987	
P. illinoensis	ILLN4	ILLN4	INHS1719.13	INHS1719	Cass	Illinois	40.0768	-89.9987	
P. illinoensis	ILLN4	ILLN4	INHS1719.14	INHS1719	Cass	Illinois	40.0768	-89.9987	
P. illinoensis	ILLN4	ILLN4	INHS1719.2	INHS1719	Cass	Illinois	40.0768	-89.9987	
P. illinoensis	ILLN4	ILLN4	INHS1719.3	INHS1719	Cass	Illinois	40.0768	-89.9987	
P. illinoensis	ILLN4	ILLN4	INHS1719.4	INHS1719	Cass	Illinois	40.0768	-89.9987	
P. illinoensis	ILLN4	ILLN4	INHS1719.5	INHS1719	Cass	Illinois	40.0768	-89.9987	
P. illinoensis	ILLN4	ILLN4	INHS1719.6	INHS1719	Cass	Illinois	40.0768	-89.9987	
P. illinoensis	ILLN4	ILLN4	INHS1719.7	INHS1719	Cass	Illinois	40.0768	-89.9987	
P. illinoensis	ILLN4	ILLN4	INHS1719.8	INHS1719	Cass	Illinois	40.0768	-89.9987	
P. illinoensis	ILLN4	ILLN4	INHS1719.9	INHS1719	Cass	Illinois	40.0768	-89.9987	
P. illinoensis	ILLN4	ILLN4	INHS1955.1	INHS1955	Cass	Illinois	40.0768	-89.9987	
P. illinoensis	ILLN4	ILLN4	INHS1955.2	INHS1955	Cass	Illinois	40.0768	-89.9987	
P. illinoensis	ILLN4	ILLN4	INHS1955.3	INHS1955	Cass	Illinois	40.0768	-89.9987	
P. illinoensis	ILLN4	ILLN4	INHS1955.4	INHS1955	Cass	Illinois	40.0768	-89.9987	
P. illinoensis	ILLN4	ILLN4	INHS1955.5	INHS1955	Cass	Illinois	40.0768	-89.9987	
P. illinoensis	ILLN4	ILLN4	INHS1955.6	INHS1955	Cass	Illinois	40.0768	-89.9987	
P. illinoensis	ILLN4	ILLN4	INHS1955.7	INHS1955	Cass	Illinois	40.0768	-89.9987	
P. illinoensis	ILLN5	ILLN5	INHS1722	INHS1722	Menard	Illinois	40.0979	-89.8746	21
P. illinoensis	ILLN6	ILLN6	INHS1890.1	INHS1890	Mason	Illinois	40.1169	-90.213	
P. illinoensis	ILLN6	ILLN6	INHS1890.10	INHS1890	Mason	Illinois	40.1169	-90.213	
P. illinoensis	ILLN6	ILLN6	INHS1890.2	INHS1890	Mason	Illinois	40.1169	-90.213	
P. illinoensis	ILLN6	ILLN6	INHS1890.3	INHS1890	Mason	Illinois	40.1169	-90.213	
P. illinoensis	ILLN6	ILLN6	INHS1890.4	INHS1890	Mason	Illinois	40.1169	-90.213	
P. illinoensis	ILLN6	ILLN6	INHS1890.5	INHS1890	Mason	Illinois	40.1169	-90.213	
P. illinoensis	ILLN6	ILLN6	INHS1890.6	INHS1890	Mason	Illinois	40.1169	-90.213	
P. illinoensis	ILLN6	ILLN6	INHS1890.7	INHS1890	Mason	Illinois	40.1169	-90.213	
P. illinoensis	ILLN6	ILLN6	INHS1890.8	INHS1890	Mason	Illinois	40.1169	-90.213	
P. illinoensis	ILLN6	ILLN6	INHS1890.9	INHS1890	Mason	Illinois	40.1169	-90.213	
P. illinoensis	ILLN7	ILLN7	INHS 1958.11	INHS1958	Mason	Illinois	40.2308	-90.1075	20
P. illinoensis	ILLN7	ILLN7	INHS1958.1	INHS1958	Mason	Illinois	40.2308	-90.1075	
P. illinoensis	ILLN7	ILLN7	INHS1958.10	INHS1958	Mason	Illinois	40.2308	-90.1075	
P. illinoensis	ILLN7	ILLN7	INHS1958.2	INHS1958	Mason	Illinois	40.2308	-90.1075	
P. illinoensis	ILLN7	ILLN7	INHS1958.3	INHS1958	Mason	Illinois	40.2308	-90.1075	
P. illinoensis	ILLN7	ILLN7	INHS1958.4	INHS1958	Mason	Illinois	40.2308	-90.1075	
P. illinoensis	ILLN7	ILLN7	INHS1958.5	INHS1958	Mason	Illinois	40.2308	-90.1075	

P. illinoensis	ILLN7	ILLN7	INHS1958.6	INHS1958	Mason	Illinois	40.2308	-90.1075	
P. illinoensis	ILLN7	ILLN7	INHS1958.7	INHS1958	Mason	Illinois	40.2308	-90.1075	
P. illinoensis	ILLN7	ILLN7	INHS1958.8	INHS1958	Mason	Illinois	40.2308	-90.1075	
P. illinoensis	ILLN7	ILLN7	INHS1958.9	INHS1958	Mason	Illinois	40.2308	-90.1075	
P. illinoensis	ILLN8	ILLN8	INHS2554	INHS2554	Mason	Illinois	40.2322	-89.6943	19
P. illinoensis	ILLN8	ILLN8	INHS1985.1	INHS1985	Mason	Illinois	40.2322	-89.6943	
P. illinoensis	ILLN8	ILLN8	INHS1985.10	INHS1985	Mason	Illinois	40.2322	-89.6943	
P. illinoensis	ILLN8	ILLN8	INHS1985.11	INHS1985	Mason	Illinois	40.2322	-89.6943	
P. illinoensis	ILLN8	ILLN8	INHS1985.12	INHS1985	Mason	Illinois	40.2322	-89.6943	
P. illinoensis	ILLN8	ILLN8	INHS1985.13	INHS1985	Mason	Illinois	40.2322	-89.6943	
P. illinoensis	ILLN8	ILLN8	INHS1985.14	INHS1985	Mason	Illinois	40.2322	-89.6943	
P. illinoensis	ILLN8	ILLN8	INHS1985.15	INHS1985	Mason	Illinois	40.2322	-89.6943	
P. illinoensis	ILLN8	ILLN8	INHS1985.16	INHS1985	Mason	Illinois	40.2322	-89.6943	
P. illinoensis	ILLN8	ILLN8	INHS1985.2	INHS1985	Mason	Illinois	40.2322	-89.6943	
P. illinoensis	ILLN8	ILLN8	INHS1985.3	INHS1985	Mason	Illinois	40.2322	-89.6943	
P. illinoensis	ILLN8	ILLN8	INHS1985.4	INHS1985	Mason	Illinois	40.2322	-89.6943	
P. illinoensis	ILLN8	ILLN8	INHS1985.5	INHS1985	Mason	Illinois	40.2322	-89.6943	
P. illinoensis	ILLN8	ILLN8	INHS1985.6	INHS1985	Mason	Illinois	40.2322	-89.6943	
P. illinoensis	ILLN8	ILLN8	INHS1985.7	INHS1985	Mason	Illinois	40.2322	-89.6943	
P. illinoensis	ILLN8	ILLN8	INHS1985.8	INHS1985	Mason	Illinois	40.2322	-89.6943	
P. illinoensis	ILLN8	ILLN8	INHS1985.9	INHS1985	Mason	Illinois	40.2322	-89.6943	
P. illinoensis	ILLN9A	ILLN9	INHS1911	INHS1911	Tazewell	Illinois	40.3807	-89.6618	
P. illinoensis	ILLN9A	ILLN9	INHS1912	INHS1912	Tazewell	Illinois	40.3807	-89.6618	
P. illinoensis	ILLN9A	ILLN9	INHS1913	INHS1913	Tazewell	Illinois	40.3807	-89.6618	
P. illinoensis	ILLN9A	ILLN9	INHS1914	INHS1914	Tazewell	Illinois	40.3807	-89.6618	
P. illinoensis	ILLN9A	ILLN9	INHS1915	INHS1915	Tazewell	Illinois	40.3807	-89.6618	
P. illinoensis	ILLN9A	ILLN9	INHS1916	INHS1916	Tazewell	Illinois	40.3807	-89.6618	
P. illinoensis	ILLN9A	ILLN9	INHS1917	INHS1917	Tazewell	Illinois	40.3807	-89.6618	
P. illinoensis	ILLN9B	ILLN9	INHS1906.2	INHS1906	Tazewell	Illinois	40.3942	-89.6823	23
P. illinoensis	ILLN9B	ILLN9	INHS1892	INHS1892	Tazewell	Illinois	40.3942	-89.6823	
P. illinoensis	ILLN9B	ILLN9	INHS1893	INHS1893	Tazewell	Illinois	40.3942	-89.6823	
P. illinoensis	ILLN9B	ILLN9	INHS1894	INHS1894	Tazewell	Illinois	40.3942	-89.6823	
P. illinoensis	ILLN9B	ILLN9	INHS1895	INHS1895	Tazewell	Illinois	40.3942	-89.6823	
P. illinoensis	ILLN9B	ILLN9	INHS1896	INHS1896	Tazewell	Illinois	40.3942	-89.6823	
P. illinoensis	ILLN9B	ILLN9	INHS1897	INHS1897	Tazewell	Illinois	40.3942	-89.6823	
P. illinoensis	ILLN9B	ILLN9	INHS1898	INHS1898	Tazewell	Illinois	40.3942	-89.6823	
P. illinoensis	ILLN9B	ILLN9	INHS1899	INHS1899	Tazewell	Illinois	40.3942	-89.6823	
P. illinoensis	ILLN9B	ILLN9	INHS1900	INHS1900	Tazewell	Illinois	40.3942	-89.6823	
P. illinoensis	ILLN9B	ILLN9	INHS1901	INHS1901	Tazewell	Illinois	40.3942	-89.6823	
P. illinoensis	ILLN9B	ILLN9	INHS1902	INHS1902	Tazewell	Illinois	40.3942	-89.6823	
P. illinoensis	ILLN9B	ILLN9	INHS1903	INHS1903	Tazewell	Illinois	40.3942	-89.6823	
P. illinoensis	ILLN9B	ILLN9	INHS1904	INHS1904	Tazewell	Illinois	40.3942	-89.6823	
P. illinoensis	ILLN9B	ILLN9	INHS1905	INHS1905	Tazewell	Illinois	40.3942	-89.6823	
P. illinoensis	ILLN10	ILLN10	INHS2221	INHS2221	Mason	Illinois	40.3829	-89.8191	18
P. illinoensis	ILLN10	ILLN10	INHS1887.1	INHS1887	Mason	Illinois	40.3829	-89.8191	
P. illinoensis	ILLN10	ILLN10	INHS1887.2	INHS1887	Mason	Illinois	40.3829	-89.8191	
P. illinoensis	ILLN10	ILLN10	INHS1887.3	INHS1887	Mason	Illinois	40.3829	-89.8191	
P. illinoensis	ILLN10	ILLN10	INHS1887.4	INHS1887	Mason	Illinois	40.3829	-89.8191	
P. illinoensis	ILLN10	ILLN10	INHS1887.5	INHS1887	Mason	Illinois	40.3829	-89.8191	
P. illinoensis	ILLN10	ILLN10	INHS1887.6	INHS1887	Mason	Illinois	40.3829	-89.8191	
P. illinoensis	ILLN10	ILLN10	INHS1907	INHS1907	Mason	Illinois	40.3829	-89.8191	
P. illinoensis	ILLN10	ILLN10	INHS1908	INHS1908	Mason	Illinois	40.3829	-89.8191	
P. illinoensis	ILLN10	ILLN10	INHS1909	INHS1909	Mason	Illinois	40.3829	-89.8191	
P. illinoensis	ILLN10	ILLN10	INHS1910	INHS1910	Mason	Illinois	40.3829	-89.8191	
P. illinoensis	ILLN10	ILLN10	INHS2212	INHS2212	Mason	Illinois	40.3829	-89.8191	
P. illinoensis	ILLN10	ILLN10	INHS2213	INHS2213	Mason	Illinois	40.3829	-89.8191	
P. illinoensis	ILLN10	ILLN10	INHS2214	INHS2214	Mason	Illinois	40.3829	-89.8191	
P. illinoensis	ILLN10	ILLN10	INHS2215	INHS2215	Mason	Illinois	40.3829	-89.8191	
P. illinoensis	ILLN10	ILLN10	INHS2216	INHS2216	Mason	Illinois	40.3829	-89.8191	
P. illinoensis	ILLN10	ILLN10	INHS2217	INHS2217	Mason	Illinois	40.3829	-89.8191	
P. illinoensis	ILLN10	ILLN10	INHS2218	INHS2218	Mason	Illinois	40.3829	-89.8191	
P. illinoensis	ILLN10	ILLN10	INHS2219	INHS2219	Mason	Illinois	40.3829	-89.8191	
P. illinoensis	ILLN10	ILLN10	INHS2220	INHS2220	Mason	Illinois	40.3829	-89.8191	
P. illinoensis	ILLCA	ILLC	ECM1119	TNHC-GDC 19670	Madison	Illinois	38.78299	-90.02459	24
P. illinoensis	ILLCA	ILLC	ECM1120	TNHC-GDC 19671	Madison	Illinois	38.78299	-90.02459	
P. illinoensis	ILLCB	ILLC	ECM1123	TNHC-GDC 19674	Madison	Illinois	38.78365	-90.0336	25
P. illinoensis	ILLCB	ILLC	ECM1124	TNHC-GDC 19675	Madison	Illinois	38.78365	-90.0336	
P. illinoensis	ILLCC	ILLC	INHS2003.9	TNHC-GDC 20286	Madison	Illinois	38.7969	-90.0389	
P. illinoensis	ILLSA	ILLS	INHS1960.1	INHS1960	Alexander	Illinois	37.11798	-89.33667	
P. illinoensis	ILLSA	ILLS	INHS1960.2	INHS1960	Alexander	Illinois	37.11798	-89.33667	
P. illinoensis	ILLSA	ILLS	INHS1960.3	INHS1960	Alexander	Illinois	37.11798	-89.33667	
P. illinoensis	ILLSA	ILLS	INHS1960.4	INHS1960	Alexander	Illinois	37.11798	-89.33667	
P. illinoensis	ILLSA	ILLS	INHS1960.5	INHS1960	Alexander	Illinois	37.11798	-89.33667	
P. illinoensis	ILLSA	ILLS	INHS1960.6	INHS1960	Alexander	Illinois	37.11798	-89.33667	
P. illinoensis	ILLSB	ILLS	ECM2856	n/a	Alexander	Illinois	37.13389	-89.38111	26
P. illinoensis	ILLSB	ILLS	ECM2857	n/a	Alexander	Illinois	37.13389	-89.38111	
P. illinoensis	ILLSB	ILLS	ECM2858	n/a	Alexander	Illinois	37.13389	-89.38111	

P. illinoensis	ILLSC	ILLS	INHS1961.12	INHS1961	Alexander	Illinois	37.1841	-89.3304	27
P. illinoensis	ILLSC	ILLS	INHS1961.1	INHS1961	Alexander	Illinois	37.1841	-89.3304	
P. illinoensis	ILLSC	ILLS	INHS1961.10	INHS1961	Alexander	Illinois	37.1841	-89.3304	
P. illinoensis	ILLSC	ILLS	INHS1961.11	INHS1961	Alexander	Illinois	37.1841	-89.3304	
P. illinoensis	ILLSC	ILLS	INHS1961.2	INHS1961	Alexander	Illinois	37.1841	-89.3304	
P. illinoensis	ILLSC	ILLS	INHS1961.3	INHS1961	Alexander	Illinois	37.1841	-89.3304	
P. illinoensis	ILLSC	ILLS	INHS1961.4	INHS1961	Alexander	Illinois	37.1841	-89.3304	
P. illinoensis	ILLSC	ILLS	INHS1961.5	INHS1961	Alexander	Illinois	37.1841	-89.3304	
P. illinoensis	ILLSC	ILLS	INHS1961.6	INHS1961	Alexander	Illinois	37.1841	-89.3304	
P. illinoensis	ILLSC	ILLS	INHS1961.7	INHS1961	Alexander	Illinois	37.1841	-89.3304	
P. illinoensis	ILLSC	ILLS	INHS1961.8	INHS1961	Alexander	Illinois	37.1841	-89.3304	
P. illinoensis	ILLSC	ILLS	INHS1961.9	INHS1961	Alexander	Illinois	37.1841	-89.3304	
P. illinoensis	MIS1A	MIS1A	ECM4395	n/a	Mississippi	Missouri	36.77651	-89.19439	30
P. illinoensis	MIS1B	MIS1B	ECM4370	n/a	Mississippi	Missouri	36.7851	-89.31423	31
P. illinoensis	MIS1B	MIS1B	ECM4361	n/a	Mississippi	Missouri	36.7851	-89.31423	
P. illinoensis	MIS1B	MIS1B	ECM4362	n/a	Mississippi	Missouri	36.7851	-89.31423	
P. illinoensis	MIS1B	MIS1B	ECM4363	n/a	Mississippi	Missouri	36.7851	-89.31423	
P. illinoensis	MIS1B	MIS1B	ECM4364	n/a	Mississippi	Missouri	36.7851	-89.31423	
P. illinoensis	MIS1B	MIS1B	ECM4365	n/a	Mississippi	Missouri	36.7851	-89.31423	
P. illinoensis	MIS1B	MIS1B	ECM4366	n/a	Mississippi	Missouri	36.7851	-89.31423	
P. illinoensis	MIS1B	MIS1B	ECM4367	n/a	Mississippi	Missouri	36.7851	-89.31423	
P. illinoensis	MIS1B	MIS1B	ECM4368	n/a	Mississippi	Missouri	36.7851	-89.31423	
P. illinoensis	MIS1B	MIS1B	ECM4369	n/a	Mississippi	Missouri	36.7851	-89.31423	
P. illinoensis	MIS1B	MIS1B	ECM4371	n/a	Mississippi	Missouri	36.7851	-89.31423	
P. illinoensis	MIS1B	MIS1B	ECM4372	n/a	Mississippi	Missouri	36.7851	-89.31423	
P. illinoensis	MIS1B	MIS1B	ECM4373	n/a	Mississippi	Missouri	36.7851	-89.31423	
P. illinoensis	MIS1B	MIS1B	ECM4374	n/a	Mississippi	Missouri	36.7851	-89.31423	
P. illinoensis	MIS1B	MIS1B	ECM4375	n/a	Mississippi	Missouri	36.7851	-89.31423	
P. illinoensis	MIS1B	MIS1B	ECM4376	n/a	Mississippi	Missouri	36.7851	-89.31423	
P. illinoensis	MIS1B	MIS1B	ECM4377	n/a	Mississippi	Missouri	36.7851	-89.31423	
P. illinoensis	MIS1B	MIS1B	ECM4378	n/a	Mississippi	Missouri	36.7851	-89.31423	
P. illinoensis	MIS1B	MIS1B	ECM4379	n/a	Mississippi	Missouri	36.7851	-89.31423	
P. illinoensis	MIS1B	MIS1B	ECM4380	n/a	Mississippi	Missouri	36.7851	-89.31423	
P. illinoensis	MIS1B	MIS1B	ECM4360	n/a	Mississippi	Missouri	36.7851	-89.31423	
P. illinoensis	MIS2	MIS2	ECM0090	TNHC62346	Scott	Missouri	37.0667	-89.5667	32
P. illinoensis	MIS2	MIS2	ECM0091	TNHC62347	Scott	Missouri	37.0667	-89.5667	
P. illinoensis	MIS2	MIS2	ECM92	TNHC62348	Scott	Missouri	37.0667	-89.5667	
P. illinoensis	MIS2	MIS2	ECM93	TNHC62349	Scott	Missouri	37.0667	-89.5667	
P. illinoensis	MIS2	MIS2	ECM94	TNHC62350	Scott	Missouri	37.0667	-89.5667	
P. illinoensis	ARK6	ARK6	ECM0002	TNHC62352	Clay	Arkansas	36.3308	-90.10899	29
P. illinoensis	ARK6	ARK6	ECM10	TNHC62345	Clay	Arkansas	36.3308	-90.10899	
P. illinoensis	ARK6	ARK6	ECM4	TNHC62339	Clay	Arkansas	36.3308	-90.10899	
P. illinoensis	ARK6	ARK6	ECM5	TNHC62340	Clay	Arkansas	36.3308	-90.10899	
P. illinoensis	ARK6	ARK6	ECM6	TNHC62341	Clay	Arkansas	36.3308	-90.10899	
P. illinoensis	ARK6	ARK6	ECM7	TNHC62342	Clay	Arkansas	36.3308	-90.10899	
P. illinoensis	ARK6	ARK6	ECMspec.3	TNHC62353	Clay	Arkansas	36.3308	-90.10899	
P. illinoensis	ARK6	ARK6	ECM0001	TNHC62351	Clay	Arkansas	36.3308	-90.10899	28
P. streckeri	ARK1A	ARK1	MHP15479	MHP15479	Conway	Arkansas	35.11889	-92.74148	
P. streckeri	ARK1A	ARK1	MHP15480	MHP15480	Conway	Arkansas	35.11889	-92.74148	
P. streckeri	ARK1A	ARK1	MHP15481	MHP15481	Conway	Arkansas	35.11889	-92.74148	
P. streckeri	ARK1A	ARK1	MHP15482	MHP15482	Conway	Arkansas	35.11889	-92.74148	
P. streckeri	ARK1A	ARK1	MHP15483	MHP15483	Conway	Arkansas	35.11889	-92.74148	
P. streckeri	ARK1B	ARK1	MHP15484	MHP15484	Conway	Arkansas	35.121284	-92.74269	
P. streckeri	ARK1B	ARK1	MHP15485	MHP15485	Conway	Arkansas	35.121284	-92.74269	
P. streckeri	ARK1B	ARK1	MHP15486	MHP15486	Conway	Arkansas	35.121284	-92.74269	
P. streckeri	ARK1B	ARK1	MHP15487	MHP15487	Conway	Arkansas	35.121284	-92.74269	
P. streckeri	ARK1B	ARK1	MHP15488	MHP15488	Conway	Arkansas	35.121284	-92.74269	
P. streckeri	ARK1B	ARK1	MHP15489	MHP15489	Conway	Arkansas	35.121284	-92.74269	
P. streckeri	ARK1B	ARK1	MHP15490	MHP15490	Conway	Arkansas	35.121284	-92.74269	
P. streckeri	ARK1B	ARK1	MHP15491	MHP15491	Conway	Arkansas	35.121284	-92.74269	
P. streckeri	ARK1B	ARK1	MHP15492	MHP15492	Conway	Arkansas	35.121284	-92.74269	
P. streckeri	ARK1B	ARK1	MHP15493	MHP15493	Conway	Arkansas	35.121284	-92.74269	
P. streckeri	ARK1B	ARK1	MHP15494	MHP15494	Conway	Arkansas	35.121284	-92.74269	
P. streckeri	ARK1B	ARK1	MHP15495	MHP15495	Conway	Arkansas	35.121284	-92.74269	
P. streckeri	ARK1B	ARK1	MHP15496	MHP15496	Conway	Arkansas	35.121284	-92.74269	
P. streckeri	ARK1B	ARK1	MHP15497	MHP15497	Conway	Arkansas	35.121284	-92.74269	
P. streckeri	ARK1B	ARK1	MHP15498	MHP15498	Conway	Arkansas	35.121284	-92.74269	
P. streckeri	ARK2	ARK2	MHP15499	MHP15499	Conway	Arkansas	35.136869	-92.82369	13
P. streckeri	ARK2	ARK2	MHP15500	MHP15500	Conway	Arkansas	35.136869	-92.82369	
P. streckeri	ARK2	ARK2	MHP15501	MHP15501	Conway	Arkansas	35.136869	-92.82369	
P. streckeri	ARK2	ARK2	MHP15502	MHP15502	Conway	Arkansas	35.136869	-92.82369	
P. streckeri	ARK2	ARK2	MHP15503	MHP15503	Conway	Arkansas	35.136869	-92.82369	
P. streckeri	ARK2	ARK2	MHP15504	MHP15504	Conway	Arkansas	35.136869	-92.82369	
P. streckeri	ARK2	ARK2	MHP15505	MHP15505	Conway	Arkansas	35.136869	-92.82369	
P. streckeri	ARK2	ARK2	MHP15506	MHP15506	Conway	Arkansas	35.136869	-92.82369	
P. streckeri	ARK2	ARK2	MHP15507	MHP15507	Conway	Arkansas	35.136869	-92.82369	
P. streckeri	ARK2	ARK2	MHP15508	MHP15508	Conway	Arkansas	35.136869	-92.82369	

P. streckeri	ARK2	ARK2	MHP15509	MHP15509	Conway	Arkansas	35.136869	-92.82369	
P. streckeri	ARK3	ARK3	JTC2581	TNHC63382	Conway	Arkansas	35.2503	-92.6833	12
P. streckeri	ARK3	ARK3	JTC2582	TNHC63383	Conway	Arkansas	35.2503	-92.6833	
P. streckeri	ARK3	ARK3	JTC2583	TNHC63384	Conway	Arkansas	35.2503	-92.6833	
P. streckeri	ARK3	ARK3	JTC2584	TNHC63385	Conway	Arkansas	35.2503	-92.6833	
P. streckeri	ARK3	ARK3	JTC2585	TNHC63386	Conway	Arkansas	35.2503	-92.6833	
P. streckeri	ARK4A	ARK4	MHP15510	MHP15510	Yell	Arkansas	35.161302	-93.12036	16
P. streckeri	ARK4B	ARK4	MHP15511	MHP15511	Yell	Arkansas	35.165822	-93.1152	
P. streckeri	ARK4B	ARK4	MHP15512	MHP15512	Yell	Arkansas	35.165822	-93.1152	
P. streckeri	ARK4B	ARK4	MHP15513	MHP15513	Yell	Arkansas	35.165822	-93.1152	
P. streckeri	ARK4B	ARK4	MHP15514	MHP15514	Yell	Arkansas	35.165822	-93.1152	
P. streckeri	ARK4B	ARK4	MHP15515	MHP15515	Yell	Arkansas	35.165822	-93.1152	
P. streckeri	ARK4B	ARK4	MHP15516	MHP15516	Yell	Arkansas	35.165822	-93.1152	
P. streckeri	ARK4B	ARK4	MHP15517	MHP15517	Yell	Arkansas	35.165822	-93.1152	
P. streckeri	ARK4B	ARK4	MHP15518	MHP15518	Yell	Arkansas	35.165822	-93.1152	
P. streckeri	ARK5A	ARK5A	MHP15473	MHP15473	Logan	Arkansas	35.365668	-93.70207	15
P. streckeri	ARK5A	ARK5A	MHP15474	MHP15474	Logan	Arkansas	35.365668	-93.70207	
P. streckeri	ARK5A	ARK5A	MHP15475	MHP15475	Logan	Arkansas	35.365668	-93.70207	
P. streckeri	ARK5A	ARK5A	MHP15476	MHP15476	Logan	Arkansas	35.365668	-93.70207	
P. streckeri	ARK5A	ARK5A	MHP15477	MHP15477	Logan	Arkansas	35.365668	-93.70207	
P. streckeri	ARK5A	ARK5A	MHP15478	MHP15478	Logan	Arkansas	35.365668	-93.70207	
P. streckeri	ARK5B	ARK5B	MHP15689	MHP15689	Johnson	Arkansas	35.38968	-93.62222	14
P. streckeri	ARK5B	ARK5B	MHP15690	MHP15690	Johnson	Arkansas	35.38968	-93.62222	
P. streckeri	ARK5B	ARK5B	MHP15691	MHP15691	Johnson	Arkansas	35.38968	-93.62222	
P. streckeri	KAN1A	KAN1	MHP8249	MHP8249	Barber	Kansas	37.44944	-98.50119	
P. streckeri	KAN1B	KAN1	MHP8259	MHP8259	Kingman	Kansas	37.45391	-98.44633	3
P. streckeri	KAN1C	KAN1	MHP8224	MHP8224	Pratt	Kansas	37.47086	-98.51404	
P. streckeri	KAN1D	KAN1	MHP8225	MHP8225	Pratt	Kansas	37.47102	-98.47065	
P. streckeri	KAN1E	KAN1	MHP8220	MHP8220	Pratt	Kansas	37.49986	-98.54001	4
P. streckeri	KAN2	KAN2	MHP8258	MHP8258	Barber	Kansas	37.19356	-98.36659	1
P. streckeri	KAN3	KAN3	P-1	TNHC-GDC 20520	Harper	Kansas	37.2	-98.0833	2
P. streckeri	OKL1	OKL1	MHP14745	MHP14745	Woodward	Oklahoma	36.45341	-99.30602	5
P. streckeri	OKL1	OKL1	MHP14746	MHP14746	Woodward	Oklahoma	36.45341	-99.30602	
P. streckeri	OKL1	OKL1	MHP14747	MHP14747	Woodward	Oklahoma	36.45341	-99.30602	
P. streckeri	OKL1	OKL1	MHP14748	MHP14748	Woodward	Oklahoma	36.45341	-99.30602	
P. streckeri	OKL1	OKL1	MHP14749	MHP14749	Woodward	Oklahoma	36.45341	-99.30602	
P. streckeri	OKL2A	OKL2	MGP 02040701	TNHC-GDC 19984	Cleveland	Oklahoma	35.066153	-97.28845	
P. streckeri	OKL2A	OKL2	MGP 02040702	TNHC-GDC 20011	Cleveland	Oklahoma	35.066153	-97.28845	
P. streckeri	OKL2A	OKL2	MGP 02040705	TNHC-GDC 19975	Cleveland	Oklahoma	35.066153	-97.28845	
P. streckeri	OKL2A	OKL2	MGP 02040707	TNHC-GDC 20038	Cleveland	Oklahoma	35.066153	-97.28845	
P. streckeri	OKL2A	OKL2	MGP 02040709	TNHC-GDC 19993	Cleveland	Oklahoma	35.066153	-97.28845	
P. streckeri	OKL2A	OKL2	MGP 02040710	TNHC-GDC 20020	Cleveland	Oklahoma	35.066153	-97.28845	
P. streckeri	OKL2A	OKL2	MGP 02040713	TNHC-GDC 20029	Cleveland	Oklahoma	35.066153	-97.28845	
P. streckeri	OKL2A	OKL2	MGP 02049704	TNHC-GDC 19967	Cleveland	Oklahoma	35.066153	-97.28845	
P. streckeri	OKL2B	OKL2	DBS 1	TNHC-GDC 21027	Cleveland	Oklahoma	35.087074	-97.21822	
P. streckeri	OKL2B	OKL2	DBS 2	TNHC-GDC 21028	Cleveland	Oklahoma	35.087074	-97.21822	
P. streckeri	OKL2B	OKL2	DBS 3	TNHC-GDC 21029	Cleveland	Oklahoma	35.087074	-97.21822	
P. streckeri	OKL2B	OKL2	DBS 4	TNHC-GDC 21019	Cleveland	Oklahoma	35.087074	-97.21822	
P. streckeri	OKL2C	OKL2	OMNH39833	OMNH39833	Cleveland	Oklahoma	35.087271	-97.22086	7
P. streckeri	OKL2C	OKL2	OMNH39834	OMNH39834	Cleveland	Oklahoma	35.087271	-97.22086	
P. streckeri	OKL2C	OKL2	OMNH39835	OMNH39835	Cleveland	Oklahoma	35.087271	-97.22086	
P. streckeri	OKL2D	OKL2	OMNH39832	OMNH39832	Cleveland	Oklahoma	35.087404	-97.21026	
P. streckeri	OKL3	OKL3	OMNH41972	OMNH41972	Atoka	Oklahoma	34.558848	-95.94736	6
P. streckeri	TEX1	TEX1	ECM 23	TNHC62302	Travis	Texas	30.32177	-97.8034	
P. streckeri	TEX1	TEX1	ECM0021	TNHC62301	Travis	Texas	30.32177	-97.8034	
P. streckeri	TEX1	TEX1	ECM0022	TNHC62300	Travis	Texas	30.32177	-97.8034	
P. streckeri	TEX1	TEX1	MGP 01020901	TNHC-GDC 20028	Travis	Texas	30.3218	-97.8034	
P. streckeri	TEX1	TEX1	MGP 01020902	TNHC-GDC 20019	Travis	Texas	30.3218	-97.8034	
P. streckeri	TEX1	TEX1	MGP 01020904	TNHC-GDC 20001	Travis	Texas	30.3218	-97.8034	
P. streckeri	TEX1	TEX1	MGP 01020905	TNHC-GDC 19966	Travis	Texas	30.3218	-97.8034	
P. streckeri	TEX1	TEX1	MGP 01021307	TNHC-GDC 20037	Travis	Texas	30.3218	-97.8034	
P. streckeri	TEX1	TEX1	MGP 01021308	TNHC-GDC 19983	Travis	Texas	30.3218	-97.8034	
P. streckeri	TEX1	TEX1	MGP 01021309	TNHC-GDC 20010	Travis	Texas	30.3218	-97.8034	
P. streckeri	TEX1	TEX1	P-2	TNHC62317	Travis	Texas	30.32177	-97.8034	
P. streckeri	TEX1	TEX1	P-4	TNHC62319	Travis	Texas	30.32177	-97.8034	
P. streckeri	TEX1	TEX1	P-5	TNHC62320	Travis	Texas	30.32177	-97.8034	
P. streckeri	TEX1	TEX1	P-6	TNHC62321	Travis	Texas	30.32177	-97.8034	
P. streckeri	TEX1	TEX1	P-7	TNHC62322	Travis	Texas	30.32177	-97.8034	
P. streckeri	TEX1	TEX1	P-8	TNHC62323	Travis	Texas	30.32177	-97.8034	
P. streckeri	TEX1	TEX1	P-3	TNHC62318	Travis	Texas	30.32177	-97.8034	10
P. streckeri	TEX1	TEX1	ECM7051	n/a	Travis	Texas	30.32177	-97.8034	11
P. streckeri	TEX2	TEX2	ECM2690	n/a	Mason	Texas	30.8255	-99.2182	9
P. streckeri	TEX3	TEX3	MHP14750	MHP14750	Bosque	Texas	31.65421	-97.47136	8
P. ornata			ECM0033	TNHC62178	Barbour	Alabama	32.0369	-85.0889	33
P. ornata			ECM0057	TNHC62185	Barnwell	South Carolina	33.3178	-81.4769	34

Table S2. Primer sequences and annealing temperatures (ºC) for the 23 nDNA loci and 4 mtDNA fragments in this study. All primers were developed in Lemmon and Lemmon (2012) unless otherwise noted.

Locus Name	Anneal. Temp.	Forward Primer (5' - 3')	Reverse Primer (5' - 3')
7	47	CTGTTCTCTCTGCTCTTACAGGA	TGGTTCATCTCCTTATCATTGAC
21	47	TTTTTCTTTCCTTGTAGAGTGTCA	ATCTGCAAATGTTTGGCTCT
23	48	GCAAAAGTACATCACATTTAGTGC	AACTACCTGCAGGCTTTTTGT
30	47	TAATATGTGGTGATGGAGATGG	TAATTAGTTCCAATGCCAGACTTA
82	51	TCTTCCCTTTCTAGTAGGCCATGT	TTTCAGAACCACTTTGTCCCTGT
91	47	GCTTTTGAGCATACTTTACATGG	TTGATCCAATCCTGCACAT
92	49	CATCTGCACTTTCAAAGGGTTT	ATGTAGTGTTTTCTTATGCCACCA
104	46	AAATGAGGAATTGACTTTAAGCTG	AAAGAGTAAGGCAAGAAATGCAC
110	49	CTTATGCCCAAAGCCCTTTCTA	CAGATAACACACCCAACATCTCC
111	47	ACACTTACCTCTGGATCGTTGA	TTTAGATATTTCTGCTTTGGGACT
117	48	TAAGACCACACAGAAGTCCATAAA	GCTGATAGCGCCTGTCCT
125	49	TAATGCAGGTGTTTGAACAAGCTA	AAAGGTCTTTGCACAGTTCCTCA
128	48	TAAGATGTAGATCCCTTGTGCTTA	AATGAGCAGAACAGTATTGTACCC
137	46	CCTGATAAGAAAATGTAGCCATTC	CGGTTAGTGTACACCAGCACAT
139	48	CTGCTGTGTATTTTGTCCTGGT	AGCTACATGTATTTGCTTTCTCAA
140	46	ATAACTGAGCTTTCCCAGCTGTA	ATTTATCAGATGGACTCCAAAAAC
149	46	ATGTTTTACTTTGCTCCCCTGT	GTATTTCAAATTCATCTTTTGTGC
151	48	ATATTATACATGCCCTTTGCACAT	GGCACAGGGGCACATAGTT
162	48	GATACACATTCTGCTCTTTTGTTG	AATCAATAACAGTTTAGCGGTTCG
166	48	ATCAGAATAAATACAGACGCAACC	ACGTCTTCATTCCCCCATGTA
168	48	GGTATTCATGCCGAATGCAAG	GCGCTGCAAAAAGTCATTC
169	46	TAAACTAGAGCTCAATGCCACCA	TTTTTCATCTTACTGAAACCAACA
182	46	ATTCTAAAAGCATTTACGCAAAAC	CATTAATAAGAACAGCGGCCAGA
cytb	42	MVZ15 = GAACTAATGGCCCACACWWTACGNAA (Moritz et al., 1992)	cytbR = GCRAAKCCRAARRYGTCTTTGTATGAGAAGTAT
COI	42	VF1-d = TTCTCAACCAACCACAARGAYATYGG (Ivanova et al., 2006)	VR1-d = TAGACTTCTGGGTGGCCRAARAAYCA (Ivanova et al., 2006)
ND2	42	L4437b = CAGCTAAAAAAGCTATCGGGCCCATACC (Kumazawa et al., 1996)	ND2r102 = CAGCCTAGGTGGGCGATTG (Sadlier et al., 2004)
16S	42	16Sc = GTRGGCCTAAAAGCAGCCAC (Moriarty and Cannatella 2004)	16Sd = CTCCGGTCTGAACTCAGATCACGTAG (Moriarty and Cannatella 2004)

Table S3. Sequence locus information including length analyzed (after excluding primer regions), ingroup variable sites, ingroup parsimony-informative sites, and model of nucleotide evolution.

Locus	Length Analyzed in bp	Number Variable Sites (%)	Number Informative Sites (%)	Model of Nucleotide Evolution
7	458	10 (2.18)	7 (1.53)	K80+I
21	522	3 (0.57)	3 (0.57)	HKY
23	521	8 (1.54)	8 (1.54)	F81+I
30	543	9 (1.66)	3 (0.55)	F81+I
82	520	7 (1.35)	4 (0.77)	HKY
91	415	2 (0.48)	1 (0.24)	HKY
92	510	3 (0.59)	1 (0.20)	F81+I
104	538	5 (0.93)	4 (0.74)	GTR
110	513	13 (2.53)	6 (1.17)	GTR+I
111	391	2 (0.51)	1 (0.26)	F81
117	491	17 (3.46)	14 (2.85)	HKY+I
125	430	4 (0.93)	2 (0.47)	HKY
128	568	6 (1.06)	3 (0.53)	GTR
137	512	2 (0.39)	2 (0.39)	HKY
139	493	14 (2.84)	11 (2.23)	HKY+I
140	473	4 (0.85)	2 (0.42)	F81
149	515	2 (0.39)	0 (0.00)	HKY
151	508	4 (0.79)	4 (0.79)	GTR+I
162	390	4 (1.03)	4 (1.03)	HKY
166	417	9 (2.16)	6 (1.44)	F81
168	457	21 (4.6)	15 (3.28)	SYM+I
169	467	2 (0.43)	0 (0.00)	GTR+I
182	472	4 (0.85)	3 (0.64)	HKY
cytb	648	65 (10.03)	53 (8.18)	GTR+I+G
COI	658	71 (10.79)	67 (10.18)	GTR+I
ND2	580	39 (6.72)	4 (0.6)	HKY+G
16S	883	27 (3.06)	21 (2.38)	HKY+I
mean nDNA:	**483.7**	**6.7**	**4.5**	
mean mtDNA:	**692.3**	**50.5**	**36.3**	
Total:	**13,893**	**357 (2.57%)**	**249 (1.79%)**	

Table S4. List of mitochondrial 16S sequences from GenBank used for divergence time estimation.

Genus	Species	GenBank Acc. No.	Field/Voucher No.	Original Published Study
Pseudacris	ocularis	AY291098	TNHC62241	Moriarty and Cannatella 2004
Pseudacris	crucifer	AY291103	TNHC62369	Moriarty and Cannatella 2004
Pseudacris	brimleyi	AY291094	TNHC62337	Moriarty and Cannatella 2004
Pseudacris	brachyphona	AY291095	TNHC62303	Moriarty and Cannatella 2004
Pseudacris	fouquettei	AY291085	TNHC62265	Moriarty and Cannatella 2004
Pseudacris	nigrita	AY291079	TNHC62364	Moriarty and Cannatella 2004
Pseudacris	triseriata	AY843738	AMNH A-168468	Faivovitch et al. 2005
Pseudacris	clarkii	AY291093	KU289035	Moriarty and Cannatella 2004
Pseudacris	maculata	AY291088	ECMK2	Moriarty and Cannatella 2004
Pseudacris	feriarum	AY291084	KU289227	Moriarty and Cannatella 2004
Pseudacris	kalmi	AY291087	KU289235	Moriarty and Cannatella 2004
Pseudacris	cadaverina	AY291114	KU207382	Moriarty and Cannatella 2004
Pseudacris	regilla	AY291112	TNHC62409	Moriarty and Cannatella 2004
Isthmohyla	zeteki	EF566968	MVZ203913	Lemmon et al. 2007
Acris	gryllus	EF566971	TNHC62372	Lemmon et al. 2007
Acris	gryllus	AY843560	AMNH A-168422	Faivovitch et al. 2005
Acris	crepitans	EF566969	DCC3535	Lemmon et al. 2007
Acris	crepitans	AY843559	LSUMZ H-2164	Faivovitch et al. 2005
Hyla	cinerea	AY680271	TNHC61054	Pauly et al. 2004
Hyla	cinerea	AY549327	MVZ1453854	Faivovitch et al. 2004
Hyla	squirella	EF566965	LSUMZ H487	Lemmon et al. 2007
Hyla	squirella	AY843678	AMNH A-168427	Faivovitch et al. 2005
Hyla	gratiosa	EF566966	LSUMZ H15929	Lemmon et al. 2007
Hyla	gratiosa	AY843630	AMNH A-168404	Faivovitch et al. 2005
Hyla	femoralis	EF566964	TNHC64108	Lemmon et al. 2007
Hyla	femoralis	AY843627	AMNH A-168425	Faivovitch et al. 2005
Hyla	versiscolor	EF566951	TNHC61055	Lemmon et al. 2007
Hyla	chrysoscelis	EF566949	TNHC64082	Lemmon et al. 2007
Hyla	chrysoscelis	AY291116	KU289034	Moriarty and Cannatella 2004
Hyla	versicolor	AY843682	UMFS 5545	Faivovitch et al. 2005
Hyla	avivoca	EF566946	HCG28	Lemmon et al. 2007
Hyla	avivoca	AY843605	AMNH A-168423	Faivovitch et al. 2005
Hyla	japonica	EF566952	TNHC uncat.	Lemmon et al. 2007
Hyla	japonica	AY843633	LSUMZ H-230	Faivovitch et al. 2005
Hyla	andersonii	AY291115	KU207335	Moriarty and Cannatella 2004
Hyla	andersonii	AY843598	AMCC 125627	Faivovitch et al. 2005
Hyla	plicata	EF566962	UTA A13372	Lemmon et al. 2007
Hyla	eximia	AY843626	MZFC 4814	Faivovitch et al. 2005
Hyla	euphorbiacea	EF566961	UTA A13237	Lemmon et al. 2007
Hyla	euphorbiacea	AY843625	UTA A-54763	Faivovitch et al. 2005
Hyla	walkeri	EF566963	UTA 13399	Lemmon et al. 2007
Hyla	eximia	JN830879	00006H	Klymus and Gerhardt 2012
Hyla	arenicolor	AY843603	UMMZ 7755	Faivovitch et al. 2005
Hyla	arenicolor	EF566958	TNHC64105	Lemmon et al. 2007
Hyla	savignyi	EF566954	KU207344	Lemmon et al. 2007
Hyla	savignyi	AY843665	ZFMK H-074	Faivovitch et al. 2005
Hyla	meridionalis	EF566953	KU207371	Lemmon et al. 2007
Hyla	meridionalis	GQ916810	HE101A	Grozdik et al. 2010
Hyla	arborea	AY843601	N/A	Faivovitch et al. 2005

Table S5. Genetic diversity estimates for 14 microsatellite loci. N = number of individuals, Na = average number of alleles per locus, Ar = allelic richness, Np = number of private alleles, Ho = observed heterozygosity, uHe = unbiased expected heterozygosity [(2N/(2N - 1)) * (1 - sum of squared allele frequencies)], F = fixation index = 1 - (Ho/He).

Region	**Site**	**N**	**Na**	**Ar**	**Np**	**Ho**	**uHe**	**F**
streckeri (N = 95 individuals)								
TEX	TEX1	18	10	5.25	42	0.755	0.843	0.083
CGP	OKL1	5	3.714	3.08	0	0.6	0.684	0.025
	OKL2A	8	5.857	4.23	4	0.781	0.774	-0.077
	OKL2B	8	4.143	3.56	2	0.732	0.695	-0.124
	KAN1	5	2.429	2.25	1	0.443	0.508	0.02
ARV	ARK1	20	4.429	3.21	1	0.622	0.609	-0.035
	ARK2	11	4.214	3.25	1	0.553	0.63	0.133
	ARK3	5	3.429	2.98	0	0.614	0.614	-0.105
	ARK4	9	4.5	3.43	0	0.651	0.672	-0.033
	ARK5A	6	3.357	2.88	0	0.583	0.594	-0.056
mean *streckeri*		**9.5**	**4.607**	**3.412**	**5.1**	**0.633**	**0.662**	**-0.017**
illinoensis (N = 186 individuals)								
ILLS	ARK6	8	2.571	2.23	2	0.381	0.41	-0.019
	MIS1	21	5.643	3.66	0	0.694	0.659	-0.081
	MIS2	5	3.929	3.28	0	0.643	0.689	-0.051
	ILLS	11	4.071	3.25	0	0.639	0.628	-0.022
ILLC	ILLC	5	2.929	2.62	0	0.6	0.551	-0.206
ILLN	ILLN1	11	3.714	2.85	1	0.536	0.567	-0.005
	ILLN3	13	3.5	2.72	0	0.483	0.538	0.037
	ILLN4	21	4.357	3.11	0	0.639	0.594	-0.105
	ILLN6	10	3.929	2.96	1	0.593	0.569	-0.098
	ILLN7	11	3.429	2.79	0	0.597	0.558	-0.111
	ILLN8	17	3.786	2.83	0	0.571	0.553	-0.055
	ILLN9	22	4.286	3.05	1	0.571	0.564	-0.028
	ILLN10	20	4.286	2.96	1	0.611	0.553	-0.135
mean *illinoensis*		**14.231**	**3.879**	**2.947**	**0.462**	**0.581**	**0.572**	**-0.068**

Table S6. Pairwise differentiation values and pairwise geographic distances between 23 sites (280 individuals) used for AMOVAs and Mantel tests. Below diagonal: Differentiation values (Top = Rst, Bottom = Fst). Bold italicized values are significant at a level of p = 0.001, using 10,000 permutations in Arlequin v. 3.5. Above diagonal: Pairwise geographic distances in km, calculated by transforming GPS coordinate data using the Geographic Distance Matrix Generator v. 1.2.3.

Rst (based on allele size differences)

	TEX1	OKL1	OKL2A	OKL2B	KAN1	ARK1	ARK2	ARK3	ARK4	ARK5A	ARK6	MIS1B	MIS2	ILLS	ILLC	ILLN1	ILLN3	ILLN4	ILLN6	ILLN7	ILLN8	ILLN9	ILLN10
TEX1	-	696.68	530.34	533.29	798.53	713.97	710.24	728.18	695.11	679.83	978.95	1065.84	1069.51	1093.85	1179.95	1231.14	1270.02	1296.14	1289.31	1304.84	1325.32	1340.52	1332.75
OKL1	0.14336	-	238.87	242.26	133.38	610.81	603.24	612.24	576.85	519.49	823.94	893.09	870.88	892.27	857.3	844.81	871.51	907.34	892.46	905.88	937.99	946.27	935.21
OKL2A	***0.22597***	0.06441	-	6.81	289.4	414.05	406.67	419.58	380.14	327.85	663.96	743.6	729.38	753.11	766.48	784.48	818.59	850.8	839.49	854.51	881.84	893.92	884.16
OKL2B	***0.16766***	0.14094	0.09007	-	289.71	407.58	400.18	413.04	373.64	321.22	657.18	736.8	722.58	746.3	759.89	778.2	812.39	844.54	833.28	848.31	875.57	887.69	877.95
KAN1	***0.20855***	0.12192	0.11773	0.22475	-	579.96	572.65	578.06	547.9	490.54	758.63	819.75	793.61	813.23	756.56	733.18	757.07	793.5	777.73	790.48	823.61	830.63	819.32
ARK1	***0.31963***	0.21513	0.1244	***0.28181***	0.13463	-	7.58	15.34	34.27	91.37	273.44	360.18	358.45	383.1	473.54	541.66	582.11	602.31	599.1	614.27	629.04	645.71	639.65
ARK2	***0.31395***	0.24286	0.18709	***0.33997***	0.15986	0.01869	-	17.96	26.73	83.81	278.98	365.55	363.23	387.91	475.75	542.61	583.03	603.62	600.18	615.39	630.54	647.13	640.95
ARK3	***0.25224***	0.17759	0.0618	***0.2225***	0.01767	-0.01427	0.02899	-	40.39	93.43	261.72	348.12	345.43	370.12	458.39	526.31	566.76	586.98	583.76	598.92	613.73	630.39	624.31
ARK4	***0.2785***	0.1857	0.11304	***0.2723***	0.09795	-0.02089	-0.03006	-0.03	-	57.79	300.95	386.92	382.84	407.55	487.06	549.63	589.86	611.75	607.53	622.86	639.29	655.58	649.02
ARK5A	***0.45362***	0.48153	0.37545	***0.5288***	0.25424	0.08074	0.07715	0.08584	0.07242	-	341.52	425.18	416.83	441.41	500.83	553.24	592.79	617.41	611.49	626.98	646.16	661.7	654.32
ARK6	***0.37461***	***0.47811***	***0.23521***	***0.43732***	***0.4199***	0.11643	***0.2599***	0.20404	***0.18611***	***0.44393***	-	87.22	95.15	117.66	273.13	374.03	411.33	417.11	421.56	434.15	435.81	453.86	451.79
MIS1B	***0.33514***	***0.20975***	0.05559	***0.21186***	***0.30365***	***0.1769***	***0.25741***	***0.17372***	***0.19301***	***0.47643***	***0.26998***	-	38.57	44.44	231.3	339.51	372.62	371.26	379.07	389.74	385.15	403.04	402.91
MIS2	***0.26676***	0.1909	0.00708	0.14876	0.26974	0.15423	0.22637	0.1404	0.15891	0.46051	***0.37242***	-0.03479	-	24.71	195.48	302.85	336.85	337.18	344.17	355.35	352.56	370.55	369.81
ILLS	***0.3886***	***0.23627***	0.05589	***0.24347***	***0.35033***	***0.23782***	***0.34284***	***0.26467***	***0.27313***	***0.56439***	***0.33748***	0.0291	0.00903	-	188.45	297.2	329.45	327.21	335.37	345.81	340.78	358.65	358.6
ILLC	***0.33245***	0.41958	0.21678	***0.38728***	0.3698	0.17173	0.21394	0.16247	0.17272	0.38456	0.42354	0.15518	0.19697	***0.32931***	-	109.08	141.4	143.98	149.22	161.22	163.86	181.8	178.98
ILLN1	***0.35946***	***0.301***	***0.17616***	***0.36147***	***0.34428***	***0.17909***	***0.24882***	***0.21478***	***0.20922***	***0.4397***	***0.27802***	0.09018	0.11524	***0.18955***	0.08552	-	40.52	66.5	58.24	73.75	97.39	110.47	101.86
ILLN3	***0.41733***	***0.40165***	***0.26728***	***0.42616***	***0.4432***	***0.2166***	***0.30607***	***0.27543***	***0.26665***	***0.48046***	***0.39567***	***0.15945***	0.18432	***0.27116***	0.10145	0.00131	-	36.86	21.12	35.92	66.57	75.74	65.59
ILLN4	***0.42845***	***0.38761***	***0.2563***	***0.41215***	***0.45746***	***0.29903***	***0.37214***	***0.35724***	***0.34554***	***0.56076***	***0.39744***	***0.16688***	***0.20289***	***0.25361***	***0.20179***	0.04071	***0.10498***	-	18.79	19.48	31.15	44.4	37.34
ILLN6	***0.39974***	***0.3932***	***0.24641***	***0.4125***	***0.40899***	***0.25836***	***0.31689***	***0.29249***	***0.29193***	***0.50358***	***0.40108***	***0.17931***	***0.23777***	***0.27765***	***0.20682***	0.04638	0.13553	-0.01136	-	15.53	45.95	54.64	44.69
ILLN7	***0.38832***	***0.32203***	***0.18003***	***0.34358***	***0.3759***	***0.24515***	***0.31816***	***0.28475***	***0.27612***	***0.52912***	***0.41557***	***0.13866***	***0.18404***	***0.196***	***0.24561***	***0.06324***	***0.12717***	***0.0809***	***0.1072***	-	35.12	40.42	29.77
ILLN8	***0.42042***	***0.3227***	***0.22091***	***0.3042***	***0.41229***	***0.36075***	***0.4412***	***0.37763***	***0.39738***	***0.6189***	***0.51227***	***0.18124***	***0.194***	***0.19941***	***0.35391***	***0.1914***	***0.24778***	***0.15697***	***0.19439***	***0.0716***	-	18.06	19.84
ILLN9	***0.44026***	***0.35937***	***0.28302***	***0.41312***	***0.41854***	***0.29347***	***0.34469***	***0.33502***	***0.31857***	***0.53065***	***0.46518***	***0.18072***	***0.21652***	***0.26605***	***0.19151***	***0.07438***	***0.08268***	***0.11168***	***0.14251***	0.04919	***0.12551***	-	11.67
ILLN10	***0.44742***	***0.38806***	***0.25849***	***0.40422***	***0.46221***	***0.32227***	***0.40907***	***0.37523***	***0.3725***	***0.60291***	***0.47535***	***0.1535***	***0.20689***	***0.22157***	***0.25486***	0.06822	***0.12443***	0.05598	0.08475	0.00377	0.04915	0.03991	-

Pairwise Fst

	TEX1	OKL1	OKL2A	OKL2B	KAN1	ARK1	ARK2	ARK3	ARK4	ARK5A	ARK6	MIS1	MIS2	ILLS	ILLC	ILLN1	ILLN3	ILLN4	ILLN6	ILLN7	ILLN8	ILLN9	ILLN10
TEX1	-	696.68	530.34	533.29	798.53	713.97	710.24	728.18	695.11	679.83	978.95	1065.84	1069.51	1093.85	1179.95	1231.14	1270.02	1296.14	1289.31	1304.84	1325.32	1340.52	1332.75
OKL1	***0.12313***	-	238.87	242.26	133.38	610.81	603.24	612.24	576.85	519.49	823.94	893.09	870.88	892.27	857.3	844.81	871.51	907.34	892.46	905.88	937.99	946.27	935.21
OKL2A	***0.10189***	0.07006	-	6.81	289.4	414.05	406.67	419.58	380.14	327.85	663.96	743.6	729.38	753.11	766.48	784.48	818.59	850.8	839.49	854.51	881.84	893.92	884.16
OKL2B	***0.14472***	0.11636	0.0442	-	289.71	407.58	400.18	413.04	373.64	321.22	657.18	736.8	722.58	746.3	759.89	778.2	812.39	844.54	833.28	848.31	875.57	887.69	877.95
KAN1	***0.21927***	0.18735	***0.16956***	0.24253	-	579.96	572.65	578.06	547.9	490.54	758.63	819.75	793.61	813.23	756.56	733.18	757.07	793.5	777.73	790.48	823.61	830.63	819.32
ARK1	***0.19935***	***0.16035***	***0.09175***	***0.16054***	***0.21649***	-	7.58	15.34	34.27	91.37	273.44	360.18	358.45	383.1	473.54	541.66	582.11	602.31	599.1	614.27	629.04	645.71	639.65
ARK2	***0.17886***	***0.1293***	***0.07485***	***0.12874***	***0.19055***	0.02064	-	17.96	26.73	83.81	278.98	365.55	363.23	387.91	475.75	542.61	583.03	603.62	600.18	615.39	630.54	647.13	640.95
ARK3	***0.17781***	0.12738	***0.08723***	0.11828	0.18426	0.05256	0.00267	-	40.39	93.43	261.72	348.12	345.43	370.12	458.39	526.31	566.76	586.98	583.76	598.92	613.73	630.39	624.31
ARK4	***0.16363***	***0.12334***	***0.0466***	***0.11119***	***0.17685***	***0.053***	0.02166	0.03929	-	57.79	300.95	386.92	382.84	407.55	487.06	549.63	589.86	611.75	607.53	622.86	639.29	655.58	649.02
ARK5A	***0.19526***	0.15771	***0.13735***	***0.18452***	0.18777	***0.07402***	***0.06379***	0.08355	***0.10338***	-	341.52	425.18	416.83	441.41	500.83	553.24	592.79	617.41	611.49	626.98	646.16	661.7	654.32
ARK6	***0.27265***	***0.37158***	***0.27116***	***0.35154***	***0.49007***	***0.32924***	***0.35218***	***0.39411***	***0.32677***	***0.43239***	-	87.22	95.15	117.66	273.13	374.03	411.33	417.11	421.56	434.15	435.81	453.86	451.79
MIS1	***0.16626***	***0.18577***	***0.12654***	***0.19675***	***0.29611***	***0.16324***	***0.18331***	***0.1948***	***0.18389***	***0.20506***	***0.18211***	-	38.57	44.44	231.3	339.51	372.62	371.26	379.07	389.74	385.15	403.04	402.91
MIS2	***0.1427***	0.18673	***0.09608***	***0.16176***	0.31888	***0.16128***	***0.18548***	0.20469	***0.15719***	0.23531	***0.26184***	0.02544	-	24.71	195.48	302.85	336.85	337.18	344.17	355.35	352.56	370.55	369.81
ILLS	***0.18772***	***0.20525***	***0.15725***	***0.22426***	***0.31553***	***0.20569***	***0.22468***	***0.22431***	***0.20842***	***0.26289***	***0.25263***	***0.06598***	0.04833	-	188.45	297.2	329.45	327.21	335.37	345.81	340.78	358.65	358.6
ILLC	***0.20623***	0.27964	***0.20212***	***0.24979***	0.38086	***0.31407***	***0.28666***	0.31753	***0.24514***	0.3208	***0.41987***	***0.23019***	0.20823	***0.26451***	-	109.08	141.4	143.98	149.22	161.22	163.86	181.8	178.98
ILLN1	***0.20799***	***0.22215***	***0.18175***	***0.24322***	***0.35217***	***0.29952***	***0.304***	***0.32325***	***0.27493***	***0.31406***	***0.36588***	***0.17595***	***0.16857***	***0.22173***	***0.22374***	-	40.52	66.5	58.24	73.75	97.39	110.47	101.86
ILLN3	***0.2356***	***0.28193***	***0.22526***	***0.26501***	***0.39039***	***0.31908***	***0.32416***	***0.34656***	***0.27713***	***0.36583***	***0.38752***	***0.2258***	***0.19447***	***0.24035***	***0.18247***	0.05288	-	36.86	21.12	35.92	66.57	75.74	65.59
ILLN4	***0.21059***	***0.24244***	***0.1864***	***0.23828***	***0.34681***	***0.26072***	***0.25803***	***0.27984***	***0.23717***	***0.27488***	***0.3675***	***0.19187***	***0.14533***	***0.22033***	***0.15978***	***0.11619***	***0.1283***	-	18.79	19.48	31.15	44.4	37.34
ILLN6	***0.21351***	***0.2222***	***0.19931***	***0.2499***	***0.33742***	***0.28353***	***0.28277***	***0.28869***	***0.25908***	***0.28543***	***0.38697***	***0.17392***	***0.14737***	***0.19397***	***0.15865***	***0.07347***	***0.10034***	***0.03628***	-	15.53	45.95	54.64	44.69
ILLN7	***0.21795***	***0.23357***	***0.21039***	***0.26009***	***0.35226***	***0.2892***	***0.27612***	***0.28959***	***0.26676***	***0.276***	***0.38712***	***0.16628***	***0.17089***	***0.19759***	***0.17845***	***0.12127***	***0.15865***	***0.04767***	0.00719	-	35.12	40.42	29.77
ILLN8	***0.23062***	***0.2554***	***0.2094***	***0.2485***	***0.35949***	***0.3029***	***0.30158***	***0.3121***	***0.28155***	***0.31338***	***0.39919***	***0.18877***	***0.16224***	***0.21681***	***0.22775***	***0.13781***	***0.18413***	***0.06591***	***0.05847***	***0.05149***	-	18.06	19.84
ILLN9	***0.21911***	***0.23514***	***0.21399***	***0.26384***	***0.35837***	***0.28835***	***0.28274***	***0.30169***	***0.2856***	***0.28708***	***0.3875***	***0.18917***	***0.16061***	***0.22654***	***0.21881***	***0.16188***	***0.21132***	***0.07277***	***0.06911***	0.03682	***0.06643***	11.67	
ILLN10	***0.22632***	***0.23749***	***0.20617***	***0.2673***	***0.34102***	***0.28707***	***0.2893***	***0.29989***	***0.27596***	***0.30164***	***0.39076***	***0.18783***	***0.15849***	***0.20889***	***0.20668***	***0.10753***	***0.15706***	***0.04867***	0.01568	0.02404	***0.03105***	***0.02862***	-

Table S7. Pairwise differentiation for entire microsatellite dataset (294 individuals, 50 locations) with combined sites highlighted. Greyed boxes are locations that were excluded from combined analyses because they had sample size n < 5 and were not within 10 km of any other sample locality. Fst values were calculated and significance testing was done using 10,000 permutations in Arlequin v. 3.5; locations with n = 1 are indicated in the left column and should not be interpreted (see Bayesian clustering analyses for evidence that combined sites are not genetically differentiated in these cases). Bold, italicized values are significant at a level of p = 0.05. Two pairs of combined sites (ILLN3B-ILLN3D and ILLN9A-ILLN9B) are significant at a level of p = 0.05, but not after correction for multiple tests.

		TEX1	TEX2	TEX3	OKL1	OKL2A	OKL2B	OKL2C	OKL2D	OKL3	KAN1A	KAN1B	KAN1C	KAN1D	KAN1E	KAN2	KAN3	ARK1A	ARK1B	ARK2	ARK3	ARK4A	ARK4B	ARK5A	ARK5B	ARK6	MIS1A	MIS1B	MIS2	ILLSA	ILLSB	ILLSC	ILLCA	ILLCB	ILLCC	ILLN1A	ILLN1B	ILLN1C	ILLN2	ILLN3A	ILLN3B	ILLN3C	ILLN3D	ILLN4	ILLN5	ILLN6	ILLN7	ILLN8	ILLN9A	ILLN9B	ILLN10
	TEX1	0																																																	
removed	TEX2	0.00291	0																																																
removed	TEX3	-0.00516	0	0																																															
	OKL1	***0.19381***	0.18262	0.17223	0																																													
	OKL2A	***0.10349***	0.12404	0.09997	***0.07183***	0																																													
	OKL2B	***0.11466***	0.13651	0.14957	0.09612	0.01005	0																																												
	OKL2C	***0.11134***	0.15052	0.15598	***0.09676***	0.01397	-0.13681	0																																											
n=1	OKL2D	0.19579	0.14286	0.15385	0.16885	0.04064	-0.08789	0.07966	0																																										
removed	OKL3	0.15881	0.30909	0.21569	0.21443	0.1334	0.20398	0.20874	0.36	0																																									
n=1	KAN1A	0.17762	0.34615	0.26531	0.18035	0.13282	0.20102	0.2218	0.37778	0.5	0																																								
n=1	KAN1B	0.17681	0.34615	0.26531	0.19106	0.16893	0.22097	0.2324	0.41667	0.54717	0.35484	0																																								
n=1	KAN1C	0.11992	0.28302	0.18367	0.1538	0.09928	0.16667	0.16335	0.34694	0.46154	0.17241	0.11111	0																																							
n=1	KAN1D	0.15704	0.32075	0.2549	0.15366	0.05116	0.19955	0.12542	0.375	0.4902	0.35294	0.15385	-0.08333	0																																						
n=1	KAN1E	0.14005	0.24528	0.19231	0.09758	0.09744	0.13078	0.10628	0.33333	0.4	0.1875	0.10345	-0.03448	0	0																																					
removed	KAN2	0.12309	0.21569	0.16	0.07954	0.03702	0.08445	0.01748	0.17073	0.38776	0.16129	0.16129	-0.11111	-0.03704	0.05882	0																																					
removed	KAN3	0.15118	0.2549	0.16667	0.1538	0.09214	0.13514	0.13223	0.31915	0.45098	0.2	0.25	0.09677	0.07143	0.09091	-0.07143	0																																					
	ARK1A	***0.16693***	0.25141	0.27538	***0.16847***	***0.08352***	***0.13706***	***0.15789***	0.18581	0.28805	0.25796	0.3709	0.23533	0.19463	0.20168	0.20923	0.2209	0																																				
	ARK1B	***0.19429***	0.2977	0.26787	***0.16765***	***0.09059***	***0.13748***	***0.15034***	0.19476	0.24916	0.19357	0.31167	0.1521	0.1434	0.1633	0.14662	0.20356	0.02373	0																																			
	ARK2	***0.17707***	0.26156	0.22576	***0.13205***	***0.07261***	***0.10248***	***0.11646***	0.14996	0.21133	0.1492	0.25981	0.16413	0.13426	0.12321	0.10118	0.16056	0.0314	***0.02129***	0																																	
	ARK3	***0.17345***	0.27541	0.21786	***0.11522***	***0.08639***	***0.09157***	***0.10767***	0.15526	0.29596	0.19594	0.25077	0.1592	0.12834	0.09706	0.08741	0.11973	***0.08994***	***0.04499***	0.00258	0																																
n=1	ARK4A	0.10424	0.13208	0.04	0.07815	-0.02754	0.0317	0.05399	0.04762	0.12595	0.2381	0.30435	0.23404	0.22727	0.11628	0.11628	0.12395	0.01947	0.04352	-0.06509	-0.00249	0																																
	ARK4B	***0.16211***	0.23957	0.22375	***0.13834***	***0.04995***	***0.08522***	***0.09429***	0.13978	0.20015	0.1754	0.24026	0.14423	0.09736	0.07779	0.09472	0.15164	***0.06393***	***0.05764***	***0.03186***	***0.04550***	-0.01256	0																																
	ARK5A	***0.1912***	0.29707	0.25658	***0.15301***	***0.13288***	***0.16617***	***0.16977***	0.24304	0.29495	0.14348	0.2682	0.15849	0.20562	0.07375	0.15156	0.17241	***0.06616***	***0.08227***	***0.06348***	***0.08328***	0.04733	***0.11313***	0																																
removed	ARK5B	***0.13734***	0.15845	0.15252	0.10653	***0.05765***	0.09373	0.08872	0.08729	0.17208	0.15391	0.26237	0.16599	0.17869	0.11433	0.10052	0.16599	0.017	***0.05082***	0.01768	0.03859	-0.08119	0.04291	0.02838	0																																
	ARK6	***0.25893***	0.4876	0.37624	***0.36719***	***0.26739***	***0.35172***	***0.37361***	0.46264	0.53666	0.55093	0.56046	0.48188	0.46999	0.52537	0.47907	0.46501	***0.37356***	***0.33416***	***0.34727***	***0.38762***	0.37335	***0.33506***	***0.42254***	***0.3926***	0																															
removed	MIS1A	0.06212	0.09434	0.03846	0.10841	0.02491	0.0903	0.08286	0.16	0.13636	0.30612	0.33333	0.19549	0.18182	0.18367	0.16667	0.22833	0.16188	0.1487	0.14142	0.16744	***0***	0.11558	0.20978	0.09683	0.34517	0																																
	MIS1B	***0.17206***	***0.22605***	***0.17801***	***0.20153***	***0.13202***	***0.18032***	***0.19257***	***0.21133***	***0.25053***	***0.2949***	***0.33524***	***0.23643***	***0.25286***	***0.29162***	***0.21935***	***0.18909***	***0.17054***	***0.1676***	***0.18799***	***0.2002***	0.12825	***0.19678***	***0.20987***	***0.19313***	***0.18695***	0.04996	0																																
	MIS2	***0.14012***	0.15018	0.15395	***0.19166***	***0.09516***	***0.13102***	***0.15186***	0.14965	0.26293	0.31929	0.3389	0.21677	0.24895	0.26489	0.20643	0.21017	***0.15601***	***0.16284***	***0.18544***	***0.20469***	0.12334	***0.15981***	***0.22178***	***0.17058***	***0.25355***	0.04643	***0.02802***	0																															
	ILLSA	***0.1678***	0.23198	0.20316	***0.20152***	***0.15083***	***0.20487***	***0.22205***	0.24101	0.30269	0.3426	0.36098	0.23946	0.28945	0.32825	0.21069	0.23946	***0.23058***	***0.20058***	***0.23093***	***0.23***	0.2066	***0.21965***	***0.26089***	***0.22575***	***0.25718***	0.06431	***0.03926***	0.01873	0																															
	ILLSB	***0.1712***	0.23688	0.23534	***0.24966***	***0.16839***	***0.2173***	0.24354	0.25859	0.37275	0.40767	0.42244	0.29498	0.35503	0.38504	0.26612	0.31496	***0.28188***	***0.2396***	***0.26737***	***0.2804***	0.26002	***0.25136***	***0.30191***	0.2272	***0.31726***	0.10946	***0.05534***	0.00511	-0.03603	0																															
	ILLSC	***0.18467***	0.2504	0.23152	***0.21217***	***0.14681***	***0.19729***	***0.21116***	0.24209	0.33079	0.32654	0.35822	0.23275	0.25384	0.31709	0.18909	0.20163	***0.22554***	***0.20022***	***0.21451***	***0.21752***	0.19371	***0.19713***	***0.20614***	***0.21941***	***0.24418***	0.08173	***0.05032***	***0.07008***	0.02571	0.0387	0																															
	ILLCA	***0.15033***	0.27273	0.1938	0.22751	***0.14273***	0.16938	0.16846	0.28389	0.33501	0.35917	0.39659	0.27671	0.33333	0.28796	0.29534	0.30709	0.29766	***0.28631***	***0.23951***	0.28722	0.33783	***0.21663***	***0.28042***	0.22625	***0.40946***	0.07879	***0.20482***	***0.15047***	***0.24203***	0.27142	***0.25297***	0																															
	ILLCB	***0.17387***	0.3253	0.25	***0.25087***	***0.16153***	0.20332	0.20887	0.33333	0.35829	0.42268	0.45098	0.36508	0.4016	0.36571	0.33867	0.34426	***0.32087***	***0.31097***	***0.26754***	***0.3061***	0.23164	***0.23788***	***0.31161***	0.24633	***0.42821***	0.11111	***0.22277***	0.17817	***0.24064***	0.29594	***0.23799***	-0.06233	0																															
n=1	ILLCC	0.15797	0.28302	0.23077	0.28659	0.18096	0.20398	0.22452	0.31915	0.42857	0.45455	0.52	0.41667	0.48	0.38776	0.38776	0.3913	0.32306	0.30524	0.26054	0.29889	0.18182	0.20877	0.30716	0.20684	0.47822	0.13636	0.23109	0.23017	0.2787	0.3384	0.26937	-0.07755	-0.0084	0																															
	ILLN1A	***0.18955***	0.2687	0.22286	***0.19411***	***0.1599***	0.21133	0.21412	0.37173	0.45098	0.44974	0.46974	0.3253	0.38462	0.37127	0.3033	0.34884	***0.32132***	***0.29289***	***0.29494***	***0.30918***	0.31183	***0.27582***	***0.30044***	0.27768	***0.42514***	0.22581	***0.16773***	***0.16014***	***0.18654***	0.28181	***0.25018***	0.22634	0.28455	0.35632	0																															
	ILLN1B	***0.16771***	0.24211	0.21485	0.22282	***0.13976***	0.16827	0.16682	0.30709	0.46811	0.3974	0.35014	0.27697	0.28144	0.28889	0.27273	0.33154	0.30934	***0.28635***	***0.27579***	0.29591	0.28389	***0.2412***	***0.28659***	0.26241	***0.42216***	0.20879	***0.19818***	0.16648	***0.22275***	0.27542	***0.2875***	0.19679	0.28788	0.33154	-0.01695	0																															
	ILLN1C	***0.19347***	0.2652	0.2691	***0.22564***	***0.17262***	***0.22575***	***0.23222***	0.3159	0.3718	0.40022	0.38849	0.32417	0.34527	0.36151	0.29772	0.31588	***0.31197***	***0.30415***	***0.30256***	***0.32843***	0.29503	***0.27399***	***0.31736***	***0.2733***	***0.36555***	0.12096	***0.17479***	***0.15777***	***0.17621***	***0.25055***	***0.22641***	***0.17192***	***0.17631***	0.22283	0.00586	0.06432	0																															
removed	ILLN2	***0.19734***	0.25672	0.27541	***0.21246***	***0.16884***	***0.19507***	***0.2054***	0.31382	0.41166	0.42599	0.41469	0.32441	0.36545	0.33665	0.32226	0.35284	***0.28549***	***0.28552***	***0.28***	***0.30522***	0.27045	***0.26102***	***0.31159***	***0.25159***	***0.39585***	0.19849	***0.18509***	***0.1398***	***0.21615***	***0.28827***	***0.26165***	0.19575	0.2381	0.24569	0.02698	-0.01072	***0.04749***	0																															
	ILLN3A	***0.18819***	0.27143	0.29412	***0.24695***	***0.17277***	***0.20801***	0.21259	0.32867	0.38803	0.43103	0.44186	0.34442	0.37931	0.35909	0.32697	0.35814	***0.30908***	***0.29522***	***0.2816***	***0.32049***	0.29907	***0.24259***	***0.33165***	0.24539	***0.41825***	0.18221	***0.21705***	***0.13021***	***0.22281***	0.277	***0.25***	0.10704	0.07578	0.18824	0.1067	0.10691	0.04402	0.04582	0																															
	ILLN3B	***0.19807***	0.31052	0.27196	***0.26101***	***0.20004***	***0.24013***	***0.2418***	0.37528	0.44269	0.46493	0.43553	0.35107	0.39334	0.3969	0.30128	0.38075	***0.3652***	***0.32814***	***0.33265***	***0.34852***	0.35044	***0.27771***	***0.36276***	***0.32044***	***0.4056***	0.21996	***0.22742***	***0.19594***	***0.18242***	***0.28649***	***0.23868***	0.263	0.2791	0.31151	0.1094	0.07184	***0.09628***	***0.12215***	0.12292	0																													
	ILLN3C	***0.21617***	0.35248	0.34694	***0.27683***	***0.2073***	0.2377	0.2393	0.42268	0.50239	0.52475	0.51515	0.41899	0.42693	0.40496	0.41779	0.46114	***0.34299***	***0.3076***	***0.31533***	***0.33236***	0.36508	***0.25758***	***0.37049***	0.29633	***0.43997***	0.20257	***0.24537***	***0.18619***	***0.24298***	0.33118	***0.29009***	0.21569	0.2381	0.26241	0.08832	0.16302	0.12322	0.09224	0.04264	0.16845	0																													
	ILLN3D	***0.25004***	0.43703	0.43941	***0.34132***	***0.25941***	***0.29457***	***0.30637***	0.45681	0.54069	0.53601	0.51069	0.46464	0.47167	0.47774	0.44557	0.48728	***0.40462***	***0.36021***	***0.36302***	***0.39245***	0.45308	***0.31112***	***0.40795***	***0.36613***	***0.4507***	0.27733	***0.27519***	***0.24687***	***0.29707***	***0.3832***	***0.32722***	0.18949	0.24312	0.27027	0.20702	0.18854	***0.1248***	***0.14619***	0.10102	***0.18174***	0.07501	0																													
	ILLN4	***0.21056***	***0.25411***	***0.25079***	***0.21064***	***0.1863***	***0.22152***	***0.2248***	***0.29637***	***0.35806***	***0.36237***	***0.33778***	***0.30412***	***0.34042***	***0.33411***	***0.30936***	***0.30689***	***0.2634***	***0.24405***	***0.25711***	***0.27586***	***0.25348***	***0.23836***	***0.27488***	***0.26117***	***0.30727***	***0.22375***	***0.19448***	***0.14513***	***0.20315***	***0.25278***	***0.23208***	***0.12476***	***0.15469***	***0.1595***	***0.09336***	***0.11783***	***0.12181***	***0.08961***	***0.09303***	***0.17634***	***0.16185***	***0.17791***	0																													
removed	ILLN5	0.16464	0.22449	0.16667	0.20775	0.15474	0.18782	0.21407	0.28889	0.45098	0.5	0.5102	0.36364	0.48	0.38776	0.31818	0.34884	0.28805	0.28385	0.25082	0.27479	0.23404	0.23154	0.27971	0.20684	0.42802	0.19149	0.15154	0.10033	0.0911	0.22113	0.18591	0.19757	0.17241	0.24324	0.06667	0.17057	0.09317	0.08931	0.11821	0.12646	0.1938	0.28775	0.01974	0																													
	ILLN6	***0.2103***	0.27014	0.24448	***0.22934***	***0.19822***	***0.235***	***0.2366***	0.33227	0.39379	0.35124	0.37545	0.27756	0.34016	0.32862	0.28675	0.28247	***0.30071***	***0.28373***	***0.28084***	***0.28869***	0.29593	***0.25997***	***0.28392***	***0.26026***	***0.38181***	0.22143	***0.17679***	***0.14737***	***0.17302***	***0.24076***	***0.20579***	***0.1257***	***0.15168***	0.16954	-0.00737	***0.12825***	***0.08794***	***0.09048***	***0.08291***	***0.16555***	***0.1074***	***0.15641***	***0.03628***	-0.03048	0																											
	ILLN7	***0.21492***	0.29771	0.23486	***0.24052***	***0.20933***	***0.24661***	***0.25126***	0.33827	0.39036	0.3538	0.37761	0.30762	0.3756	0.34777	0.3028	0.28741	***0.30701***	***0.29017***	***0.27432***	***0.28559***	0.26893	***0.27253***	***0.27478***	***0.26649***	***0.38433***	0.25613	***0.16725***	***0.17089***	***0.17885***	***0.24168***	***0.21497***	***0.16069***	***0.16755***	0.17967	0.07126	***0.16322***	***0.13268***	***0.12374***	***0.17001***	***0.19235***	***0.18783***	***0.20445***	***0.04767***	-0.00332	0.00719	0																											
	ILLN8	***0.22892***	0.28209	0.27402	***0.26305***	***0.20889***	***0.23456***	***0.23432***	0.3353	0.39652	0.39769	0.3827	0.33092	0.36255	0.35209	0.31856	0.3412	***0.32171***	***0.30295***	***0.3002***	***0.3121***	0.31027	***0.28374***	***0.31272***	***0.29735***	***0.39786***	0.24987	***0.19118***	***0.16224***	***0.1985***	***0.23969***	***0.21965***	***0.18596***	***0.22676***	0.26353	***0.10955***	***0.14699***	***0.11397***	***0.12442***	***0.17878***	***0.20528***	***0.22418***	***0.24307***	***0.06093***	0.11585	***0.05847***	***0.05149***	0																											
	ILLN9A	***0.20532***	0.332	0.25125	***0.23171***	***0.20356***	***0.24179***	***0.2441***	0.3596	0.37004	0.38795	0.41762	0.34631	0.40415	0.36289	0.34503	0.30718	***0.2963***	***0.28767***	***0.27331***	***0.30882***	0.2627	***0.29587***	***0.2837***	***0.2613***	***0.39526***	0.27426	***0.17905***	***0.18423***	***0.25072***	***0.32086***	***0.27007***	***0.20251***	***0.21348***	0.28334	***0.12903***	***0.19784***	***0.16001***	***0.14715***	***0.18366***	***0.20671***	***0.26873***	***0.28183***	***0.09887***	0.16896	***0.10332***	***0.06295***	***0.12355***	0																											
	ILLN9B	***0.22043***	0.28752	0.24857	***0.2617***	***0.22105***	***0.26316***	***0.27022***	0.34488	0.38857	0.38361	0.39555	0.33558	0.39567	0.37211	0.3341	0.33462	***0.31793***	***0.30389***	***0.29543***	***0.31427***	0.30687	***0.29797***	***0.30466***	***0.28225***	***0.41048***	0.2732	***0.20298***	***0.16404***	***0.22537***	***0.25104***	***0.23408***	***0.21403***	***0.21564***	0.27711	***0.16407***	***0.22427***	***0.1926***	***0.18252***	***0.18126***	***0.26818***	***0.25971***	***0.28472***	***0.08037***	0.15648	***0.07613***	***0.04018***	***0.06207***	***0.07809***	0	
	ILLN10	***0.22548***	***0.2907***	***0.25869***	***0.24621***	***0.20587***	***0.25418***	***0.2537***	***0.35004***	***0.38323***	***0.36772***	***0.36837***	***0.29129***	***0.34784***	***0.34218***	***0.30454***	***0.30974***	***0.31189***	***0.28007***	***0.28815***	***0.29989***	***0.29178***	***0.27951***	***0.30136***	***0.27877***	***0.39606***	0.24096	***0.19053***	***0.15849***	***0.20245***	***0.25363***	***0.22035***	***0.17807***	***0.20483***	***0.23865***	0.05116	***0.15486***	***0.1199***	***0.11128***	***0.14608***	***0.20063***	***0.18042***	***0.21344***	***0.04867***	0.10168	***0.01568***	***0.02404***	***0.03105***	***0.07084***	***0.03282***	0